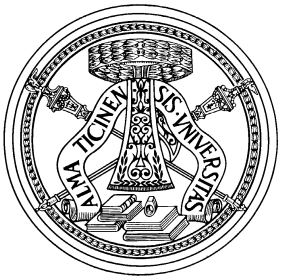

UNIVERSITÀ DEGLI STUDI DI PAVIA
Department of Biology and Biotechnology

Roles of Amyloid Precursor Protein in Platelet Function

Caterina Visconte

Dottorato di Ricerca in Scienze Biomediche
XXX Ciclo - A.A. 2014-2017

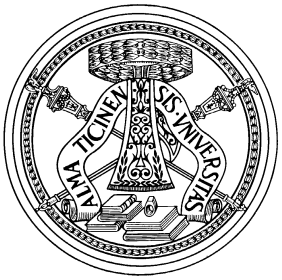

UNIVERSITÀ DEGLI STUDI DI PAVIA
Department of Biology and Biotechnology

Roles of Amyloid Precursor Protein in Platelet Function

Caterina Visconte

Doctoral Thesis
Supervisor: Prof. Mauro Torti

Dottorato di Ricerca in Scienze Biomediche
XXX Ciclo - A.A. 2014-2017

Alla mia famiglia,

Table of Contents

ABSTRACT

Role of Amyloid Precursor Protein APP in platelet function

Alzheimer's disease (AD) is an age-related neurodegenerative disorder, characterized by the presence of numerous senile plaques and neurofibrillary tangles in cerebral cortex and hippocampus of affected individuals. The principal protein in plaques is Aβ, a 4kDa amyloidogenic peptide derived from larger integral membrane glycoprotein APP. In recent years, AD has been recognized to be a systemic disorder that affects other peripheral tissues beside brain. Indeed, alterations in AD patients occur not only in the central nervous system but also in blood vessels and blood cells leading to Aβ deposits in cerebral vessels known as cerebral amyloid angiopathy (CAA). In addition to CAA, recent studies demonstrated that AD is strongly related to vascular system and is associated to vascular diseases such as stroke, atherosclerosis and hypertension. Conversely, many risk factors predisposing to vascular disorders may increase the risk for AD. Therefore, AD and cardiovascular disease are strongly related.

Circulating blood platelets are considered an important link between AD and cardiovascular disease. Besides being responsible to haemostasis and thrombosis, platelets represent the principal source of Aβ peptides in plasma, and express amount of APP similar to those detected in the brain. In addition, platelets store APP and Aβ peptides in α-granules and release them in circulation upon activation with physiological agonists. In turn, platelet derived Aβ peptides stimulate platelet activation. Importantly, APP isoforms expressed in platelet contain the additional Kunitz type protease inhibitor (KPI) domain, probably involved in the regulation of proteolytic events occurring near the cell membrane where may modulate haemostasis by inhibiting the activity of blood coagulation factors.

Neuronal APP influences cell proliferation, differentiation and neurite outgrown and acts either as a soluble molecule or as a cell surface

receptor. However, the exact biological function of platelet APP is still unknown.

Therefore, my project is based on the need to better define 1) the interrelation between platelets and AD and 2) the physiopathological role of APP in platelets. Two different kind of murine transgenic models were used to study these aspects: 3xTg-AD mice and APP KO mice, respectively.

3xTgAD transgenic mice represent a well characterized murine models of AD with propensity to accumulate Aβ in the brain over time. In the present PhD thesis, I explored platelet adhesion, activation and thrombus formation in old 3xTg-AD mice compared to aged matched control mice. I have demonstrated that circulating platelets isolated from 3xTg-AD mice exhibited a greater tendency to adhere to components of the subendothelial matrix, such as collagen, vWF and fibrinogen and to form thrombi under arterial blood flow, compared to platelets from control mice. Increased adhesion to collagen results in enhanced signalling in collagen adherent 3xTg-AD platelets.
The strong adhesive propensity described in platelets from AD mice suggest a new explanation for the increased pro-thrombotic risk state described in many patients affected by AD.

During my PhD I have also investigated the role of APP in platelet function, haemostasis and thrombosis, through the use of APP KO. Platelets from APP-deficient mice show abnormalities in platelet count and size, despite major glycoprotein expression and granule content are normal. APP is dispensable for platelet activation and aggregation, but it is required for platelet adhesion to immobilized Aβ peptides, supporting the hypothesis that APP functions as an adhesion receptor for Aβ peptides. Moreover, the absence of APP did not affect peripheral arterial thrombosis. In contrast, the analysis of venous thrombosis through IVC ligation model revealed that APP KO mice developed larger thrombi, with a significant increased length and weight, compare to control animals. Consistent with this result, APP KO shown larger occlusive thrombi in the lungs following pulmonary thromboembolism, hence suggesting an inhibitory role for platelet APP in venous thromboembolism. I further investigated the possible contribution of APP either in blood coagulation and in Neutrophil extracellular traps (NETs)

formation, two important pathways leading to the propagation of venous thrombosis. I found that APP have an important inhibitory action on the intrinsic coagulation pathway by targeting factor XI. Moreover, APP KO neutrophils exhibited a greater tendency to protrude neutrophils extracellular traps, that were also highly incorporated into venous thrombi. APP KO displayed significant increased platelet-leukocyte aggregates. These results indicated that platelet APP controls venous thrombosis through a dual mechanism: it inhibits the intrinsic coagulation pathway (namely through the FXIa inhibition) and it negatively regulates neutrophil functions.

INTRODUCTION

PLATELETS

Platelets were discovered by Giulio Bizzozzero in 1882. He was the first to clearly described platelets and their function in the bloodstream, demonstrating the role of platelets in promoting thrombosis. Later, for many years, a great deal of effort has been devoted to unravel the dynamic and multifunctional nature of platelets.

Anucleated, discoid platelets are originated from megakaryocytes, the only polyploid hematopoietic cells in the bone marrow (Schulze and Shivdasani, 2005). During megakaryocytes maturation, all platelet-specific organelles, proteins, membrane systems and other contents essential for platelet function are formed. Subsequently megakaryocytes extend long branching proplatelet-like protrusions into the sinusoidal blood vessels. The released proplatelets further mature in the circulation (Italiano et al., 1999). The normal platelet concentration in blood of mammals is 150-400 x 10^9 cells/L. Their average lifespan is normally 10-12 days, after that they are removed from the bloodstream and cleared by macrophages in liver and spleen.

New evidences suggested that blood platelets are involved in many processes, ranging from promoting inflammation and fighting microbial infection to endorsing tumour angiogenesis and metastasis (Leslie M., 2010). In addition, blood platelets appear to be involved in neurodegenerative disorders. Nevertheless, the principal physiological function of platelets remains to contribute to primary haemostasis, stopping haemorrhage when the continuity of the vasculature is interrupted (Cimmino et al., 2013). Indeed, under normal conditions, platelets circulate in the blood singly as smooth-surfaced discs, without interacting with each other or with the vascular endothelium. Conversely, upon tissue trauma, platelets initially tether and roll over the exposed extracellular matrix (ECM), eventually resulting in firm adhesion that in turns triggers full platelet activation and concomitant granules release. Platelet adhesion and activation leads to aggregation, ultimately resulting in platelet-rich clot formation (Broos, et al. 2011).

Platelet morphology

Platelets are about 1,5 -3 µm in diameter, 1µm in thickness and have a discoid shape. Resting platelets have an asymmetrical **plasma membrane**. The internal membrane layer contains anionic aminophospholipids, such as phosphatidyl serine, whereas the external layer contains several neutral phospholipids. Platelet activation triggers a rearrangement in membrane composition that causes the exposure of negative charged phospholipids to the outer membrane to promote their pro-coagulant activity (Wang et al., 2014).

Platelets possess two peculiar intracellular membrane systems: the open canalicular system and the dense tubular system. The **open canalicular system (OCS)** is an elaborate channel system, which begins as indentations of the plasma membrane and tunnels throughout the interior of the platelet, greatly increasing their available surface area and providing a route for the release of granules content to the outside. The **dense tubular system (DTS)** is an internal closed network, derived from endoplasmic reticulum of megakaryocytes. It represents the principal site of storage of Ca^{2+} that is released upon platelet activation, leading to shape change, granules centralization and secretion (Menashi et al., 1982). The dense tubular system membranes are also probably the principle site of prostaglandin (PG) and thromboxane synthesis (Gerrard et al., 1978).

Platelets are characterized by the presence of peroxisomes, lysosomes, glycosomes and few mitochondria randomly dispersed in the cytoplasm. Moreover, platelets also contain two types of peculiar platelet granules: dense bodies and α-granules. **Dense bodies** are electron-dense, 20-30 nm in diameter and each platelet contains, on average, approximately three to eight of these organelles; they contain organic and inorganic small molecules, with pro-aggregating activity, among which calcium, ADP, ATP and serotonin. (Rendu & Brohard-Bohn, 2002). **α-granules** represent the typical secretory vesicles, which carry many soluble proteins and membrane receptors to the cell surface. They are the most abundant granules in platelets (about 50-80 per platelet) and bigger than the dense bodies (they are about 200 nm in diameter). α-granules contain a vast number of biologically active molecules, including platelets specific proteins, such as platelet factor 4 and the α-thromboglobulin; there are also many adhesive proteins (e.g. von Willebrand factor and fibrinogen), hemostatic factors (e.g. Factor V, Factor IX, Factor XIII), membrane glycoproteins and protease inhibitors. Furthermore, platelet α-granules present high concentration of amyloid β-precursor protein APP and amyloid β-peptides. Both

dense-bodies and α-granules contents are released from activated platelets in the circulation.

Platelet function

The main physiological role of platelets is to contribute to **primary haemostasis**, a defense mechanism aimed at preventing blood loss when the continuity of the vasculature is interrupted.

Platelet **adhesion** represents the first response to vascular injury during which platelets immediately adhere to the exposed subendothelial extracellular matrix (ECM), through specific membrane receptors. After adhering to vascular injuries, platelets can rapidly undergo **activation** and recruit additional platelets, which are necessary to achieve haemostasis, or different types of leukocytes, which start the host defense responses. Platelet adhesion and activation lead to platelet **aggregation** to form hemostatic plug. Platelet activation must be carefully controlled in order to avoid unnecessary or excessive responses, which can lead to vessel occlusion and tissue infarction. For this reason, platelet activation also triggers endothelial cells to produce inhibitory compounds that limit the growth of the platelet thrombus in the damaged area.

Platelet adhesion

The first step in the hemostatic cascade is represented by the interaction of platelets with the exposed components of subendothelial extracellular matrix (ECM). The subendothelial ECM contains several adhesive macromolecules, such as collagens, von Willebrand Factor (vWF), laminin, fibronectin and thrombospondin, all of which serve as ligands and support platelet adhesion through the engagement of specific platelet surface receptors (Broos et al., 2011).

The mechanism of platelet adhesion at the site of vascular injury is largely determined by the local rheological conditions. Shear rate and shear stress have different effects on cellular adhesive interactions. Shear rate is directly related to flow velocity, indicating the velocity of cells in the fluid layer adjacent to the vessel wall and limits the time of contact between platelet membrane receptors and immobilized substrates on the vessel wall, in other words the rate of adhesive interaction. Therefore, the efficiency of cell recruitment onto the surface decreases with increasing shear rate. In contrast, shear stress influences the lifetime of an adhesive bond once formed, that is the off-rate of the interaction. The consequence is the decrease of efficiency of cell

recruitment with increasing shear stress, due to the detachment of adherent cells (Ruggeri, 1997). Blood flows with a greater velocity in the center of the vessel than near the wall, thereby generating shear forces between adjacent layers of fluid that become maximal at the wall. The drag, which opposes platelet adhesion and aggregation, increases with the prevailing shear rates (Varga-Szabo et al., 2008). At low share rate, such as in veins and larger arteries, platelet adhesion primarily involves the direct binding to collagen, laminin and fibronectin; whereas, at higher share rate, characteristic of small arteries and stenotic vessels, platelets are unable to efficiently interact with the exposed collagen fibers. In these conditions, the interaction between the platelet receptor glycoprotein GPIbα and vWF bound to collagen becomes critical.

VWF is a large, multimeric adhesive glycoprotein synthesized by endothelial cells and megakaryocytes. VWF is present in plasma, subendothelial matrix and storage granules in both platelets (α-granules) and endothelial cells (Weibel-Palade bodies) (De Mayer et al., 2009). The mature vWF is composed of four different repeating domains (A–D). There are three homologous A domains, that regulate interaction with different receptors and prothrombotic ligands of the subendothelial matrix. In particular, the A1 domain exclusively binds collagen type VI, whereas collagen I and III are bound via the A3 domain. In addition, the C1 domain contains the sequence Arg-Gly-Asp (RGD), which represents a binding motif for both platelet β_3-integrins, namely $\alpha_{IIb}\beta_3$ and $\alpha_v\beta_3$ (Varga-Szabo et al., 2008).

At sites of vascular damage, circulating vWF rapidly binds to exposed collagen, via collagen binding sites in its A1 and especially A3 domains. Another mechanism of vWF immobilization is via self-association with matrix-bound, platelet-bound or endogenous subendothelial vWF. After immobilization, vWF is able to capture platelets from the circulation via binding of its A1 domain with GPIbα. GPIbα represents the only receptor on a non-active platelet with significant affinity for vWF. It is part of the **GPIb-IX-V** complex, a highly abundant complex exclusively expressed in platelets (25000 copies per platelet) and megakaryocytes. Four different genes encode the receptor complex proteins, namely the α- and β- subunits of GPIb, GPIX and GPV, all of which belong to the leucine-rich repeat protein superfamily. In particular, GPIbα (135 kDa), which represents the major functional subunit of the receptor complex, is linked by disulphide bonds to two GPIb β subunits (25 kDa). GPIX (22 kDa) and GPV (88 kDa) are non-covalently associated, resulting in an overall receptor stoichiometry of 2:4:2:1 (Clemetson and Clemetson,1995; Berndt at al., 2001). Under conditions of high share rate, as occurs in arterioles and stenotic

arteries, the instantaneous onset of the interaction between GPIbα and vWF immobilized on collagen or on the surface of activated platelet is crucial for the initial adhesion of flowing platelets. The bond between vWF and GPIbα is characterized by fast on- and off-rates, resulting only in transient interaction that is not sufficient to mediate stable adhesion. Thus, the principal function of this interaction is to decelerate platelets, maintaining them in close contact with the exposed subendothelium and allowing the engagement of other platelet receptors leading to activation and eventually firm adhesion (Broos et al., 2011). After the initial slowing down mediated by vWF, the platelet interaction with the matrix is stabilized by the binding to collagen, principally via glycoprotein VI (GPVI) and integrin $\alpha_2\beta_1$.

Subendothelial fibrillar **collagen** is considered the highly thrombogenic component, since it directly induces powerful platelet activation and supports platelet adhesion and aggregation. Collagens consist of repeat GXY motifs where G is glycine and X and Y are frequently proline and hydroxyproline. Of the more than 20 forms of collagen in the human genome, fibrillar types I and III are the major components of the ECM of blood vessels, whereas, type IV collagen is the principal form in the subendothelial basement membrane (Varga-Szabo et al., 2008). Platelets possess two receptors for collagen, namely glycoprotein VI (GPVI) and the integrin $\alpha_2\beta_1$ (Broos et al., 2011; Rivera et al., 2009).

GPVI (62 kDa) is a platelet-specific transmembrane type I receptor that has two extracellular immunoglobulin-like domains, a mucin-like core, a transmembrane region and a short cytoplasmic tail (Clementson J.M. et al., 1999). GPVI harbors a positively charged arginine in its transmembrane region, which allows it to undergo a non-covalent association with the Fc receptor-γ (FcRγ) chain that bears an immunoreceptor tyrosine-based activation motif (ITAM) subunit for signal transduction (Watson S.P. and Gibbins J., 1998). Similarly to GPIbα, GPVI binds collagen with low affinity and thus is unable to mediate stable platelet adhesion by itself. Nevertheless, GPVI is crucial for stable platelet adhesion on exposed extracellular collagen because it induces strong signaling via the associated FcRγ chain (Broos et al., 2011). In fact, together with G protein coupled receptors (GPCRs) activation by locally produced or released agonists, GPVI mediates cellular activation and triggers intracellular signals that shift platelet integrins to a high-affinity state, thereby allowing firm adhesion and thrombus growth (Varga-Szabo et al., 2008).

Collagen also interacts with integrin **$\alpha_2\beta_1$** (GPIa/IIa or CD49b/CD29) in a Mg^{2+}-dependent manner. Integrins are widely expressed heterodimeric

transmembrane receptors, which are composed of a big α- and a small β-subunits which are non-covalently linked to each other. Both subunits consist of a large N-terminal extracellular domain, a single transmembrane domain and a short cytoplasmic tail (Varga-Szabo et al., 2008). Ligand binding to integrins is regulated by a process known as "inside-out" signaling, in which platelet activation determines the receptor conversion from a low-affinity to a high affinity state. In turn, binding of such ligands to integrins triggers "outside-in" signals that cooperate with signals resulting from occupancy of immunoreceptors or G protein coupled receptors (GPCRs) to induce anchorage-dependent responses. As with other integrin receptors, ligand binding to $\alpha_2\beta_1$ is engaged by a shift from the low-affinity to the high-affinity conformation. Otherwise, the exact signaling pathway leading to $\alpha_2\beta_1$ activation is still not completely clear but it probably involves GPVI signaling. Although structurally unrelated, the two major collagen receptors act in a synergistic cooperation, indeed, $\alpha_2\beta_1$ binding to collagen reinforces and enhances GPVI-collagen interaction promoting indirectly platelet activation.

The final step of platelet adhesion is firm arrest on ECM, a process that requires platelet activation, shifting several β_1 and β_3 integrins to their high-affinity ligand binding state. Platelets express three different β_1-integrins, namely $\alpha_2\beta_1$ (collagen receptor), $\alpha_5\beta_1$ (fibronectin receptor), and $\alpha_6\beta_1$ (laminin receptor) and two β_3-integrins: $\alpha_{IIb}\beta_3$ (fibrinogen, fibronectin, fibrin, trombospondin, vitronectin and vWF receptors) and $\alpha_V\beta_3$ (vibronectin, fibronectin and osteopontin receptors) (Varga-Szabo et al., 2008). Among them, $\alpha_{IIb}\beta_3$ (GPIIb/GPIIIa), the most abundant glycoprotein on platelet surface (60000-80000 copies per platelet), not only is the main platelet aggregating receptor, but also mediates firm adhesion of platelets by binding vWF and immobilized fibrinogen (Broos et al., 2011). Other integrins such as $\alpha_5\beta_1$, $\alpha_V\beta_3$ and $\alpha_6\beta_1$ probably play a role in modulating platelet responses according to the nature of the exposed ECM, which is dependent of the site, type and severity of the injury (Varga-Szabo et al., 2008).

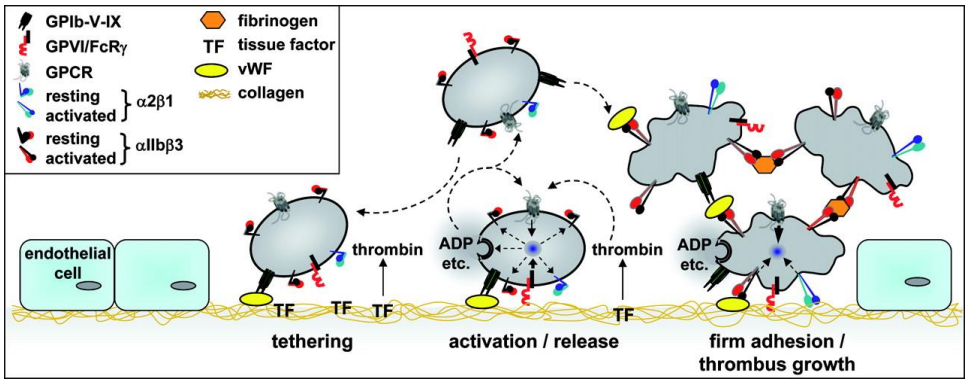

Figure 1: Platelet adhesion mechanism. (Varga-Szabo et al., 2008)

Platelet activation

Once platelets firmly adhere to the vessel wall or to the surface of a growing thrombus, they undergo remarkably complex series of morphological and biochemical changes leading to the release of the platelet granules, upregulation of the adhesive function of integrins, cytoskeletal rearrangements, which cause platelet shape change and finally aggregation.

Platelet activation and signaling downstream adhesion receptors

Platelet adhesion receptors are the key initiators of platelet activation at sites of vascular injury where platelets become exposed to adhesive proteins in the matrix or on endothelial cells. Interestingly, despite significant differences in their functions and signaling pathways, several platelet adhesion receptors share many similarities in their signal transduction mechanisms (Li Z., et al., 2010).

Increasing evidences suggest that signal generated by GPIb, GPVI and $\alpha_{IIb}\beta_3$ requires carefully regulated tyrosine phosphorylation. The phosphorylation of key tyrosine residues in signaling proteins by protein tyrosine kinases (PTKs) provides docking sites for proteins containing Src homology 2 (SH2) domain. This tyrosine phosphorylation is mainly mediated by Src family kinases (SFKs) and spleen tyrosine kinase (Syk). This signal transduction cascade also depends on PLCγ2 isoform and several other adaptor proteins (Asazuma et al., 1997; Falati et al., 1999; Jackson et al., 1994; Marshall et al., 2002; Torti et al., 1999; Wu et al., 2001).

The initial entrapment of platelets on subendothelial collagens requires the plasma protein vWF, which under high shear stress binds simultaneously to collagen

and to GPIb-V-IX, or to the integrin $\alpha_{IIb}\beta_3$ in its activated conformation (Li et al., 2010). VWF/GPIb-IX interaction also induces platelet activation signaling events, leading to integrin activation and integrin-dependent stable platelet adhesion and aggregation. There has been evidence that GPIb-IX is associated with the ITAM receptors FcγRIIA or FcRγ, two receptors that can initiate signaling via tyrosine phosphorylation of their cytoplasmic ITAM sequences by SFKs and recruitment of Syk (Sullam et al., 1998; Wu Y., 2001). Moreover, GPIbα interacts with 14-3-3ζ, which can bind PI3Ks and may be implicated in GPIb-mediated intracellular signaling that results in $\alpha_{IIb}\beta_3$ activation. Both SFKs and PI3Ks are important for transmitting the "early" activation signals from GPIb-IX, leading to calcium elevation and integrin activation independent of other receptors (Kasirer-Friede et al., 2004). Interestingly, VWF/GPIb-IX interaction also induces elevation of intracellular cGMP levels and sequential activation of cGMP-dependent protein kinase (PKG) and the p38-mitogen activated protein kinase (MAPK) and extracellular signal-regulated kinase (ERK) (Yin et al., 2008; Li et al 2006). Finally, GPIb-IX binds thrombin and sensitizes platelets to low-dose thrombin.

Subsequently, collagen helps to stabilize platelets interaction with the matrix. In particular, integrin $\alpha_2\beta_1$ is important for platelet adhesion to collagen, whereas GPVI is required for collagen-induced platelet activation. GPVI is non-covalently coupled to the Fc receptor γ chain (FcRγ). Collagen binding causes GPVI clustering, leading to phosphorylation of the ITAM domain within the FcRγ by SFKs (mainly Lyn and Fyn) bound to the cytoplasmic domain of GPVI. ITAM phosphorylation leads to binding and activation of the tyrosine kinase Syk, which phosphorylates downstream targets, such as the transmembrane adaptor linker for activated T cells (LAT) and the Src homology 2 domain-containing leukocytes phosphoprotein of 76 kDa (SLP-76). This induces the formation of a signaling complex, including LAT, SLP-76, Bruton tyrosine kinase (Btk), Gads, and phospholipase Cγ (PLCγ) 2, leading to thromboxane A_2 (TXA_2) synthesis, granule secretion and integrin activation (Watson et al., 2005).

Platelet activation and signalling downstream G-protein coupled receptors.

Beyond the first monolayer of platelets adherent to collagen and vWF, the addition of subsequent layers of platelets to the growing thrombus is strongly potentiated by a variety of soluble platelet agonists. Soluble platelet agonists produced

during coagulation (like thrombin) and inflammation (such as platelet-activating factor) or released from damaged cells (like ADP) are important in platelet activation and thrombus formation processes. In addition, platelet soluble agonists, such as TXA_2, ADP and serotonin are released from stimulated platelets and serve to amplify platelet activation and to recruit other circulating platelets. All these platelet agonists stimulate platelets by interacting with specific G-protein coupled receptors (GPCRs), a family of seven-transmembrane domain receptors with the N-terminus lying the outside and the C-terminus pointing in the cytoplasm, where it associates with heterotrimeric G proteins. G proteins consist of three subunits (α, β, and γ) and are characterized by two different functional states: when the α subunit is bound to GDP, it forms an inactive heterotrimeric complex with β/γ subunits. Upon receptor ligation, GPCR functions as a guanine exchange factor (GEF), inducing the replacement of the GDP to GTP on the α subunit, leading to the activated α form. The activated GTP-bound α form dissociates from both the receptor and the β/γ complex, and interacts with specific downstream targets to transmit GPCR signals (Offermanns, 2006). The β/γ complex can also interact with and activate downstream effectors. Platelets express four types of α subunits: Gq, G12/G13, Gi/Gz, and Gs, each of which is coupled to selective receptors and downstream effectors (Li et al., 2010). For example, signaling through receptor coupled to Gq-family members activates of phospholipase C β(PLC β) and induces the consequent release of IP3 and DAG, leading to granule secretion, integrin activation and platelet aggregation. Conversely, stimulation of G12/13-coupled receptors contributes to shape changes by promoting actin cytoskeleton reorganization through the activation of the monomeric G-protein Rho. Whereas, activation of Gi mediates both inhibition of adenylyl cyclase and activation of PI3K.

The principal soluble platelet agonists are thrombin, ADP and TxA_2. **Thromboxane A_2** (**TxA_2**) is produced by the increase of intracellular Ca^{2+} concentration that leads to phospholipase A_2 (PLA_2) activation, by p38 phosphorylation. In turn, PLA_2 cleaves fatty acids from the sn-2 acyl bond of phospholipids with the release of several compounds, among which arachidonic acid.

This represents the substrate for ciclooxygenase (COX-1) to the production of prostaglandin cyclo-endoperoxydases, which are further transformed in TxA_2 by the thromboxane synthase.

Released thromboxane A_2 (TxA_2) activates platelets via the TXA_2/prostaglandin H2 receptor (TP), which couples to Gq and G_{13}. Through TP receptor, TXA_2 induces smooth muscle cell contraction, but also activates additional platelets.

The exposure of phosphatidylserine on the outer leaflet of plasma membrane provides a catalytic surface for the assembly of coagulation complexes necessary for **thrombin** generation. Thrombin signals through the protease-activated receptor (PAR) family of GPCRs. PARs 1 and 4 are expressed on human platelets, while PARs 3 and 4 are expressed on mouse platelets. PAR1 and PAR4 directly couple to Gq and G_{12}/G_{13} (Kahn et al., 1998). Thrombin cleaves the N-terminus of these receptors, exposing a new N-terminus that serves as a tethered ligand for these receptors. Kinetic studies have shown that the human platelet response to thrombin is biphasic and involves first signaling through PAR1 and subsequent signaling through PAR4 (Covic et al., 2000). Thrombin causes fast mobilization of intracellular Ca^{2+}, activation PLA_2 and subsequent TxA_2 generation (all mediated by Gq). Moreover, thrombin can trigger Rho dependent signaling pathways in platelets (mediated by G_{13}), that contribute to actin modeling and shape change. In addition to the PAR receptors, GP1bα has high affinity for thrombin.

ADP is stored at high dose in platelet dense granules and is released upon platelet activation. The released ADP strongly activates platelets in an autocrine and paracrine fashion. It can also be released from damaged cells at sites of vascular injury. Platelet activation by ADP is mediated by two G protein-coupled receptors, $P2Y_1$ (coupled to Gq) and $P2Y_{12}$ (coupled to Gi). In particular, ADP is able to generate a second feedback amplification loop by activating additional platelets via $P2Y_1$ that causes platelet shape change and aggregation through Gq mediated PLCβ2 activation. Otherwise, ADP can also bind to $P2Y_{12}$ thus inhibiting adenylyl cyclase and stimulating phosphoinositide3-kinase β (PI3K β). In addition, ADP induces auxiliary granule secretion through activation of specific protein kinase C (PKC) isoforms.

Although the initial signalling mechanisms of various platelet receptors differ, they ultimately converge into common intracellular signalling events. In particular, almost all agonists induce activation of PLC. Indeed, PLCγ and PLCβ are activated by the ITAM and Gq pathways, respectively. PLC catalyzes the hydrolysis of phosphor-inositol 4,5-bisphosphate (PIP_2) to produce the second messenger inositol 1,4,5-trisphosphate (IP_3) and the membrane bound 1,2-diacylglycerol (DAG) (Rivera et al., 2009). IP_3 binds to the IP_3 receptor on the platelet DTS, that is a calcium-selective

cation channel and allows efflux of Ca^{2+} from the DTS resulting in increased cytosolic Ca^{2+} levels. In addition, membrane bound DAG stimulates several effectors, such as PKC isoforms. Raising cytosolic Ca^{2+} and DAG concentrations within the adherent platelet results in a burst of activating events, including the activation of PLA_2, a change in platelet shape, granule secretion and ultimately aggregation.

Another common platelet response to all agonists is the secretion of granule content. Granule secretion plays critical roles in platelet activation, in the recruitment of circulating platelets into aggregates, and thrombus stabilization. Thus, it can be considered a signalling amplification mechanism (Reed G.L. 2000).

Shape change

When platelets adhere to the subendothelial matrix, they change their shape from discoid to spherical with the extrusion of pseudopods (White, 1974), that represent a morphological evidence of activation. Platelet morphology represents an important factor influencing cell rolling behavior during the process of thrombus formation. The majority of platelets translocate on the vessel wall and on the surface of thrombi in vivo as flat, sliding discs (Maxwell et al., 2007). The flat disc morphology also enables maximal surface contact area with the adhesive surface, increasing the potential for multiple adhesive interactions. Shape change is an event that occurs downstream of agonist induced platelet activation, such as thrombin, ADP, or TxA_2. This process is based on the reorganization of the cytoskeleton: new actin filaments are created, leading to the formation of submembranous actin filament network and the extension of four distinct actin structures, with peculiar composition and function: filopodia, lamellipodia, stress fibers and contractile ring. In addition, shape change also induces actomyosin-based contractile processes, resulting in centralization of dense and α-granules, fusion of granules with each other and with the open canalicular system and the plasma membrane and finally release of granules content.

Negative Regulation of platelets.

The activation of platelets by agonists is counterbalanced by inactivation by specific platelet antagonists: in particular prostacyclins and prostaglandins (**PGI_2** and **PGE1**), nitric oxide (**NO**) and **cGMP**. They are strong negative regulators able to interfere with platelet adhesion, activation, aggregation, secretion and shape change (Broos et al., 2011). Physiological platelet inhibitors (prostacyclin and adenosine) activate receptor coupled to Gs subunit and mediate inhibitory signals by stimulating

adenylyl cyclase–dependent cAMP synthesis. Moreover, recent investigations demonstrate a biphasic role of NO and cGMP during platelet activation: stimulatory role at low concentrations of NO and cGMP, whereas inhibitory effect at high concentrations of NO and cGMP.

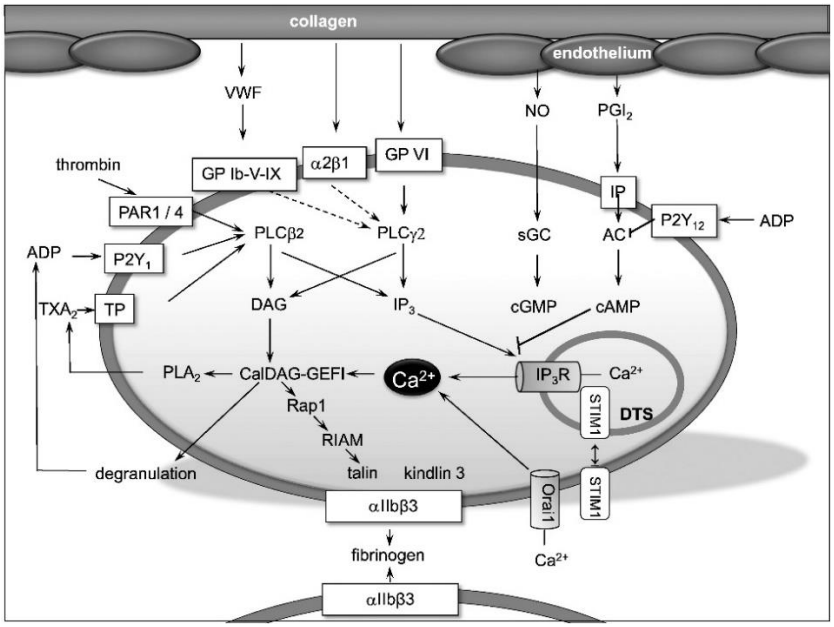

Figure 2. Schematic overview of the main platelet receptors and effectors involved in platelet signalling. (Broos et al., 2011).

Platelet aggregation

The accumulation of platelets into the hemostatic thrombus is based on the formation of multiple platelet/platelet interactions. Stable platelet adhesion, platelet aggregation and thrombus formation are mediated by integrin **$\alpha_{IIb}\beta_3$**, which binds various extracellular macromolecular ligands including fibrinogen and vWF and other matrix components containing RGD like sequences. In particular, the dimeric structure of fibrinogen and the multimeric structure of vWF allow these ligands to cross-bridge platelets and to generate a platelet aggregate. In resting platelets, $\alpha_{IIb}\beta_3$ is normally in a "low affinity" state, in which ligand binding affinities are low and no signaling occurs.

Platelet activation induces intracellular signaling mechanism that causes changes in the extracellular ligand binding domain of integrins, rapidly converting $\alpha_{IIb}\beta_3$ into an active conformation (**inside-out signaling**) (Shattil et al., 2010).

Ca^{2+} and DAG-regulated guanine nucleotide exchange factor I (CalDAG-GEFI) play a crucial role in integrin $\alpha_{IIb}\beta_3$ inside-out activation. Activated CalDAG-GEFI converts Rap1b, a member family of small GTPases named Ras, from the GDP-bound form to the active GTP-bound form, which interacts with RIAM (Rap1-interacting adaptor molecule) and talin. This event results in the cytoskeletal rearrangements accompanied by conformational changes in the integrin molecules, from a bent inactive form to a more extended activated form with exposed fibrinogen binding site. Rap1b activation is also mediated by GPCRs following soluble platelet agonist activation and by membrane platelet receptors stimulation.

Once activated, integrin $\alpha_{IIb}\beta_3$ is able to signal inside the cell through an **outside-in mechanism**, promoting activation and phosphorylation of signaling enzymes, calcium mobilization and reorganization of platelet cytoskeleton, which finally lead to platelet spreading, granule secretion, stable adhesion and clot retraction (Shattil and Newman, 2004). Integrin outside-in signaling is also regulated by the binding of the G_{13} subunits to the cytoplasmic domain of β_3. The interaction of G_{13} with β_3 stimulates the activation of SFKs, which mediates outside-in signaling through different mechanisms. For example, activation of a major RhoA GTPase activating protein by Src phosphorylation, with the result of RhoA inactivation. Another way is the activation of Syk that facilitates the assembly of an SLP-76/LAT/Btk/Vav complex that mediates stimulation of PLCγ2 and subsequent platelet activation events.

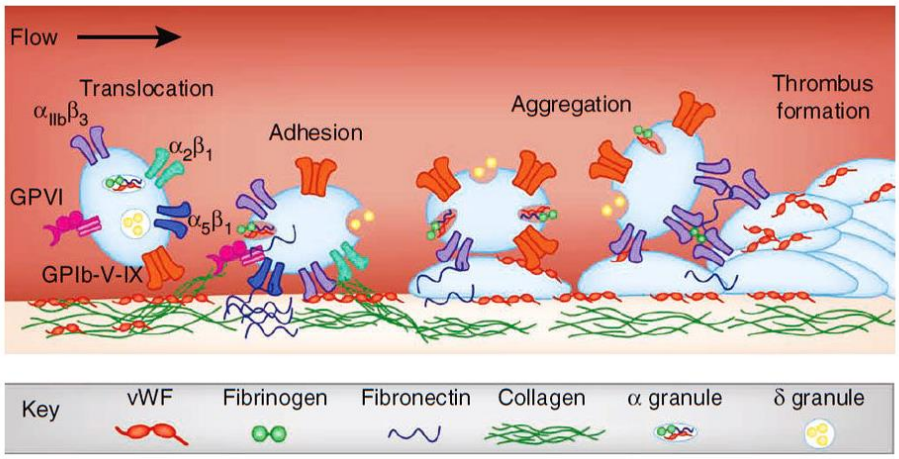

Figure 3: Adhesion and activation mechanisms supporting the haemostatic and protrombotic function of platelets. Platelets are captured in the injured vessel wall from flowing blood through the specific interaction of the platelet GPIb-V-IX complex with collagen-bound vWF exposed on the subendothelium. This ligand-receptor interaction has a rapid on-off rate that supports platelet translocation at the vessel wall. Stable platelet adhesion occurs through the binding of platelet GPVI to fibrillar collagen as well as the ligation of multiple β1 integrins, including the collagen α2β1 interaction and fibronectin engagement of α5β1. Once firmly adhered, platelets undergo a series of biochemical changes that induce integrin αIIbβ3 activation, leading to the high affinity interaction with adhesion proteins including vWF, fibrinogen and fibronectin. These adhesive interactions are indispensable in the ability of platelets to form stable aggregates with other activated platelets and promote thrombus growth. (modified from Jackson, 2011).

BLOOD COAGULATION

Haemostasis is the physiological response to stop bleeding at the site of injury while maintaining normal blood flow elsewhere in the circulation, and removes blood clots after restoration of vascular integrity. The two main components of haemostasis are primary and secondary haemostasis. **Primary haemostasis** refers to platelet aggregation and platelet plug formation. Platelets are activated through several processes and, as a result, they adhere to the site of injury and to each other, plugging the injury. **Secondary haemostasis** refers to the progression of coagulation cascade, with the generation of insoluble fibrin mesh that is incorporated into and around the platelet plug and serves to strengthen and stabilize the blood clot. These two processes happen simultaneously and are mechanistically intertwined.

Primary haemostasis

In a healthy blood vessel and under normal blood flow, platelets flow singly without adhere to surfaces or aggregate with each other. However, as a result of injury, platelets are exposed to subendothelial matrix and, as previously described, adhesion and activation of platelets begin. Multiplereceptors on the surface of platelets are involved in these adhesive interactions with likewise adhesive proteins. In particular, the formation of platelet plug occurs through platelet GPIb-IX-V receptor, which connects to immobilized vWF and GPVI receptor, bound to collagen. Both GPVI and GPIb-IX-V are critical for platelet adhesion to subendothelial matrix at the site of injury and for their subsequent activation (Kehrel et al., 1998; Nieswandt et al., 2001).

The platelet-injured vessel wall interaction involves a series of events that includes activation and shape change, release of platelet granular contents (dense bodies and α granules) with subsequent formation of fibrin-stabilized platelet aggregates and clot retraction (Triplett, 2000).

Secondary haemostasis

With platelet activation, phosphatidylserine is mobilized from the inner leaflet of platelet membrane and exposed on the external surface. This represents the perfect catalytic surface for assembling the enzyme complexes of the blood coagulation system. The coagulation system consists of a number of serine proteases cofactors, calcium and cell membrane components, and culminates in cleavage of soluble fibrinogen by thrombin. Thrombin cleavage forms insoluble fibrin that assembles into

fibrin mesh at the site of injury. Fibrin generation occurs simultaneously to platelet aggregation (Falati et al., 2002; Furie, 2009).

Figure 4 represents a simplified coagulation cascade incorporating the **intrinsic pathway** (dependent on contact activation by a negatively-charged surface), which involves coagulation Factors XII, XI, IX, VIII and V, and the **extrinsic pathway**, which involves tissue factor and Factor VII. These two pathways converge on a **common pathway** to activate Factor X, leading to conversion of prothrombin (Factor II) to thrombin (Factor IIa) and culminating in the conversion of fibrinogen to fibrin.

In more detail, when the vascular system is injured, blood is exposed to extravascular tissues, which are rich in tissue factor (TF), a cofactor for the serine protease Factor VIIa (Kirchhofer and Nemerson, 1996). The complex of TF and Factor VIIa activates both Factor X and Factor IX. Factor IXa, in the presence of its cofactor Factor VIIIa, also catalyses the formation of Factor Xa, hence amplifying this pathway. Moreover, Factor Xa can also activate Factor VII to VIIa. This activation pathway is known as extrinsic or TF pathway of coagulation. Then, Factor Xa, in the presence of its cofactor Factor Va and Ca^{2+}, catalyses the conversion of prothrombin to thrombin on anionic phospholipid surface (Dahlbäck, 2000). Thrombin represents the central serine protease in the coagulation cascade and it cleaves fibrinogen to generate insoluble fibrin in a multi-step reaction, which finally leads to the formation of cross-linked and insoluble interconnecting networks of fibrin. Thrombin also activates directly coagulation Factor IX and cofactors VIII and V to generates the active forms IXa, VIIIa and Va (Lane et al., 2005). Finally, thrombin is responsible for positive feedback activation of coagulation that is critical for clot propagation.

The APTT (activated partial thromboplastin time) is a test that evaluate the intrinsic pathway of coagulation. The APTT reagents comprise an activator (such as Kaolin, allergic acid) and phospholipids. APTT evaluates all the coagulation factors, except for Factor VII and XII. The PT (prothrombin time) is most common performed test for the extrinsic coagulation pathway of coagulation.

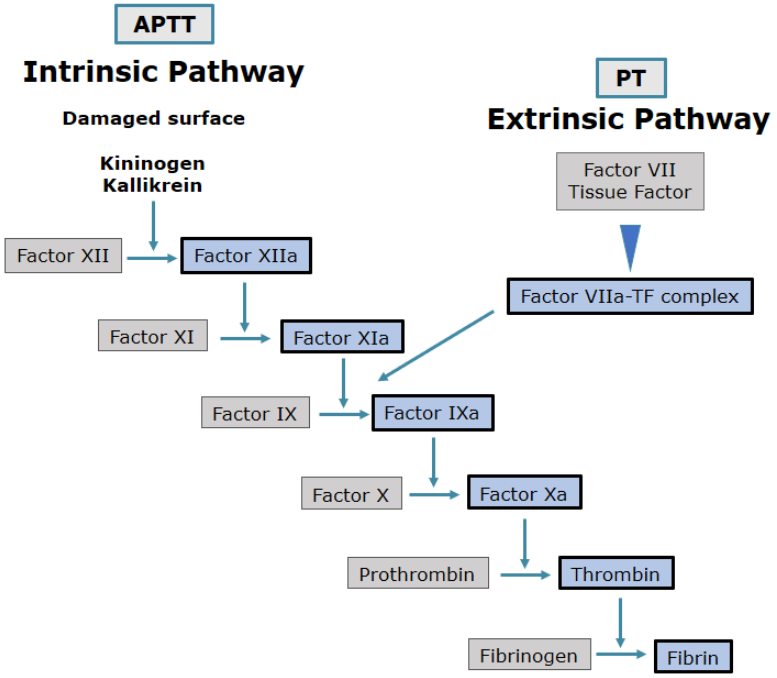

Figure 4: Schematic diagram of coagulation cascade.

Although all these reactions are frequently illustrated as simple sequential events in the coagulation cascade model, they represent highly complex interactions, subject to regulation at a number of levels. Current model describes three different separate phases of coagulation: initiation, amplification and propagation phases. The **initiation phase**, classically referred to as the extrinsic pathway of coagulation, starts with the expression of TF in damage vessel which binds coagulation Factor VIIa, in a TF/FVIIa complex. The TF/FVIIa complex converts of Factor IX and Factor X into Factor IXa and Factor Xa, respectively. This allows Factor Xa to associate with cofactor FVa to form a prothrombinase complex on TF-expressing cells which serves to convert prothrombin (Factor II) into thrombin. Thrombin generated through this reaction is not robust and can be effectively finished by TF pathway inhibitor. In the **amplification phase** the little amount of generated thrombin is able to activates platelets that adhere to a site of injury. In parallel, thrombin further converts Factor V into Factor Va, thus amplifying prothrombinase activity and converts Factor VIII into Factor VIIIa, which serves as a cofactor to Factor IXa on the surface of activated

platelets to support Factor Xa generation. In addition, thrombin also activates Factor XI. The **propagation phase** occurs on surfaces containing procoagulant phospholipids, such as activated platelets. The accumulated enzyme complexes on platelet surface support thrombin generation and platelet activation. Indeed, activated Factor XI converts Factor IX into Factor IXa, which then associates with Factor VIIIa. Then, the tenase complex of FIXa/FVIIIa catalyzes the conversion of Factor X to Factor Xa, after which the Factor Xa/ Factor Va complex produces sufficient amounts of thrombin to form fibrin fibers. As a final step, thrombin generation leads to the activation of Factor XIIIa, which catalyzes the formation of covalent crosslinks between adjacent fibrin chains and provide strength and stability to fibrin incorporated into the platelet plug (Ariëns et al., 2000).

There are physiological inhibitors in plasma that serve to localize procoagulant activity at the site of injury and maintain haemostatic balance. These include antithrombin, the principle inhibitor of thrombin and Factor Xa, and the other serine proteases inhibitors (Triplett, 2000). Antithrombin acts as a "pseudosubstrate" for thrombin and after binding, the antithrombin-thrombin complex is further cleared from the circulation. In general, antithrombin and the other members of the serpin (serine protease inhibitors) family of inhibitors down-regulate the coagulation cascade by acting on different serine proteases (Rau J.C. et al., 2007). In addition, thrombin binds to an endothelial receptor thrombomodulin, forming the thrombin-thrombomodulin complex that induces the activation of protein C (Esmon and Owen, 1981). The activated protein C (APC) in turn cleaves and inactivates the procoagulant cofactors VIIIa and Va (Fulcher et al., 1984; Guinto and Esmon, 1984). Protein S, a vitamin K-dependent protein, is an important cofactor for this reaction.

THROMBOSIS

A balance between clotting and bleeding is always maintained in the body under normal physiology. However, any pathological scenario will alter this balance to either haemorrhagic or thrombotic complications. Thrombosis can occur in the arterial or venous circulation and has an important medical impact (Mackman N., 2008). The pathophysiology of **arterial thrombosis** differs from that of **venous thrombosis**, as reflected by the different ways in which they are treated. Indeed, **a**rterial thrombosis is generally treated with drugs that inhibit platelet aggregation, whereas venous thrombosis is treated with drugs that target proteins of the coagulation cascade. Although arterial and venous thrombosis are thought to have different risk factors, recent studies have suggested that some of the classic risk factors for arterial thrombosis, such as obesity and high cholesterol, are also risk factors for venous thrombosis (Franchini and Mannucci, 2008).

Arterial thrombosis

Acute arterial thrombosis is the proximal cause of most cases of myocardial infarction and of about 80% of strokes, collectively the most common cause of death in the developed world (Mackman, 2008). The arterial circulation is characterized by higher flow rates and therefore higher sheer forces (Tangelder et al., 1988). The primary trigger of arterial thrombosis is rupture of an atherosclerotic plaque. This involves disruption of the endothelium and release of constituents of the plaque into the lumen of the blood vessel. The thrombi that form at ruptured plaques are composed largely of aggregated platelets and therefore are known as "white clots". In broad terms, when the accumulation of lipid deposits and lipid-laden macrophages in artery wall induces the atherosclerotic plaque rupture, platelets are rapidly recruited to the site, through the interaction of specific platelet cell-surface receptors with collagen and vWF. After this initial adhesion to the vessel wall, platelets also become activated and start to recruit additional platelets, resulting in rapid growth of thrombus. Then activated platelets release the content of granules, which further promotes platelet recruitment, adhesion, activation and aggregation. Another critical part of arterial thrombosis is represented by the activation of the blood coagulation cascade by thrombin. Moreover, atherosclerotic plaques contain high concentrations of tissue factor protein, which exposure triggers the coagulation cascade (Tremoli et al., 1999). Since platelets are the major components in arterial thrombi and their critical role in

thrombus stabilization and propagation, antiplatelet therapy has been widely used. At present, the primary targets of antiplatelet therapy are molecules involved in platelet activation and aggregation, among which cyclooxygenase inhibitors, such as aspirin, platelet $P2Y_{12}$ receptor antagonist, such as clopidrogrel and prasugrel, and $\alpha_{IIb}\beta_3$ antagonist.

Venous thrombosis

Venous thrombosis is a leading cause of morbidity and mortality in industrialized countries and is now recognized as a multifactorial disease caused by acquired and genetic risk factors, which cause a hypercoagulable state and result in an increased tendency for activation of the coagulation cascade (Mackmann, 2012). The genetic risk factors consist of multiple variants in the coagulation cascade, which can increase activity or abundance of proteins that promote coagulation and/or decrease abundance of proteins that inhibit coagulation. The acquired risk factors include cancer, surgery, immobilization, fractures, hospitalization, obesity and pregnancy. The risk factors for venous thrombosis are primarily due to stasis and changes of blood composition. Thrombi that form in veins are rich in fibrin and trapped red blood cells and are referred to as "red clots". The two main classes of anticoagulant drugs currently used for the treatment of venous thrombosis are vitamin K antagonists and heparins, which target multiple proteases in the coagulation cascade.

Deep vein thrombosis (**DVT**) is associated with **pulmonary embolism** (**PE**), and they are collectively referred to as **venous thromboembolism** (**VTE**). Deep vein thrombosis mostly occurs in the large veins of the legs. Pulmonary embolism represents a complication of deep vein thrombosis that can occur if part of the thrombus breaks away, travels to the lungs and lodges in a pulmonary artery, resulting in the disruption of blood flow (Mackmann, 2008). Deep vein thrombosis mainly occurs because of changes in the composition of the blood that promote thrombosis, changes that reduce or abolish blood flow and changes to the vessel wall.

In more details, reduced blood flow and stasis allow the accumulation of procoagulant proteases, such as thrombin, that may overcome the local anticoagulant pathways and induce thrombosis (Mackmann N., 2012). Recently, investigators have developed a new mouse model of venous thrombosis that involves stenosis of the inferior vena cava, which reduce the lumen of the vessel of about 80%, without denuding the endothelium (von Brühl et al., 2012). In this model, they found that the endothelium is activated and releases vWF and P-selectin from Weibel-Palade bodies.

Subsequently, P-selectin captures leukocytes by binding their P-selectin glycoprotein ligand-1 (PSGL-1) receptor, whereas GP1bα on the surface of platelets interacts with vWF. In addition, activated endothelial cells downregulate expression of the anticoagulant protein thrombomodulin and upregulate expression of the procoagulant protein TF (Esmon C.T. et al., 2011). In addition, it was found that a genetic deficiency of TF in either hematopoietic cells or myeloid cells dramatically reduced venous thrombosis, which indicates that TF expression by leukocytes initiated thrombosis in this model (von Bruhl et al., 2012). Moreover, this study also demonstrated a novel role of FXII and platelets in the propagation of the thrombus. However, TF is not the only factor that may trigger thrombosis; recent studies have also shown that vWF and extracellular chromatin from neutrophils play important role in venous thrombosis in animal models (Brill et al., 2011; Fuchs et al., 2010). Importantly, neutrophils promote thrombosis by releasing either **extracellular DNA traps** (Fuchs et al., 2010; Brill et al., 2012) or serine proteases that inactivated the anticoagulant TF pathway inhibitor (Massberg et al., 2010).

Neutrophil extracellular traps (NETs)

Neutrophils promote thrombosis in vitro and in vivo by releasing neutrophil extracellular DNA known as neutrophil extracellular traps (NETs) (Massberg et al., 2010). Neutrophil extracellular traps (NETs) are structures of chromatin filaments coated with histones, proteases and granular and cytosolic proteins, and the process by which neutrophils produce and release NETs are defined **NETosis** (Jorch et al., 2017). Netosis is a specific type of cell death different from both necrosis and apoptosis but its mechanism is still poorly understood (Fuchs et al., 2007). NETosis helps neutrophils to immobilize and catch bacteria, fungi or viruses, which results in more efficient elimination of pathogens.

Stimulation with phorbol-12-myristate-13-acetate (PMA), a useful chemical tool that activates many intracellular pathways in neutrophils, led to the original discovery that neutrophils make NETs (Brinkmann et al., 2004).

After stimulation, the neutrophil chromatin undergoes decondensation followed by mixing of euchromatin and heterochromatin (Fuchs et al., 2007). This process is mediated by neutrophil elastase (NE) and myeloperoxidase (MPO), two enzymes stored in the azurophilic granules which are further relocated to the nucleus. Initially, NE degrades the linker histone H1 and the core histones, leading to chromatin decondensation which is enhanced by MPO (Papayannopoulos et al., 2010; Metzler et al., 2011). Then, NADPH-oxidase production of reactive oxygen species (ROS)

results in the activation of protein-arginine deiminase 4 (PAD4), an enzyme localized in the nucleus of neutrophils that converts arginine to citrulline on histones H3, this modification is referred to "citrullination" (Wang et al., 2009; Leshner et al., 2012; Neeli and Radic, 2013). As a consequence of the chromatin decondensation in the neutrophil nucleus, the nuclear membrane is damaged, and chromatin is released into the cytosol and is mixed with granular antimicrobial factors. Finally, the cell membrane breaks releasing NETs (Brinkmann and Zychlinsky, 2012).

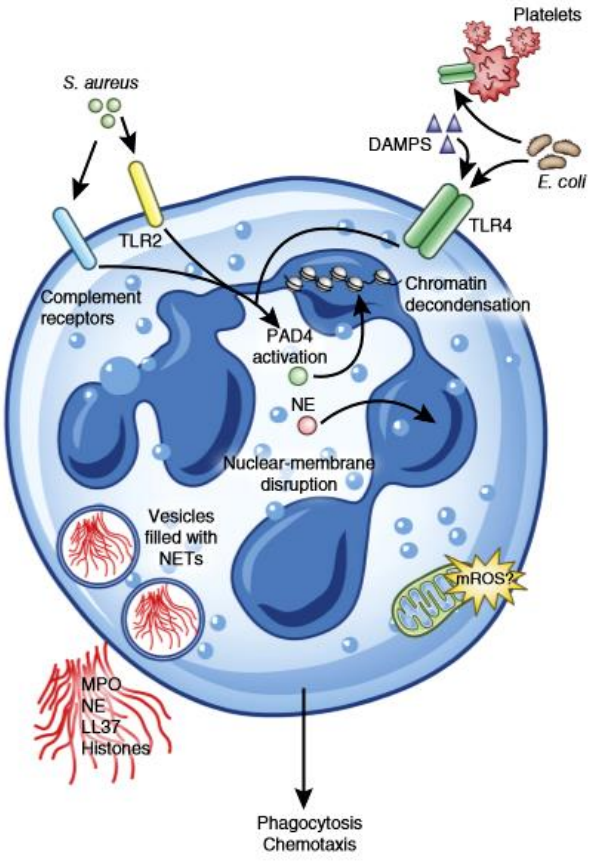

Figure 5 Overview of NETosis (from Jorch et al., 2017). NETosis is induced by *S. aureus* through both complement receptors and TLR2 ligands, or by *E. coli* directly via TLR4 or indirectly via TLR4-activated platelets. PAD4 is activated and induces chromatin decondensation. Then. neutrophil elastase (NE) and myeloperoxidase (MPO) are translocated into the nucleus to promote further unfolding of chromatin, with resultant disruption of the nuclear membrane. Chromatin is expelled into the cytosol, where it becomes decorated with granular and cytosolic proteins. Finally, NETs are released through disruption of the plasma membrane.

Recent studies suggest that NETs provide a scaffold and stimulus for thrombus formation (Martinod and Wagner, 2014). In particular, markers of extracellular DNA traps are abundant in DVT.

Tissue factor (TF) is considered as the central coagulation-triggering molecule in DVT (Manly et al., 2011). A latest finding that TF can be produced by neutrophils and expulsed to the vein during NET formation is the first evidence that neutrophils and Netosis provide a link between inflammation and thrombosis (Von Brühl et al., 2012; Fuchs et al., 2012). Additionally, DNA and histones in NETs may play an important role in stimulating coagulation as well. In fact, nucleic acids enhance the activity of coagulation serine proteases, whereas histones promote coagulation indirectly by activating platelets and stimulating release of procoagulant polyphosphates from platelet granules.

In more details, NETs stimulate the extrinsic and intrinsic coagulation pathways. NE present in NETs can regulate coagulation pathway by proteolytic cleavage of TF pathway inhibitors and enhancement of Factor Xa activity (Steppich et al., 2008). NETs also bind Factor XII thereby stimulating fibrin formation via the intrinsic coagulation pathway *(*Von Brühl et al., 2012). Another way of NET contribution to thrombus formation is through interaction with platelets. Platelets may bind to NETs directly and indirectly (Fuchs et al., 2012). Principally platelet binding involves Toll- like receptors (Semeraro et al., 2011) or is based on electrostatic interaction between histones located in NETs and phospholipids or carbohydrates of platelets (Pereira et al., 1994; Watson et al., 1999).

Platelet-NET interactions may also be mediated by adhesion molecules, such as VWF, fibrinogen, or fibronectin, possibly because of their affinity for histones (Fuchs et al., 2010; Brill et al., 2012). Finally, platelets bound to NETs can be activated by components of traps, especially by histones (Fuchs et al., 2011) and neutrophil proteases (Si-Tahar et al., 1997). This process may be accelerated, as activated platelets cause further NET release that increases endothelial permeability (Fuchs et al., 2010; Brill et al., 2012).

Numerous observations indicate that NETs could influence initiation and growth of DVT, suggesting that NETs might be considered a potential therapeutic target for the treatment and prevention of this specific disease.

ALZHEIMER'S DISEASE

Alzheimer's disease (**AD**) is a chronic progressive neurodegenerative disorder that affects about 45 million people worldwide and it is characterized by devastating cognitive and memory decline. AD represents the most common cause of dementia in the elderly, whose prevalence has been calculated to rise in the next decade.

The first neuropathological case of a patient affected by AD was described by Dr. Alois Alzheimer in 1906 (Möller and Graeber, 1998).

AD pathological diagnosis is established post-mortem by the presence of characteristic lesions consisting of extracellular senile plaques and intracellular neurofibrillary tangles in cortical and hippocampal regions (Gandy, 2005), and a major loss of grey matter.

Senile plaques are characterized by abnormal accumulation of amyloid β-peptide (Aβ) that is able to spontaneously self-aggregates into multiple coexisting physical forms. One form consists of oligomers (2 to 6 peptides), which associate into intermediate assemblies. Aβ can also grow into fibrils, which arrange themselves into β-pleated sheets to form the insoluble fibers of advanced amyloid plaques (Querfurth, 2010). The amyloid plaques are mostly constituted of self-aggregating Aβ peptides. Aβ peptides are natural products consisting of 36 to 43 amino acids, which derive from the metabolism of amyloid precursor protein (APP) through the amyloidogenic pathway. An imbalance between production and clearance causes Aβ accumulation and this excess may be the initiating factor in AD (Gandy, 2005).

Neurofibrillary tangles result from the self-association of hyperphosphorylated, microtubule-associated protein, called tau (Goedert, 1993). Normally abundant soluble protein tau in axons promotes assembly and stability of microtubules while hyperphosphorylated tau is insoluble, lacks affinity for microtubules, and self-associates into paired helical filament structures. Like Aβ oligomers, intermediate aggregates of abnormal tau molecules are cytotoxic and impair cognition.

Post-mortem pathological examinations also suggest an association of cerebral vascular diseases (CVD) with AD. To date, cerebral amyloid angiopathy (CAA), microvasculature degeneration, microvessels inflammation, microinfarcts, subcortical lacunes and microhemorrhages, are frequently observed in the brain of AD patients (Jellinger, 2002).

Two forms of AD have been described: a Sporadic or Late Onset (SAD or LOAD) senile form, and Familial (FAD) or presenil form.

The **sporadic form** of AD develops in 95-98% of cases of AD and typically occurs in patients after 65 years of age old. No genes are directly responsible for the onset of the sporadic AD, but an association with polymorphisms of the gene ApoE has been reported, in particular, ε4 allele of apolipoprotein E (ApoE) predisposes to AD and thus provides a major genetic risk factor for the disorder in the typical late-onset senile form of AD (Struhl and Adachi, 2000). In addition, many vascular risk factors for cardiovascular disease, such as hypertension, diabetes, hypercholesterolemia and smoke predispose to sporadic AD (Honjo et al., 2012).

The **familial form** of AD represents only 2-5% of the cases and its onset occurs generally before the age of 65 years old. The familial form is transmitted as an autosomal dominant trait and it is mainly due to mutations in three genes: amyloid precursor protein (*APP*), presenilin-1 (*PSEN1)* and presenilin-2 (*PSEN2)*. The first specific genetic cause of AD to be identified was the occurrence of missense mutations found on gene encoding amyloid-β precursor protein (APP). These mutations are strategically located either immediately before the β-secretase cleavage site, or shortly after the α- secretase site, or close to the COOH-terminal of the γ- secretase cleavage site. These missense mutations lead to AD by altering proteolytic processing of APP in different ways, principally because all these proteolytic cleavage sites concern Aβ. Alterations in the APP gene can predispose to the development of AD also in another way: the overexpression of structurally normal APP owing to elevated gene dosage in trisomy 21 (Down's syndrome) leads to the premature occurrence of classical AD neuropathology (neuritic plaques and neurofibrillary tangles) during middle adult years.

In addition, missense mutations in the genes on chromosome 14 and 1, which encode the presenilin 1 (*PSEN1*) and presenilin 2 (*PSEN2*) genes, respectively, represent the most common cause of autosomal dominant AD. In fact, the presenilin genes (*PSEN1* and *PSEN2*) also affect APP processing as they encode γ- secretase proteolytic subunits which, in their mutated form promote the production of aggregating forms of Aβ (Selkoe, 2001).

Altogether mutations in *APP*, *PSEN1* and *PSEN2* leads to a common molecular phenotype: an increase in the ratio of $A\beta_{42}$:$A\beta_{40}$ (Tanzi and Bertram, 2005). The relative increase in $A\beta_{42}$ promotes the aggregation of the peptide into oligomers and ultimately amyloid fibrils (Jarrett et al. 1993).

Although AD is prevalently known as a neurological disorder, it is now well recognized that it represents a systemic disease that affects peripheral tissues with alterations in blood cells and vessels (Canobbio et al., 2016). Indeed, in AD patients, abnormal accumulation of Aβ peptides is not restricted to the brain parenchyma, but it also occurs in the brain vessel walls, in peripheral tissues and in biological fluids, such as the cerebrospinal fluid and plasma (Blennow et al., 2010). A number of recent evidences have led to the proposal of a novel **vascular hypothesis** for AD pathogenesis suggesting that early cerebrovascular dysfunction play a central role in the onset of the disease. The vascular hypothesis for AD was first proposed in 1993 after the observation of extensive angio-architectural distortions of cerebral capillaries and reduced cerebral blood flow in Alzheimer's brains (de la Torre and Mussivand, 1993). It has been demonstrated that sporadic AD and cardiovascular diseases share numerous risk factors, such as aging, hypercholesterolemia, hypertension, diabetes and obesity. Moreover, cardiovascular diseases quicken $A\beta_{40}$ and $A\beta_{42}$ production and deposition in the cerebral vasculature (Hohjo et al., 2012) and enables cerebral amyloid angiopathy (CAA), which is frequently associated with AD. Conversely, a growing number of studies established that AD patients have substantially increased risk of ischemic and hemorrhagic strokes if compared to non-AD patients, and microinfarctions arise more frequently in AD patients than in non-demented controls (Chi et al., 2013). Therefore, it is now clear that AD and cardiovascular diseases are strongly connected.

Circulating blood platelets are necessarily involved in the development of cardiovascular diseases. In addition, platelets may represent a valid peripheral model to study the metabolic mechanisms occurring in the central nervous system and associated to AD. In fact, platelets are the major source of amyloid peptides found in plasma. Then, platelets express amounts of APP comparable to those detected in the brain and all the enzymes responsible for its metabolism and for the generation of Aβ peptides. Moreover, several studies have documented alterations in platelet functions in AD patients. Hence, platelets appear suited to provide an important functional link between Alzheimer's and cardiovascular diseases.

AMYLOID PRECURSOR PROTEIN APP

Amyloid precursor protein APP is a transmembrane glycoprotein, principally known as the precursor molecule of the amyloid β-peptides (Aβ), which abnormal accumulation in the brain parenchyma and cerebral vessel walls is correlated with Alzheimer's disease (AD).

Because of the central role of APP in AD pathogenesis, the great deal of effort has been devoted to understand its function particularly in the central nervous system, where APP seems to influence cell proliferation, differentiation, neurite outgrowth, cell adhesion and synaptogenesis. Moreover, APP may have receptor-like properties. However, APP is more than just and "amyloid precursor", thus it is expressed ubiquitously, with specific biochemical and pathological roles in other tissues which require further studies.

APP gene and isoforms

***APP* gene** is located on the long arm of chromosome 21 (21q21.3) and contains at least 18 exons. Alternative splicing generates APP mRNAs encoding several isoforms that range from 365 to 770 amino acid residues (Zheng and Koo, 2011). However, the three principal isoforms are **APP_{695}**, **APP_{751}** and **APP_{770}**, which derived by the alternative mRNA splicing, principally of exons 7, 8, and 15 of the *APP* gene (Ling, 2003).

The larger two isoforms (APP_{751} and APP_{770}) are expressed in most tissues examined, whereas APP_{695} isoform is predominately or even exclusively expressed in neurons and accounts for the primary source of APP in brain. In human cortex the ratio of different APP isoform mRNAs is approx $APP_{770}/APP_{751}/APP_{695}$ = 1:10:20, although there are regional differences (Nalivaeva and Tunder, 2013).

The APP isoforms APP_{751} and APP_{770} contain an additional 56 aminoacid domain in the extracellular sequences, that is structurally and functionally related to Kunitz-type serine proteinase inhibitors (KPI). These two isoforms are known as Kunitz-type serine proteinase inhibitor domain-containing isoforms (KPI^+-APP) and represent the predominant forms expressed in non neuronal cells, such as glia, platelets and leukocytes, under normal conditions (Li et al., 1994). This Kunitz-type protease inhibitor domain is believed to be involved in the regulation of proteolytic events occurring near the cell membrane. Conversely, the alternative splicing of exon 7 on *APP* gene generates the Kunitz-type protease inhibitor domain-lacking isoform (KPI^-

-APP), represented by APP_{695} isoform and it is the predominant form expressed in neurons.

Whereas the deletion of exon 15 generates isoforms containing consensus sequence for the attachment of chondroitin sulphate proteoglycans (Pangalos et al., 1995). The proteoglycan form of APP (called 'appican' or L-APP isoforms) has been found mostly in glia rather than in neurons. The binding of glycosaminoglycan chain close to Aβ sequence of APP may affect the processing of APP and the production of Aβ and p3 peptides. L-APP isoforms are expressed in the lymphocyte/monocyte lineage and in non-neuronal cells within the central nervous system.

Finally, the exon 8 codes for a domain with homology to the MRC OX-2 antigen (OX-2) and its splicing occurs in APP_{695} and APP_{751} isoforms, whereas the APP_{770} expresses all exons.

APP family

APP belongs to a family of evolutionary and functionally conserved type I membrane proteins. The APP orthologues have been identified in diverse organisms, among which C. elegans (APL-1), Drosophila (APPL), Zebrafish and Xenopus Laevis. Mammalian homologues of APP include other two proteins, namely APP like protein 1 (APLP1) and APP like protein 2 (APLP2). The human *APLP 1* gene is located on chromosome 19, whereas *APLP 2* gene is located on chromosome 11 (Wasco W. et al., 1992 and Wasco et al., 1993). All APP family proteins share conserved aminoacid sequences and protein subdomains, particularly in the extracellular and cytoplasmic regions. Importantly, the Aβ sequence is unique to APP. Both, APP and APLP2 are ubiquitously expressed transmembrane proteins containing the protease inhibitor domain of Kunitz type (KPI domain) and are predominantly expressed in peripheral cells (Tanzi et al., 1988). Moreover, secreted APP and APLP2 molecules are present in blood plasma and the cerebrospinal fluid (CSF) (Palmert et al., 1989). Unlike APP and APLP2, the expression pattern of APLP1 is restricted to cells of the central nervous system being strongest in the brain (Wasco et al., 1992 and Wasco et al., 1995).

The existence of a family of APP-like proteins implies that they may share common functions. Functional redundancy was described in knockout animals demonstrating that the conserved structure of the proteins appears also to extend to their physiological role (Coulson et al. 2000).

APP protein structure

The APP is a type I transmembrane glycoprotein with a large ectodomain, a single membrane-spanning domain and a short cytosolic domain. The N-terminal globular domain in the extracellular side includes binding site for heparin, zinc and copper and is connected through an unstructured acidic domain followed by KPI domain and OX-2 domain to a large glycosylated domain that may be involved in homo- and hetero-dimerization (Soba P. et al., 2005). The Aβ region comprises the C-terminal moiety of the extracellular domain and part of the membrane-spanning domain.

The cytoplasmic carboxyl-terminal domain of APP contains transduction and internalization signals (Koo et al., 1996). In particular, the cytoplasmic domain contains two consensus motifs, YENPTY and YTS, which mediate interactions with adaptor proteins that control endocytosis (Thinakaran et al., 2008).

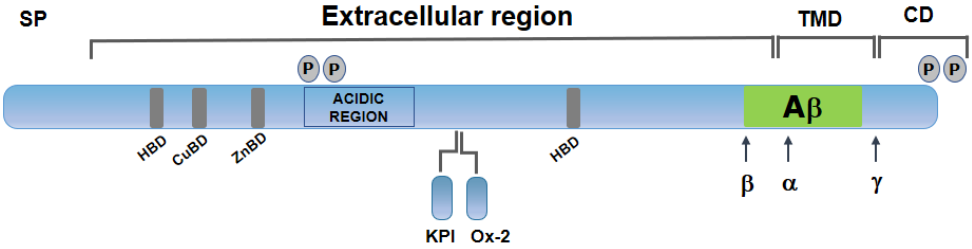

Figure 6. APP structure.

Extracellular region

The structure of the APP N-terminal domain consists of nine β-strands (34% β-sheet) and one α-helix (12% helix) which fold into a compact, globular domain (Rossjohn et al. 1999).

The large ectodomain of APP includes a **cysteine-rich globular domain** (**E1**), an **acidic domain** and a **carbohydrate domain**, further subdivided into the **helix-rich domain** (**E2**) and the **linker or juxtamembrane domain**.

In the **cysteine-rich E1 domain** of APP is recognized into two distinct regions, the heparin-binding domain (**HBD**) and the copper/metal binding domain (**CuBD**).

The N-terminal head of APP (aminoacid residues 23-128) is called growth factor-like domain (**GFLD**) and includes the heparin binding domain (HBD). In particular, the location of the heparin-binding site is formed of a single α-helix and an anti-parallel

β-sheet, with a loop rich in positively charged residues (aminoacid residues 96-110) that bind to heparin (Small et al. 1994; Rossjohn et al. 1999). Moreover, the disulfide bridge between Cys 98 and Cys 105 has a crucial role in conformation maintenance of the loop, that it has been found to be critical for neurite outgrowth (Small D.H. et al., 1994) and MAP kinase activation (Greenberg et al., 1995). Immediately adjacent to the HBD is a conserved hydrophobic pocket, which could form either a protein-binding site or a dimerization site (Rossjohn et al. 1999).

Then, a high affinity fibrillar Aβ binding domain was also identified between residues 95 and 118 in the amino terminal region of AβPP (Van Nostrand W.F. et al., 2002). Soba and colleagues have identified the E1 domain together with the transmembrane region as the major interaction interface for lateral (cis-) dimerization of cellular APP and APLPs, while the formation of adhesive complexes (trans-cellular dimers) only requires the E1 domain (Soba P. et al., 2005).

Adjacent to the HBD is the **copper/metal binding domain (CuBD)**, which comprises the aminoacid residues 124-189 of APP and contains a single α-helix packed against a short triple-stranded β-sheet (Barnham et al, 2003). Three disulfide bonds and a small hydrophobic core stabilize the structure. This region can bind several metal ions (Bush et al. 1993).

A Zn^{2+}-binding site resides was identified within APP residues 181 to 200, at the border between the cysteine-rich and the acidic domain of APP. Whereas, a Cu^{2+}-binding site resides are located within APP residues 135 to 155. Zn^{2+} and Cu^{2+} binding influences APP conformation, stability and homophilic interactions (Hesse et al., 1994). In addition, the presence of Zn^{2+} increases the affinity of APP to bind to heparin and it potentiates the inhibition of Factor XIa activity by the KPI^{+}-APP isoforms (Komiyama et al., 1992). Furthermore, it has been suggested that Cu^{2+} binding and reduction may have important functions (Multhaup et al. 1996), participating in electron transfer reactions and thus contributing to aggregation and toxicity of Aβ amyloid (Hesse et al., 1994).

On the C-terminal side of the E1 domain is an **acidic region** that is rich in negatively charged amino acids, such as glutamic acid and aspartic acid residues. In addition, this region also contains a stretch of seven threonine residues (Kang et al. 1987). This unstructured and flexible acidic region connects E1 domain to the carbohydrate domain.

Another important functional region on the extracellular portion of the APP_{770} and APP_{751} isoforms is **the Kunitz proteinase inhibitor (KPI) domain** (Kitaguchi N. et al., 1988). The secreted KPI^{+}-APP are analogous to the cell-secreted proteinase inhibitor known as protease nexin-2 (PN2), which was first purified and characterized in 1987, prior to the known existence of AβPP. Then, it was shown to also inhibit trypsin and chymotrypsin (Van Nostrand W.E. et al., 1989). In addition, purified PN2/AßPP is a tight-binding inhibitor of several enzymes of the blood coagulation cascade including Factors XIa, IXa, Xa, and VIIa:tissue factor complex (Van Nostrand W.E. et al., 1990; Smith R.P. et al., 1990; Schmaier A.H. et al., 1993; Mahdi F. et al., 1995; Mahdi F. et al., 2000).

Importantly, KPI-containing isoforms APP_{770} and APP_{751} are highly expressed in platelets where they can influence wound repair by regulating blood clotting serine proteases (Van Nostrand et al. 1991b). As serine proteases are also implicated in neuronal cell growth (Wang and Reiser 2003), it is possible that KPI-containing APP isoforms regulate cell growth by inhibiting one or more of these proteases.

In addition, the APP_{770} isoform also presents the **Ox-2 antigen domain**. The Ox-2 domain in APP_{770} consists of 19 amino acids, whose role is less clear. The Ox-2 domain is similar to a region of the Ox-2 antigen that is a lymphoid and neuronal cell-surface glycoprotein, which has homology to Thy-1 and immunoglobulin light chains. Since immunoglobulin loop domains are commonly found in cell-surface receptors and are involved in cell-surface binding and recognition, it seems likely that the Ox-2 domain in APP has a similar function (Dawkins and Small, 2014).

The **carbohydrate region** can be divided into **E2 domain**, also known as central APP domain (**CAPPD**) and the **linker region**.

The **E2 domain** two distinct coiled-coil substructures composed of six α-helices in total (Wang and Ha, 2004). This α-helix rich region can readily dimerize and may therefore be involved in APP self-association.
In addition, the E2 domain contains a sequence of five amino acids, **RERMS** (aminoacid residues 328-332), uniquely required for the growth- promoting properties of APP (Ninomiya H. et al., 1993). Another interesting feature of the E2 domain is the heparan sulfate proteoglycan (HSPG)-binding site, which forms a groove on the surface (Multhaup 1994; Clarris et al. 1997), as well as a number of putative metal-binding sites that may hold the E2 domain in a rigid conformation (Dahms et al. 2012).

Dimerization of the E2 domain buries the hydrophobic surface cluster and also generates a better groove for the heparin-binding site.

Moreover, the **collagen binding peptide CBP1** was mapped to a conserved motif in the carbohydrate domain of E2 domain, corresponding to amino acid residues 448-465. APP interacts directly with the α1(I)CB6 fragment of collagen type I, independent from integrin-mediated adhesion. In particular, collagen binding is negatively regulated by heparin, suggesting that both molecules share the same binding site on collagen. In addition, the collagen binding is regulated by Zn^{2+} and Cu^{2+} (Beher et al., 1996).

Importantly, the carbohydrate domain of E2 domain is also involved in **APP-APP interactions**. APP may exist as a homodimer on the cell surface. Two highly conserved regions of APP, residues 91-111 and collagen binding site (residues 448-465) are of critical importance for the regulation of homo-oligomerization of full-length APP (Coulson, E. J., et al., 2000). The homodimer is stabilized as an inactive dimer by multiple dimerization interfaces. Dimerization would provide a potential mechanism for negative regulation of proposed APP functions and a concomitant increase of amyloid formation (Scheuermann S. et al., 2001).
Finally, it has been demonstrated that APP and APLPs (APLP1 and APLP2) specifically interact in a homophilic fashion and can form heterocomplexes (Soba et al., 2005).

The C-terminal side of the E2 domain contains the **Aβ region**, which lies on partly within the ectodomain and partly within the transmembrane domain.

Transmembrane domain

A GxxxG sequence motif within the **transmembrane domain** has been implicated in homodimerization (Munter et al. 2007) and in cholesterol binding (Barrett et al. 2012).

Intracellular domain

The cytoplasmic domain of APP (referred to as the APP intracellular domain, or AICD) comprises about 47 amino acid residues (Zheng and Koo, 2011). The **intracellular domain** of APP is highly conserved among APP family members predicting that it is a critical domain mediating APP function. Indeed, this relatively short cytoplasmic domain contains one well described phosphorylation site as well as

multiple functional motifs and multiple binding partners that contribute to trafficking, metabolism and possibly cell signalling functions of APP.

The cytoplasmic region of APP (amino acid residues 657-676 of the APP_{695} isoform) shows a specific binding site for Goα protein, a major GTP-binding protein in brain. APP forms a complex with Go and is necessary for complex formation, providing evidence that APP functions as a receptor coupled to Go through this Go-activating cytoplasmic domain (Nishimoto et al., 1993).

Importantly, the intracellular domain of APP contains a YENPTY sorting motif located between residues 682-687 of the APP_{695} isoform. Several studies have demonstrated that the YENPTY motif is involved in the regulation of APP trafficking and is important for clathrin-mediated endocytosis and binding to numerous proteins including Fe65, JIP and X11/Mint (De Stroopper and Annaert, 2000). In particular, the phosphorylation of Tyr682 is required to interact with various adaptor proteins, including Mint-1/X11a, Fe65 and c-Jun N-terminal kinase.

Another important phosphorylation site in the APP intracellular domain is located in the threonine 668 residue within the VTPEER motif (amino acids residues 667-672). Several kinases have been implicated in this phosphorylation event, including cyclin-dependent kinase 5 (CDK5), c-Jun N-terminal kinase 1 (JNK1) and JNK3, CDK1/CDC2 kinase and GSK3b (Iijima, et al., 2000; Kimberly et al., 2005; Muresan and Muresan, 2005; Scheinfeld et al., 2003). Phosphorylation at this residue has been reported to regulate APP localization to the growth cones and neurites (Ando et al., 1999) and to contribute to Aβ generation, a finding consistent with an increase of Thr668 phosphorylated APP fragments in brains of AD individuals (Lee M.S. 2003). In addition, threonine668 phosphorylation leads to resistance of APP to be cleaved by caspases, an event that has been proposed to result in increased vulnerability to neuronal death.

Thus, phosphorylation of the AICD might regulate multiple signalling pathways ranging from phosphoinositide-mediated calcium signalling (Leissring et al, 2002) and apoptosis (Passer et al, 2000) to gene transcription regulation (Kimberly et al., 2001; Walsh et al., 2003; von Rotz et al., 2004).

APP metabolism

APP can be proteolytically processed by specific proteases, termed α-, β- and γ- secretases which cleave APP in different sites. APP ectodomain can be shed from the membrane by two alternative cleavages: α- secretase cleavage splits Aβ domain

and precludes Aβ formation, whereas β-secretase cleavage exposes the amino-terminus of the Aβ peptide. α- and β-secretases shedding of APP leads to the production of a membrane-anchored carboxy terminal fragment (CTFα/β) and to the extracellular release of the large soluble APP fragment (sAPPα/ β).

Therefore, two different metabolic pathways of APP have been identified depending on the type of secretase involved: non-amyloidogenic pathway (α- γ) and amyloidogenic pathway (β- γ). These two pathways are mutually exclusive.

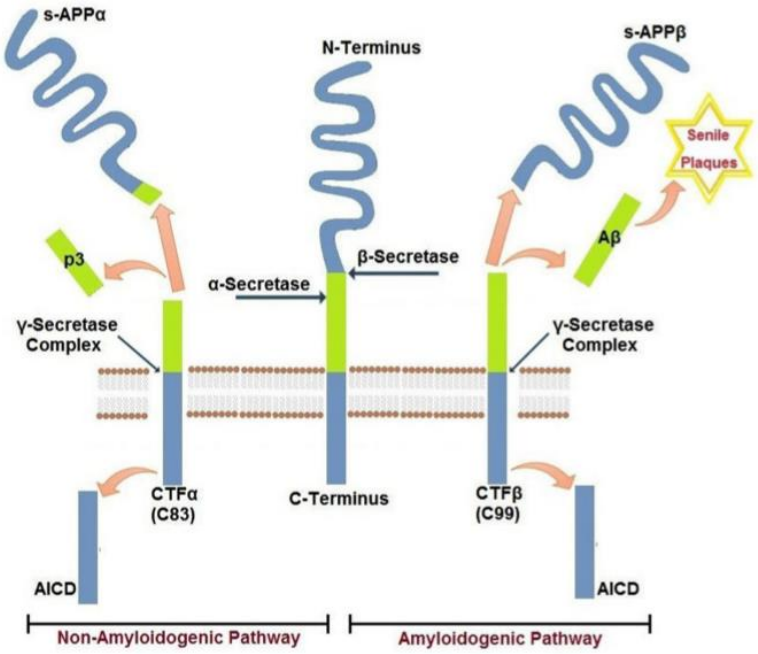

Figure 7 APP metabolism (from Canobbio et al., 2015).

Non-amyloidogenic pathway

In most peripheral cells and in platelets, APP is processed through the non-amyloidogenic pathway. In this case the proteolytic cleavage of APP is performed by α- secretase, that cleaves between Lys 16 and Leu 17 (aminoacids residues 612 and 613 of APP) within the Aβ sequence, precluding the generation of Aβ peptide (Allison et al., 2003). Cleavage within Aβ sequence of APP by α- secretase generates soluble amino terminal fragments of 100-130 kDa termed soluble amyloid precursor protein α(sAPPα) and an 83 amino acids, membrane associated C-terminal fragment, termed

CTF83, which is about 10kDa and consists of the C-terminal portion of Aβ and APP cytosolic domain (Esch et al., 1990).

sAPPα generated by α- secretase cleavage of APP might have neurotrophic and neuroprotective functions and, in the case of sAPPα containing the Kunitz proteinase inhibitor domain, they may potentially regulate blood coagulation.

The non-amyloidogenic pathway takes place in the secretory pathway, at the plasma membrane and in secretory vesicles. In addition, protein kinase C activation stimulates sAPPα production by mechanisms involving the formation and release of secretory vesicles from TGN (trans-Golgi network), thus enhancing trafficking to cell surface (Thinekoran and Koo, 2008). The non-amyloidogenic pathway involves α-secretase enzymes that belong to the family of ADAM proteinases (a disintegrin and metalloproteinase). Some members of the ADAM family have been identified as critical in several physiological and pathological processed ranging from cell growth, adhesion, migration and signalling. ADAM 9, ADAM10 and ADAM17 are, for instance, three members of ADAMs family that can cleave APP at the α-secretase site. ADAM9 (MDC9 or meltrin gamma) possesses an α-secretase-like activity, and although physiologically it was not able to cleave APP, ADAM9 might have a role in APP processing in particular conditions and cell types. ADAM10 mediates proteolysis of Notch, Eph/ephrin, or classic cadherins, which is a pre-requisite for their proper function (Marambaud and Robakis 2005). ADAM17 also known as TACE (Tumor necrosis factor-α converting enzyme) plays a role the proteolytic activation of TNF-α and epidermal growth factor (EGF) receptor ligands, which are regulators of several fundamental functions, such as inflammation or cell growth during development or cancer (Blobel 2005). ADAM17 is considered to be responsible in large part for the regulated α-secretase proteolysis of APP.

Besides ADAM9, ADAM10 and ADAM17, other ADAM members have been suggested to possess α-secretase-like activity toward APP. The mechanisms of regulation of α-secretase cleavage involve complex and indirect mechanisms of signal transduction or protein maturation and trafficking of the different ADAMs involved.

Amyloidogenic pathway

APP can be processed by the alternative amyloidogenic pathway (Seubert et al 1993) that is predominant in neuronal cells. This alternative pathway involves cleavage of APP at the amino terminus of Aβ domain by a protease termed β-secretase. β-secretase cleavage produces the soluble N-terminal fragment, sAPPβ,

and the remaining 99 amino acid membrane tethered C-terminal fragment (CTF99), which is further processed by γ-secretase to release Aβ and AICD peptides (Evin et al., 2002).

The membrane-bound aspartyl protease beta-site APP cleaving enzyme (BACE)-1 with β-secretase activity represents the major neuronal β-secretase (Vassar et al., 2004). Cleavage by BACE1 occurs in two different positions in APP: the classical β-secretase-clipping site is in the Asp1 that generates the N-terminus of Aβ , the other site is the β′-cleavage site, within the Aβ domain between Tyr10 and Glu11, which releases a shorter form of Aβ peptide (Gouras et al.,1998). The functional significance of these two variable cleavage sites and their relative pathological impact remains largely unknown. The preference of the protease for either β- or β′- cleavage sites was strongly dependent on intracellular localization. Within the endoplasmic reticulum, β-site proteolysis predominated, whereas in the trans-Golgi network, β′- cleavage was preferential (Huse et al., 2002).

Another member of this family of membrane bound aspartyl proteases is BACE-2, the homologue of BACE-1. While BACE-1 is highly expressed in neurons, BACE-2 expression is low in the central nervous system, but higher in peripheral tissues including pancreas, placenta and stomach (Vassar and Citron, 2000). The role BACE-2 in amyloidogenesis is less clear. Indeed, BACE-2 cleaves βAPP between Phe19 and Phe20 within the Aβ domain, close to the α-secretase site increasing the secretion of an APPs-α-like variants (Fluhrer et al., 2002).

γ-secretase activity is contained within a molecular complex formed by the association of four essential subunits: presenilin-1 or -2 (either PS1 or PS2), nicastrin, presenilin-enhancer-2 (PEN-2) and anterior-pharynx-defective 1 (APH-1) (Iwatsubo, 2004). The presenilins are ubiquitously expressed and represent the catalytic subunits of γ- secretase, whereas the other subunits help to stabilize the complex and to recruit the substrates to be cleaved.

The β-carboxyl-terminal fragment CTF β from APP is cleaved by γ-secretase generating both Aβ peptides via γ-cleavage and also APP intracellular domain (AICD) via ε-cleavage (Sato et al., 2005).

Aβ peptides generated range in length from 38 to 43 residues (Selkoe et al., 2007) depending on where the cleavage occurs, therefore producing different kinds of Aβ peptide. If γ-secretase cleaves APP after the Val40 there will be the production of the soluble $A\beta_{1-40}$, which is the most common species; while, if the cleavage site is

following Ala42 there will be the production of $A\beta_{1-42}$, the less abundant but more aggregating species.

Moreover, the γ-secretase also cleaves after Leu49 to release the APP intracellular domain, termed AICD, in the cytosol, then this fragment can diffuse to the nucleus to activate signal transduction.

In conclusion, a plethora of other γ- secretase substrates have been identified, including Erb-B4, E and N-cadherins, CD44, the low-density lipoprotein receptor, Nectin-1, and the Notch ligands Delta and Jagged. In addition to APP, γ- secretase appears to play an important role in Notch signalling and Ire1p signalling, where control the release of the intracellular domains of these proteins (De Stropper and Annaert, 2000).

APP functions

The structural multi-domain function of APP suggests that it may have different biological functions. APP may act as a cell-surface receptor or as a growth factor. APP has been reported to influence cell proliferation, differentiation, neurite outgrowth, cell adhesion and synaptogenesis.

Indeed, APP is co-ordinately expressed in neuroblasts and neurons at the time of cell proliferation and differentiation, this has led to the idea that APP may play a role in the regulation of stem-cell proliferation or differentiation. It has been demonstrated that APP is able to stimulate the proliferation of neural stem or progenitor cells (NSPCs). In addition, APP can promote neurite outgrowth in cell culture (Small et al., 1994). APP expression is upregulated rapidly in axons in response to axonal injury, possibly as part of a repair mechanism. One possible mechanism by which APP promotes neurite outgrowth is by regulating cell-substrate adhesion.

APP is reported to bind to laminin, collagen type I and heparan sulphate, all of which can influence neurite outgrowth. APP may also promote cell-cell adhesion. Then, during development, APP is expressed in both pre- and postsynaptic sites and its level is dramatically increased during the critical period of synaptogenesis.

In particular, skeletal muscle APP may well play a role in the differentiation of skeletal muscle and in the formation and maturation of neuromuscular junctions. These data suggest that APP may also be involved in the regulation of synaptogenesis (Akaaboune et al., 2000).

APP has been proposed to be capable to form homo- and hetero- complexes, a process that could promote cell adhesion properties of APP/APLPs (Soba et al., 2005). The homo and hetero- dimerization processes together with the presence of binding site for heparin, collagen, laminin and proteoglycans within APP structure support the hypothesis that it may be involved in adhesion processes. Moreover, several studies suggest that APP may interact with integrins to mediate neurite outgrowth. APP contains the sequence RHDS within the Aβ region (corresponding to amino acid residues 601-604 of APP_{695}) that might interact integrin-like surface receptors modulating cell-cell or cell-matrix interactions (Ghiso et al., 1992). In addition, APP and integrins (α_5, α_1 and β_1) co-localize in developing neurons in both growth cones and along axons (Yamazaki et al., 1997).

Secreted forms of APP comprise almost the entire extracellular domain containing the KPI domain and have been identified as protease nexin II (PN2), a serine-proteinase inhibitor (Van Nostrand et al., 1989). It has been demonstrated that PN2/APP is a potent inhibitor of several proteinases involved in blood coagulation including Factors XIa, IXa, Xa, and the VIIa:tissue factor complex (van Nostrand et al., 1990). Moreover, the predominant forms of APP in blood contain the KPI domain. This finding suggest that APP may play a role in the regulation of blood coagulation (Xu et al., 2017).

Therefore, several evidences indicate that APP controls cholesterol turnover needed for neuronal activity (Pierrot et al., 2013). APP proteolytic processing not only regulates lipid metabolism (Grimm et al, 2012) but also synaptic transmission and ion channel function (Dawson et al, 1999). Indeed, another important function of APP is to maintain neuronal calcium homeostasis, which is essential for synaptic transmission (Berridge 1998).

Finally, APP is involved in the regulation of gene expression. For example, the intracellular domain of APP (AICD) forms part of a transcriptional complex involving the nuclear mediator component MED12 along with the histone acetyltransferase Tip60 and Fe65 protein (Turner et al. 2011; Müller et al. 2013). Hence, AICD acts as a key epigenetic controlling regulator of gene expression of several genes, including EGFR, GSK3 β, the amyloid-degrading enzyme neprilysin, aquaporin-1, and APP itself (Octave et al., 2013).

APP AND PLATELETS

Among the different peripheral cells expressing APP, platelets are the second source of APP after neurons, thus representing the most important peripheral source of APP (Van Nostrand et al., 1990). Platelets produce up to 90% of the Aβ peptides in circulation (Li et al, 1998).

Platelet APP is encoded by mRNA that is synthesized by the platelet precursor, the megakaryocyte, in the bone marrow (Bush et al, 1990). The two major APP isoforms expressed in human platelets are APP770 and APP_{751}, which contain the Kunitz-type protease inhibitor domain KPI. Moreover, platelets express all the required enzymatic activities (α, β- and γ- secretases) and are able to produce all APP fragments similar to those identified in neurons: sAPPα and sAPPβ soluble isoforms, and CTF83 and CTF99 fragments and Aβ peptides (Li et al., 1998).

Non amyloidogenic/α- secretase cleavage is the predominant pathway for APP processing in platelets, as the levels of sAPPα levels detected are much higher than those of Aβ (Li et al., 1998) Calmodulin stimulates the proteolysis of platelet APP by the non-amyloidogenic pathway, and is a key regulator of APP processing by α-secretase (Canobbio et al., 2011).

Platelet APP can be also metabolized through the amyloidogenic pathway mostly in pathological conditions (Catricalá et al.,2012)

The main species of Aβ released from activated human platelets in pathological condition is $Aβ_{1-40}$, while the predominant form in neuronal plaques is $Aβ_{1-42}$. Immunoassay analysis has revealed that the inactivated platelets had an average of 84 ng/g tissue of $Aβ_{1-40}$ and activated platelets contained an average of 57 ng/g tissue, while in both cases there were very low levels $Aβ_{1-42}$: 1.6 ng/g tissue and 1.7 ng/g tissue, respectively (Kokjohn et al., 2011).

Approximately 10% of platelet APP is associated with the membrane and among this pool of APP there are two different types: full length APP ($APPFL\text{-}KPI^{+}$) and carboxyl-terminal truncated membrane-associated APP ($APPMem\text{-}KPI^{+}$) (Li et al., 1994). The remaining 90% of APP is metabolized by secretases and stored as soluble APP (sAPPα/β) and Aβ peptides in α-granules. Upon platelets activation with thrombin, collagen and other agonists granules are released and sAPPα/β and Aβ peptides are exocytated in the circulation.

Physiological role of APP in platelets.

The physiological role of APP and its metabolites in platelets is not yet well understood. The high expression of APP in the platelets, with a total number of 9300 copies/platelet (Burkhart et al., 2012), together with the presence of KPI domain-containing isoforms indicate that it may have an important physiological role in events associated with coagulation.

A breach of the vascular endothelial wall starts a cascade of events which include the activation and aggregation of circulating platelets and the release of the glycoprotein contents of their α-granules. The proteins released by the platelets include substrates for the coagulation cascade and numerous growth factors, and thus platelets not only locally repair the defect but also promote reparative tissue. It has been shown, indeed, that activation of platelets by thrombin increases the surface expression of APP up to threefold, suggesting that APP-KPI$^+$ may regulate haemostatic protease inhibitory activity on the platelet surface. The full-length APP may act as a receptor on the platelet surface, thanks to the cysteine-rich domain that can be proteolytically cleaved by cysteine protease during platelet activation (Li et al., 1998). Then, the released soluble APP (sAPP) isoforms may participate to the coagulation cascade by inhibiting activated coagulation pathway enzymes through their KPI domain. It has been shown that sAPP-KPI$^+$ inhibit the activity of the blood coagulation Factors IXa, XIa, and Xa, and, to a lesser extent, of factor VIIa-tissues factor complex (Van Nostrand et al., 1989), thus modulating haemostasis following vascular injury by limiting thrombosis.

In vivo the physiological role of APP has been investigated though the generation of transgenic mice overexpressing APP either in platelets under control of the rat platelet factor 4 promoter (Tg-rPF4/APP) or in neurons under control of the mouse Thy1 promoter (Tg-Thy1/APP). These studies found reduced thrombosis in vivo, suggesting that APP may contribute to the severity of the haemorrhage causing inhibition of prothrombotic proteinases and further bleeding.

Xu and co-workers examined the antithrombotic function of cerebral secreted isoforms of amyloid β-protein precursor (AβPP) that contain the Kunitz proteinase inhibitor domain, also known as proteinase nexin-2 (PN2). They investigated the PN2/AβPP function comparing transgenic mice with specific and modest overexpression of PN2/AβPP in brain and in platelets. They found that, in a strain of transgenic mice overexpressing the APP/PN2, the thrombotic capacity is reduced and the extent of cerebral hemorrhage is increased accordingly (Xu et al., 2005; Xu et al., 2007).

In addition, these studies indicate that when cerebral vessel rupture occurs modest increases in brain parenchymal PN2/AβPP can significantly reduce thrombosis and increase the severity of haemorrhage (Xu et al., 2007).

Aβ peptides in platelets

The inhibitory role of APP appears to be in direct contrast to the Aβ effects on platelet function. Indeed, Aβ has been shown to augment platelet aggregation and support platelet adhesion (Wolozin et al., 1998; Canobbio et al 2013).

Once $A\beta_{1-40}$ is released from activated platelets it can in turn activate platelets through specific signaling pathway (Shen et al., 2008). Studying the role of misfolded proteins, Herzenik and his coworkers shown that proteins with amyloid properties have also platelets activation properties. They used $A\beta_{1-40}$ peptide and observed the capacity of amyloid to activate platelets, which might underlie the development of atherothrombosis observed in disease known to be associated with formation of amyloid or fibrils (Herznik at al., 2007).

In particular, the synthetic undecapeptide $A\beta_{25-35}$ has been very useful to investigate the pathophysiological properties of Aβ in platelets. $A\beta_{25-35}$ is located in the intermembrane domain of APP (Kang et al. 1987) and it retains both physical and biological properties of the full-length APP (Kaminsky et al., 2009). In fact, it has been proposed that $A\beta_{25-35}$ represents the biologically active region of Aβ and it has the ability to form oxygen radicals, nitric oxide and to disrupt calcium homeostasis as $A\beta_{1-42}$.

They found that $A\beta_{25-35}$ potentiated agonist-induced platelet aggregation, and at higher concentrations (2-10μM) $A\beta_{25-35}$ itself directly activated the aggregatory responses (Shen et al., 2008). $A\beta_{25-35}$ activated platelet through the activation of the thrombin receptor PAR1 and activation of p38 MAPK pathway, which results in the stimulation of cytosolic phospholipase A2 (cPLA2) that catalyses the release of arachidonic acid (AA) for TXA_2 synthesis. TXA_2 augments the activation of platelets and the consequent secretion of $A\beta_{1-40}$, which initiates a vicious cycle of platelets activation and $A\beta_{1-40}$ overproduction (Shen et al., 2008). Thus, association of platelet activation and Aβ overproduction may represent a mechanism through which Aβ deposition in the walls of cerebral vessels leads to cerebral amyloid angiopathy (CAA) during AD.

In addition, Aβ-induced platelet aggregation involves PLCγ2 activation, through PKC activation (Shen et al., 2008). Furthermore, Sonkar and his colleagues have demonstrated that Aβ induces platelet activation through the activation of small

GTPase RhoA, which leads to cytoskeletal reorganization and the activation of specific cellular responses, such as aggregation, shape change, granule release and clot retraction (Sonkar et al., 2014).

More recently Gowert et al., have demonstrated platelet-released amyloid peptides contribute to aggregation and thrombus formation in cerebral vasculature thus contributing to cerebral amyloid angiopathy CAA (Gowert et al., 2014). The ability of Aβ to induce platelet activation may account for the haemostatic abnormalities observed in AD as well as in the pathogenesis of CAA. In fact, high local Aβ concentration may be detected in plasma after the Aβ release from stimulated platelets at the site of thrombus formation, and at the site of CAA and atherosclerotic plaques, thus initiating an endless cycle of platelet stimulation and further Aβ release (Sonkar et al., 2014). In another study, Aβ-induced platelet activation is principally triggered by Ca^{2+} dependent release of ADP (Canobbio et al., 2015).

Finally, it has been shown that human platelets are able to adhere and spread over immobilized Aβ peptides, and that the presence of Aβ peptides fasten deposition of platelets on subendothelial matrices (collagen). Adherent platelets activate several intracellular signalling pathways associated with platelet stimulation. These evidences suggest that deposits of Aβ peptides which are present in blood vessels wall of AD patients' lesions can reinforce platelet adhesion and activation at the site of injury, contributing to further inflammation and degeneration, and the initiation of thrombus formation (Canobbio et al., 2013).

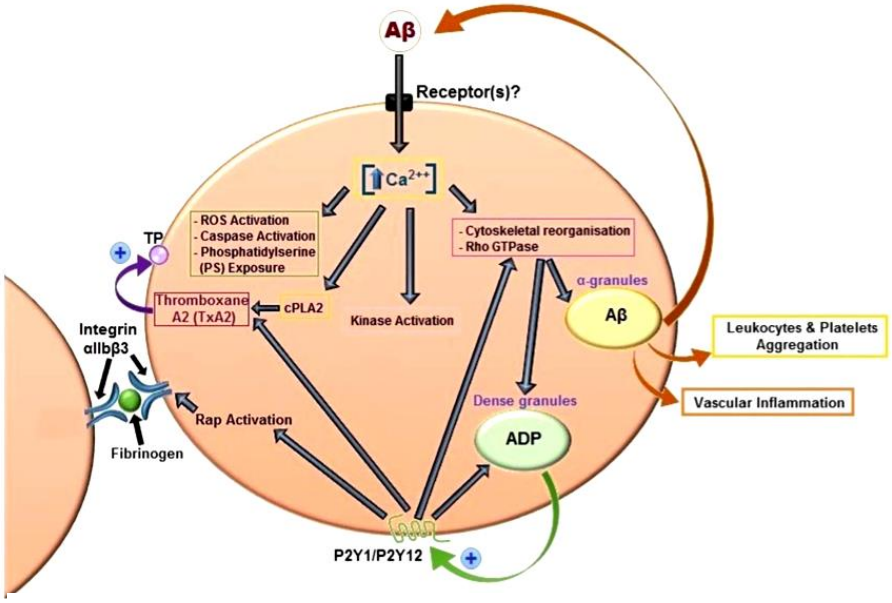

Fig. 8. Aβ peptide-induced platelet activation (from Canobbio et al., 2015).

Platelets, vascular disease and inflammation.

In haemostasis, platelets circulate in close contact with the endothelial cell lining of the vessel wall without adhering to it. Under pathological conditions, however, platelets respond rapidly to alterations of endothelial cells (e.g. fatty streak formation or plaque rupture) and to exposure of subendothelial structures by attaching firmly to the site of the lesion. Platelet aggregates subsequently form and are associated with cardiovascular ischaemic events (Willoughby et al., 2002). Furthermore, there is evidence demonstrating a platelet hyperaggregable state in subjects who have various risk factors that are associated with atherosclerosis/coronary artery disease, including diabetes mellitus, hypercholesterolaemia, hypertension and smoking.

Platelets are major players in vascular diseases associated with AD, such as atherosclerosis and stroke (Gawaz et al., 2005). In addition, recently, increasing evidence suggests that platelet activation can also mediate the onset and development of CAA. First, platelet activation and adhesion to a vessel wall is the initial step of vascular injury. Activated platelets contribute to more than 90% circulating Aβ (mainly $A\beta_{1-40}$), which in turn activates platelets and results in the vicious cycle of Aβ overproduction in damaged vessel. Second, the uncontrolled activation of platelets leads to a chronic inflammatory reaction by secretion of chemokines, interleukins, prostaglandins, and CD40 ligand. The interaction of these biological response modulators with platelets, endothelial cells and leukocytes establishes a localized inflammatory response that contributes to CAA formation.

The blood flow alterations induced by CAA or AD-related vascular diseases with consecutively hypoperfusion induced by vessel occlusion indicate a second effect of Aβ in the brain besides its neurotoxic effect (Thal et al., 2008). Aβ peptides are intimately involved in the inflammatory pathology of atherosclerotic vascular disease (AVD) and Alzheimer's disease (AD). The fact that the main species of Aβ released from the activated human platelets is $A\beta_{1-40}$ is supported to the observation that $A\beta_{1-40}$ is the primary component of the vascular amyloid deposits. Two theories have been proposed to explain the origin of Aβ peptide in the blood. The first one suggests that circulating Aβ could derive from the central nervous system and further absorbed by blood cells, mostly platelets, but also lymphocytes and monocytes. The second theory suggests that there is an additional release of Aβ from the blood cells and from other non neuronal cells.

Besides their normal function in haemostasis, platelets play an important role in inflammatory processes. Moreover, inflammatory reaction is in turn important in

the pathogenesis of AD, in fact it represents an important risk factor for AD occurrence. Platelet activation and consequent degranulation can result in the secretion of numerous potent inflammatory signalling molecules that are stored in platelet α-granules. Among these biological mediators secreted by platelets there are chemokines, such as platelet factor 4 (PF4), regulated upon activation normal T-cell expressed and presumably secreted (RANTES), macrophage inflammatory protein (MIP)-1α interleukins (IL-1β, IL-7, and IL-8), prostaglandins and CD40 ligand (CD40L). In addition, various proteins of the complement system interact specifically with platelets, activate them and promote inflammation and thrombosis. The direct products of complement activation, the membrane attack complex C5b-9, and the anaphylotoxins C3a and C5a, have been shown to activate platelets. A reciprocal interaction also exists, whereby activated platelets can initiate the complement cascade (Del Conde et al. 2005). The uncontrolled activation of platelets present in AD, results in a chronic inflammatory reaction that can induce endothelial cell stress. This, in turn, determines further platelet activation creating a vicious circle that causes increased inflammation and release of Aβ. Moreover, during a chronic inflammatory reaction the interaction of these biological response modulators with platelets, endothelial cells and leukocytes establishes a localized inflammatory response that contributes to CAA formation (Zhang et al., 2013).

Platelet abnormalities in Alzheimer's disease.

There is no doubt that platelet APP processing in AD patients is altered compared to the normal control subjects.

It has been demonstrated that AD patients have **altered APP ratio**, with significant alteration of the immunoreactivity of the APP isoforms in platelets (Borroni et al. 2005; Borroni et al. 2010). The difference in molecular mass between the 130 kDa and the 106-110 kDa isoforms has been attributed to the presence or absence of KPI. Recent studies performed on platelets obtained from patients affected by sporadic AD established a decrease of the level of 130 kDa band, when compared to platelet prepared from control subjects and patients affected by other kind of dementia (Di Luca et al., 2000). This APP altered level in platelet shows a positive correlation to the progression of the disease. The declining ratio of APP isoforms in platelets may result from increased release of the 130 kDa species in plasma during platelet activation. This alteration is present also in preclinical stages of AD and correlates with disease severity, suggesting that it can be considered as a useful biomarker for AD progression.

Platelets from AD patients show alteration in membrane fluidity (Davies et al., 1988), cytoskeletal abnormalities, cytochrome oxidase deficiency, abnormal glutamate transportes activity, decreased phospholipase C activity, and increased cytosolic protein kinase C levels (Matsushima et al., 1994, 1995). Moreover, serotonin levels in platelets of AD patients are significantly reduced. Cholesterol and ganglioside GM1 content of lipid rafts from platelets was significantly higher in patients with AD than aged-matched control subjects. Additional data suggest that increased membrane cholesterol found in AD can result in increased Aβ-secretase activity which can generate more $A\beta_{1\text{-}40}$.

Many studies have indicated that AD patients have **altered platelet functions**. Alterations in the pattern of platelet activation have been reported in AD (Sevush et al., 1998), demonstrating that platelets of patients with AD exhibit greater unstimulated activation than those of controls possibly due to stimulation of platelets by damaged endothelial cells or to platelet membrane abnormalities (Borroni et al., 2002). Another potential source of platelet activation could be Aβ peptide itself, that seem to activate and potentiate platelet aggregation.

Atypical metabolism of precursor protein has been shown in **coated-platelets**. Coated-platelets are a subset of activated platelets observed upon dual-agonist stimulation with collagen and thrombin. In contrast to platelets activated with a single agonist, coated-platelets retain full-length APP on their surface upon activation. These platelets are elevated in patients with amnestic as compared to non amnestic mild cognitive impairment (MCI), and correlate with disease progression in Alzheimer disease (AD) (Prodan et al. 2009). Coated-platelet synthesis is associated with an altered metabolism of APP characterized by retention and derivatization of full-length APP on the surface of these activated cells. This alteration is not present in platelets activated with a single agonist. Although the exact mechanism for retention of APP remains unclear, a covalent alteration of APP appears to be involved with formation of coated-platelets. Recently, it has been demonstrated a correlation between initial coated-platelet levels and the rate of AD progression, with the most severe decline noted in individuals with the highest initial coated-platelet production. In addition, recent studies showed abnormal coated-platelet synthesis in patients with cerebrovascular disease, with elevated coated-platelet levels in patients with non-lacunar ischemic stroke and decreased coated-platelet levels in patients with spontaneous intracerebral haemorrhage. Finally, limited studies have indicated that coated-platelets are potentiated by inflammation. Perhaps coated-platelet synthesis represents a sensitive biomarker of the disease process that includes APP

abnormalities, cerebrovascular disease, and inflammatory components (Prodan et al., 2009).

Platelets play a central role in pathological thrombus formation, which is an important risk factor for AD occurrence. In addition, cardiovascular risk factors and atherosclerosis, frequently present in AD, could influence platelet function in AD patients. The uncontrolled activation of platelets could result in an excessive Aβ production and thus may contribute to the pathogenesis of AD (Casoli et al., 2010).

Platelets as peripheral biomarker for AD

The diagnosis of AD is based on clinical assessments, confirmed post-mortem by the presence of typical neuropathological lesions. In the last decade, different biochemical parameters, assessed in biological fluids, have been proposed as possible markers for AD, most of them have been evaluated in the cerebrospinal fluid (CSF) and in plasma. Nevertheless, the results obtained by different authors are controversial, and in general, the measurements of Aβ in plasma have so far provided inconsistent results (Blennow et al., 2010).

However, it has been postulated that platelets represent a useful peripheral model to study changes in APP expression and processing both in physiological and pathological conditions, since they express APP and metabolize it as it occurs in neurons (Di Luca et al., 2000). Moreover, studies have shown that platelets may also be used as peripheral models for the analysis of metabolic pathways related to the pathogenesis of AD, in particular to the amyloid cascade and the regulation of oxidative stress.

Based on the observations that the majority of full length APP and its metabolites found in blood plasma may derive from platelets, platelet provide an easily accessible source of human material to study pathogenic mechanism related to AD.

Furthermore, evidence suggesting that vascular risk factors and vascular pathology play a role in the onset and progression of AD, together with the knowledge that platelets are important in the development of atherosclerosis and vascular events and their altered functions in AD, support the hypothesis that there is a positive association between the degree of platelet activation and the risk for progression of AD in patient with MCI, and progression of the rate of cognitive decline in AD patients.

MATERIALS AND METHODS

MATERIALS

Fluoresceinisothiocyanate-conjugatedanti-CD41and peridinin chlorophyll protein complex–conjugated anti-CD45 were from Biolegend. Antibodies against P-selectin, GPVI, GPV, CD42b, CD41, CD49b, AlexaFluor488-conjugated anti-GPIX (clone Xia.B4), and phycoerythrin-conjugated anti-GPIba (clone Xia. G5) were from Emfret Analytics. Fluorescein isothiocyanate-fibrinogen was from Molecular Probes. Thrombin, the thromboxane A2 analogue U46619, PGE1, apyrase, $A\beta_{25-35}$ (GSNKGAIIGLM), bovine serum albumin, TRITC-conjugated phalloidin, fibrinogen and CFSE were purchased from Sigma-Aldrich. $A\beta_{1-40}$ (DAEFRHDSGYEVHHQKLVFFAEDVGSNKGAIIGLMVGGVV) and $A\beta_{1-42}$ (DAE FRHDSGYE VHHQKLVFFAEDVGSNKGAIIGLMVGGVVIA) were kindly provided by Prof. Giordano Pula from University of Exterer, UK. Bicinchoninic acid assay was from Thermo Fisher. Enhanced chemiluminescence (ECL) substrate was from Millipore. Convulxin was provided by Dr K. J. Clemetson (Theodore Kocher Institute, University of Berne, Switzerland). Collagen type I was kindly provided by Prof. M. E. Tira (University of Pavia, Italy). Von Willebrand factor (Koate) was from Bayer. Stromatol was from Mascia Brunelli.

The monoclonal anti-tubulin (DM1A) was from Santa Cruz Biotechnology. Antibodies against APP: 22C11 and 6E10 were Chemicon, and Covance, respectively. Anti-phospho Pyk2(Y402), anti-phospho Akt(S473), anti-phospho p38MAPK(T180-Y182) and anti-phospho MLC(S19) were from Cell Signaling Technology. Antibody against citrullinate histone H3 (cit-H3) was from Abcam, and anti-cathelicidin-related antimicrobial peptide (CRAMP) antibody was from Innovagen.

Reagents for activated partial thromboplastin time (APTT), prothrombin time (PT), fibrinogen, and coagulation factors were from Instrumentation Laboratories. All other reagents were from Sigma Aldrich.

Mouse models

3xTg-AD mice were kindly provided by Dr. Dimtry Lim (University of Piemonte Orientale, Italy) and were generated as described elsewhere (Oddo et al.,

2003). 3xTg-AD mice were used at 18 months of age and age-matched wild type B6129SF2 served as control. All mice will be housed in groups of 4 same sex littermates in plastic cages in specific rooms at the animal care facilities under controlled conditions (temperature 21-23°C, humidity 50-60% and a 12:12 light/dark cycle). Health conditions of the mice are periodically controlled by veterinary and by blood screening.

APP KO mice in a C57BL/6J background were generated as described previously (Müller et al., 1994) and kindly provided by U. Müller (University Heidelberg, Germany). APP KO mice used were 4 to 6 months of age (average weight, 25-30g) and balanced for sex distribution. Age-matched C57BL/6J wild-type (WT) mice were used as control. All mice were bred as homozygous lines and were maintained with a 12:12-h light/dark cycle and had free access to food and water.

The table shows buffers utilized in this study.

Buffer:	**Composition:**
ACD	130 mM Sodium Citrate, 152 mM Citric Acid, 112 mM Glucose
PIPES	20 mM PIPES, 136 mM NaCl, pH 6.5
HEPES Buffer	10 mM HEPES, 137 mM NaCl, 2.9 mM KCl, 12 mM $NaHCO_3$, pH 7.4
Ripa Buffer + inhibitors	50 mM Tris/HCl, 200 mM NaCl, 2.5 mM $MgCl_2$, 1% Nonidet-P, 10% glycerol, 2 mM PMSF, 100 µg/ml leupeptin, 100 µg/ml aprotinin, 2 mM NaF, 2 mM Na_3VO_4, pH 7.4
Hank's Buffer	137 mM NaCl, 5.4 mM KCl, 4.5 mM KH_2PO_4, 5.5 mM D-Glucose, 0.34 mM Na_2HPO_4, 4.2 mM $NaHCO_3$, pH 7.4
Red Blood Cells Lysis Buffer	0.1 mM EDTA, 0.1 mM $KHCO_3$, 154.42 mM NH_4Cl
PBS 1X	8 mM Na_2HPO_4, 2 mM NaH_2PO_4, 140 mM NaCl, pH 7.4
HEPES Flow Buffer	2 mM $CaCl_2$, 2 mM $MgCl_2$, 5.5 mM Glucose, 0.1 % BSA, 1 U/mL Heparin in HEPES Buffer, pH 7.4, 37°C
Running Buffer	25 mM Tris-HCl pH 8.3, 192 mM Glycine, 0.1 % (w/v) SDS
Transfer Buffer	48 mM Tris, 39 mM Glycine, 1.3 mM SDS, 10 % (w/v) Methanol
Sample Buffer 3X	25 mM Tris, 192 mM Glycine, 6% SDS (w/v), 1.5 % Dithiothreitol, 30 % Glycerol, 0.03 % Bromophenol blue, 3 % (v/v) 2-β-mercaptoethanol, pH 8.3
SDS Sample Buffer 1X	12.5 mM Tris, 96 mM Glycine, 2 % SDS, 0.5 % dithiothreitol, 10 % Glycerol, 0.01 % bromophenol blue, 1 % β-mercaptoethanol, pH 8.3

METHODS

1. Preparation of murine platelets

Mice were anaesthetized with xylazine (5 mg/kg, i.p.) and ketamine (50 mg/kg, i.p.).

Whole blood was collected from inferior vena cava and was anticoagulated with citric acid/citrate/dextrose (ACD) and sodium citrate 3.8%, at the ratio 2:1. The blood was diluted with HEPES buffer and centrifuged at room temperature (20°C-25°C) using an ALC-PK130 centrifuge with a swinging-bucket rotor ALC-T535 at 180g for 10 minutes to obtain platelet-rich-plasma (PRP). PRP was then transferred to new tubes and the remaining red blood cells were diluted with HEPES buffer to a final volume of 2 ml and centrifuged again at 180 g for 7 min. PRP was collected and this step was repeated. The upper phase was added to the previously collected PRP, and 0.02 U/ml Apyrase I plus 1 μM prostaglandin E1 (PGE_1) were added before centrifugation at 550 g for 10 min. The apyrase I degrades ADP secreted by platelets, which being a platelet agonist could stimulate aggregation; while PGE_1 is a prostaglandin that inhibits platelet activation. Now the platelets are deposited on the bottom of the tube. Once separated from platelet-poor plasma (PPP), the platelet pellet was resuspended in 1 ml of PIPES buffer and then the sample was centrifuged at 550g for 8 minutes. The supernatant was again removed, and platelets were finally gently resuspended in HEPES buffer. Platelets were diluted 1:200 and counted using a Bürker chamber and brought to the suitable concentration, adding an appropriate volume of HEPES buffer.

Finally, 5.5 mM glucose is added, and platelets were allowed to rest for 30 minutes at 37°C before being used for experiments.

2. Preparation and extraction of brain tissue

Brain was dissected from euthanized mouse and homogenized in 1mL of ice-cold RIPA buffer for 4 hours at 4°C. After homogenization, lysates were cleared at 18000g for 10 minutes at 4°C to eliminates debris and insoluble materials.

Supernatants were collected, and protein concentration was determined by bicinchonicic acid assay (method 10).

3. Electron microscopy

Resting washed platelets were analyzed by electron microscopy through a method described previously (Momi et al., 2009). Briefly, platelets were fixed for 4 hours at 4°C using cacodylate 0.1N-HCl buffer (pH 7.4) containing 4% wt/vol of glutaraldehyde. The samples were then washed, maintained in cacodylate buffer for further 4 hours, then placed in 1% osmium tetraoxide and centrifuge at 10000g for 30 seconds. Ultrathin sections of platelet pellets were labelled with uranyl acetate and citrate and observed with a Philips Optic EM208 transmission electron microscope at 80 kv.

4. Flow cytometry

Samples of washed murine platelets obtained according to the method 1 are resuspended at the final concentration 10^6 cells/mL in 0.05 ml of HEPES buffer containing 1mM $CaCl_2$ and 1mM $MgCl_2$, 5.5mM glucose, and 0.1% BSA. Platelet samples, untreated or stimulated with the addition of different doses of TRAP4, convulxin, U46619, ADP or $A\beta_{25\text{-}35}$, were then labelled for 3 minutes at room temperature with different specific antibodies: Fluorescein isothiocyanate (FITC)-conjugated anti-P-selectin, or FITC-conjugated fibrinogen. Additionally, surface expression of different glycoproteins was determined using specific antibodies: glycoprotein VI, V, CD42b, CD41, CD61, CD9 and CD49b.

Reaction was stopped by diluting samples with 0.5% PFA and samples were immediately analyzed by flow cytometry using a FACSCalibur instrument equipped with CellQuest Pro software (BD Bioscience, Milan Italy). Data analyses were performed using FlowJo 7.6.1 software (Tree Star Inc., Ashland, US).

5. Megakaryocyte isolation

Bone marrow cells were flushed from femurs and tibia in DMEM supplemented with 1% penicillin/streptomycin, 1% L-glutamine, 10% of fetal bovine serum in sterile conditions. Cells were cultured for 5 days in supplemented DMEM in the presence of 10 ng/ml of recombinant mouse thrombopoietin (TPO) (Peprotech, UK). Megakaryocytes were recovered by centrifugation on 1.5/ 3 % gradient BSA for 30 minutes and counted. For evaluation of proplatelet formation, $1x10^5$ cells were seeded onto glass coverslips, previously coated with 100µg/ml of fibrinogen and cultured for additional 6 hours at 37°C and 5% CO_2. Cells were then fixed with 2%

PFA, permeabilized with 0.25% Triton X-100 for 10 minutes, and stained with anti-tubulin antibody (1:500) for 1 hour at room temperature followed by incubation with AlexaFluor488-conjugated secondary antibody for1 hour at room temperature. Nuclear counterstaining was performed with Hoechst 33258 (100 ng/ml). The coverslips were mounted onto glass slides with ProLong Gold antifade reagent and images acquired by an Olympus BX51 microscope (Olympus) using a 20X/0.5 UPlanF1 objective. Megakaryocytes protruding proplatelets were counted in twenty fields and expressed as percentage on the total number of megakaryocytes.

6. Neutrophils isolation and analysis of NETs formation

Bone marrow cells were flushed in RPMI medium supplemented with 10% FBS and 1% penicillin/streptomycin. After dispersion of the cell clumps, the cell suspension was filtered with 70 μm cell strainer, centrifugated (400g for 7 min at room temperature), resuspended in Red Blood cell lysis buffer and centrifuged again at 400g for 7 minutes. Finally, the cell pellet was resuspended in 1ml Ca-Mg-free HBSS and centrifuged on 62.5 % gradient Percoll for 30 minutes at 1000g at room temperature. Typically, 1-2 × 10^6 bone marrow-derived neutrophils were harvested per mouse.

For analysis of NETs formation, neutrophils (3 × 10^5 cells) were left untreated or stimulated with PMA (100 nM) or by addition of platelets (1 × 10^9 platelets) before plating onto glass coverslips on 24 wells plates. Neutrophils were incubated 3 hours (for PMA stimulation) or 30 minutes (for platelets stimulation) in humidified incubator (37 °C, 5 % CO_2). The cell culture plate was citospun and adherent cells were fixed with 2 % PFA and then permeabilized with ice-cold 0.25 % TRITON 100X for 10 minutes. For immunofluorescence labelling of NETs, cells were stained for citrullinated histone H3 (1:500 dilution) for 1 hour at room temperature followed by incubation with Goat anti-Rabbit (TRITC)-(ab6718) antibody for1 hour at room temperature and finally counterstained for DNA with Hoechst 33342 (1:1000 dilution).

7. Aggregation assay

Murine washed platelets were used to perform platelet aggregation analysis on a lumiaggregometer from from Chrono-Log Corporation using the turbidometric method developed by Born. Platelet samples (3x10^8/mL, 0.25 mL) were stimulated

under constant stirring with different concentrations of thrombin, TRAP4, U46619, convulxin, ADP and Aβ peptides in the presence of 1 mM $CaCl_2$. Platelet aggregation was continuously monitored for 5 minutes.

8. Adhesion and spreading assay

Glass coverslips were coated overnight at room temperature with 25 μg/ml collagen,100 μg/ml fibrinogen, 10 μM vWF, 10 U/mL Heparin, or 10 μM $Aβ_{25-35}$, $Aβ_{1-40}$ and $Aβ_{1-42}$ in PBS and then blocked with 1% BSA for 1 hour at room temperature. Washed platelets (0.5 mL, $4x10^7$/mL) were added dishes coated with fibrinogen, heparin and Aβ peptides in the presence of 1 mM $CaCl_2$, collagen in the presence of 2mM $MgCl_2$, and vWF in the presence of 5 μM cofactor brotrocetin. Adherent platelets were fixed, permeabilized with 0.25 % TRITON X-100 and stained by TRITC-conjugated phalloidin, as previously described (Cipolla et al., 2013).

Platelets were viewed on fluorescence microscope (Olympus BX51), and digital images (400x and 1000x) were acquired. The number of adherent cells were determined using the Image J Version 1.42 software and the statistical analysis was performed using Prism Version 4 software (GraphPad).

9. Platelet protein preparation

Polystyrene dishes (60mm) were coated overnight at room temperature with 25 μg/ml collagen. Dishes were washed two times with 2mL of PBS and then blocked with 1% BSA for 2 hours at room temperature. Murine platelets ($5x10^8$ /mL, 0.6 mL) were added to collagen-coated dishes in the presence of 2mM $MgCl_2$ and 1mg/ml BSA. After 60 minutes of adhesion at room temperature, non-adherent cells were removed, and dishes were washed, and adherent cells were directly solubilized by adding 0.3mL of 2% SDS in HEPES buffer and then collected. Lysates were centrifuge at 18000g for 10 minutes and protein concentration were determined by bicinchoninic acid assay (method 10).

Aliquots of each sample containing the same amount of proteins were used for immunoblotting analysis.

10. The bicinchoninic acid assay (BCA assay)

The bicinchoninic acid assay (BCA assay) is a biochemical assay for determining the total concentration of protein in a solution. The BCA assay depend on

two subsequent reactions. First, the peptide bonds in proteins can reduce Cu^{2+} to Cu^{+} and the amount of Cu^{2+} reduced is proportional to the amount of protein present in the solution. Then two molecules of bicinchoninic acid chelate a single Cu^{+} ion, resulting in an intense purple-colored reaction product that strongly absorbs light at 562 nm. Consequently, the unknown protein concentration of samples was determined by the creation of a standard curve using increasing concentrations of the standard protein Bovine Serum Albumin (BSA).

11. Electrophoresis and immunoblotting

Samples to be run on SDS-PAGE are first boiled at 95°C for 3 minutes in SDS sample buffer 1XR. Aliquots of brain and platelet lysates were separated by SDS-PAGE on 7.5 % acrylamide gel and 5-15% or 10-20% acrylamide gradient gels.

	Running gel					Stacking gel
	10%	20%	5%	15%	7.5%	3%
	µl	µl	µl	µl	µl	µl
Acrylamide 30%	1500	3000	750	2250	2250	250
Tris/HCl 1.50M pH 8.8	1125	1125	1125	1125	2250	-
Tris/HCl 1.25M pH 6.8	-	-	-	-	-	250
SDS 10%	45	45	45	45	90	25
H_2O	1560	60	2310	810	3870	1700
Temed 1%	225	225	225	225	450	250
Total volume	4500	4500	4500	4500	9000	2500

\Proteins separated through SDS-PAGE were transferred onto a PVDF (Polyvinylidene fluoride) membrane and the separated proteins were examined further by probing the membrane with an antibody to detect a specific protein. The membrane was first incubated for 1 hour with 5% BSA in TBS to block all remaining hydrophobic binding site on the PVDF membrane. After blocking membranes were incubated over night at 4°C with the desired primary antibodies diluted in TBS, 5% BSA, 0.02% NaN3, 0.01% Tween20. Anti-APP (22C11 and 6E10); anti-phopsho-Pyk (Y402) anti-phospho-Akt (S473), anti-phospho-p38MAPK (T180/Y182), anti-phospho-ERK1/2 (T202/Y204), anti-phospho-MLC (S19), anti-tubulin (DM1A)

were diluted 1:1000. The membrane is then washed with PBS additionated with 0.1% Tween 20, and then incubated with the appropriate peroxidase-conjugated secondary antibody (1:2000 dilution). Finally, proteins were visualized using an enhanced chemi-luminescence (ECL) kit (Millipore). The enzyme linked to the secondary antibody is a horseradish-peroxidase that in presence of hydrogen peroxide and the chemiluminescent substrate luminol oxidizes the luminol producing light. The light emission was detected by ChemiDoc XRS (BIORAD).

12. Cell colture

Human embryonic kidney 293T (HEK 293) cells, HEK 293 stably transfected with endogenous APP751 (HEK293/APP751) cells and malignant human breast cancer (MDA-MB-231) cells were grown in Dulbecco's modified Eagle medium (DMEM) supplemented with 10% (v/v) fetal bovine serum (FBS), 2 mM L-glutamine, 100 U/mL penicillin and 0.1 mg/mL streptomycin. Cells were maintained at 37°C in a 5% CO2 water saturated incubator. For the passaging of cells, cells were washed with PBS and then incubated with Trypsin/EDTA to detach the cells. Detached cells were resuspended in cell culture medium and split at 1:2–1:20 ratios for continued culture.

13. Thrombus formation under flow

Thrombus formation was performed essentially as previously described (Consonni et al., 2012). Glass coverslips were coated with fibrillar type I collagen (50μg/ml) or with collagen in the presence of Aβ peptides: $A\beta_{25-35}$ and $A\beta_{1-42}$ (10μM). Coverslips were mounted in a 50 μm-deep parallel-plate flow chamber (RC-31 from warner instruments) under a fluorescence microscope and blocked with 1% BSA and then rinsed with HEPES Flow Buffer. Blood was withdrawn from euthanized mice in PPACK/ heparin and incubated with 3μg/ml CFSE for 15 minutes in dark at 37°C. Subsequently, blood was flowed over collagen or collagen plus Aβ peptides at the typical arterial share rate of 1000 /s for 5 minutes using a pump system (Harvard Apparatus PHD 2000). After perfusion the flow chamber was rinsed with washing buffer, and at least 10 fluorescence microscopic images were collected after 5 minutes of rinse. Images were analyzed by ImageJ Version 1.92 software and the extent of thrombus formation was calculated as the percentage of platelet covered area.

14. Blood clotting assay

Blood was collected from anesthetized mice and anticoagulated with 3.8% sodium citrate (1:10 vol). Anticoagulated blood was centrifuged immediately for 10 minutes at 180g to obtain PRP. PRP was further centrifugated for 10 minutes at 18000g at 4°C to obtain PPP. PPP and PRP were tested as indicated. Activated partial thromboplastin time (APTT) and prothrombin time (PT) were measured by standard assays in an automatic coagulometer (ACL 300R; Instrumentation Laboratory) using the Instrumentation Laboratory kits, according to the manufacturer's instructions. Plasma fibrinogen was measured by the Clauss method in a Coagulab MJ coagulometer (Ortho Diagnostic Systems), using bovine thrombin. Plasma levels of Factors XIIa and XIa were assayed by one-stage clotting methods using commercially available human plasmas deficient in the respective coagulation factor.

15. Tail bleeding time and blood loss

Mice were positioned in a special immobilization cage which keeps the tail of the animal steady and immersed in saline thermostated at 37°C. After two minutes the tip of the tail was transected with a razor blade at 2 mm from its end. The tail was immediately re-immersed in thermostated saline and the time taken to stop bleeding was measured; the end point was the arrest of bleeding lasting for more than 30 seconds. Quantification of blood loss was performed essentially as previously described (Momi et al., 2009). Bleeding time was carried out in tubes containing saline plus sodium citrate. Tubes were centrifuged at 1000g for 10 min to collect erythrocytes, that were resuspended in 6 ml of lysis buffer (NH4Cl 8.3 g/l; KHCO3 1.0 g/l; EDTA 0.04 g/l). The amount of released haemoglobin in the sample was estimated spectrophotometrically by measuring the absorbance at 575 nm using a standard curve constructed with increasing amount of bovine haemoglobin.

16. Platelet pulmonary thromboembolism and lung histology

Thrombin-induced pulmonary thromboembolism was carried out essentially as previously described with slight modifications (Gresele et al., 1998). Briefly, mice were challenged with 0.1 ml of 500 U/kg thrombin, rapidly injected into one of the tail veins. Mice were sacrificed after 15 min by an overdose of anesthesia and the chest was opened, trachea was cannulated and lungs were perfused with a fixing solution

(10% formalin buffered with calcium carbonate). The trachea was then ligated and removed together with the lungs which were rinsed in cold saline and then fixed in 10% formalin for 24 hours. The right-lower lobe was embedded in paraffin and several sections, 5-6 μm thick, were cut and stained with hematoxylin and eosin to reveal platelet rich thrombi and with phosphotungstic acid hematoxylin to show fibrin in tissues. The specimens were examined under a light microscope (Axio LAb A.1, Carl Zeiss MicroImaging) by a pathologist unaware of the experimental groups. At least ten fields, at a magnification of 100- 400x, were observed for every specimen. The total number of identifiable lung vessels per field was counted and the percentage of them occluded by platelet thrombi as well as their diameter was annotated.

17. Femoral artery thrombosis.

Photochemical- induced femoral artery thrombosis was induced in anesthetized mice by a method described previously (Momi et al., 2014). Briefly, mice were anaesthetized by xylazine (5mg/kg) and ketamine (60 mg/kg) and placed on a heated operating table. A 25G needle venous butterfly was inserted in one of the tail veins for the infusion of rose Bengal. The left femoral artery was carefully exposed and a laser Doppler probe (Transonic Systems) was positioned onto the branch point of the deep femoral artery distal to the inguinal ligament for monitoring blood flow. The exposed artery was irradiated with green light (wavelength, 540 nm) of a Xenon lamp (L4887; Hamamatsu Photonics) equipped with a heat-absorbing filter via a 3-mm-diameter optic fiber attached to a manipulator. Light irradiation was protracted for 20 minutes; the infusion of rose bengal (20mg/kg) was started 5 minutes after the beginning of irradiation and lasted for 5 minutes. The end point was set as the cessation of blood flow for 30 seconds; if no occlusion occurred after 30 minutes, the time was recorded as 30 minutes.

18. Inferior vena cava ligation

Inferior vena cava (IVC) ligation was obtained as previously described (Momi et al., 2014) Briefly, mice were anesthetized with xylazine (5mg/kg) and ketamine (50mg/kg) and placed in a supine position. After laparotomy, intestines were exteriorized and sterile saline was applied during the whole procedure to prevent drying. After gentle separation from aorta, IVC was ligated by a 7.0 polypropylene suture immediately below the renal veins (toward the tail) over a 30-gauge needle and then the needle was removed to obtain a partial flow restriction. After surgery,

peritoneum and skin were closed by monofilament absorbable suture and 6.0 silk, respectively. Mice were euthanized after 24 hours, and thrombi developed in the IVC below the suture (toward the tail) were taken for analysis. Thrombus weight and thrombus length were measured.

19: Bone marrow transplantation

Generation of chimeric mice was performed essentially as described previously (Momi et al., 2009). Bone marrow cells were harvested from the femurs and tibias of donor WT and APP KO mice. Then, 1 $x10^7$ cells (in 300 µL) from APP KO bone marrows were transplanted by intravenous injection into irradiated recipient WT mice. Control experiments were performed by transplanting bone marrow from WT donors into irradiated WT recipient mice. 6 WT^{WT} and 6 $WT^{APP\ KO}$ chimeric mice were generated.

20: Data analysis

Statistical analysis was performed using GraphPad Prism 5 Software. Data were analysed by non-parametric t-test (for comparisons of two groups) or one-way ANOVA followed by Bonferroni post-doc analysis (for multiple comparisons). Data are expressed as mean ± SEM value of $p<0.05$ were considered statistical significant.

Part I:

Analysis of platelet adhesion and thrombus formation in a mouse model of Alzheimer's disease

AIM OF THE STUDY I

In recent years, Alzheimer's disease (AD) has been recognized to be a systemic disorder that affects other peripheral tissues beside brain. Alterations in AD patients occurs not only in the central nervous system but also in blood vessels and blood cells leading to amyloid-β deposition in cerebral vessels known as cerebral amyloid angiopathy (CAA). Beside CAA, recent studies demonstrated that AD is strongly related to vascular system and is associated to vascular diseases such as stroke, atherosclerosis and hypertension (Honig et al., 2003). Conversely, many risk factors that predispose to vascular disorders may increase the risk for AD (Mielke et al., 2007).

Platelets are responsible for haemostasis and thrombosis and appear suited to study the metabolic mechanisms occurring in the central nervous system and related to AD. Indeed, platelets express amount of APP like those detected in the brain and display the enzymatic activities to generate amyloid-β (Aβ) peptides (Van Nostrand et al., 1989). Platelets store APP soluble fragments and Aβ peptides in α-granules and release them in plasma upon activation with physiological agonists (Casoli et al., 2007). In turn, Aβ peptides in circulation can induce platelet activation (Canobbio et al., 2014; Sonkar et al. 2014) and promote ROS production (Gowert et al., 2014). In addition, platelets express Tau (Mukaetova-Ladinska et al., 2013). Therefore, platelets are considered an important link between AD and cardiovascular diseases.

The association between AD and platelet functionality remains to be clarified, even though recently several alterations have been detected in platelets from AD patients compared to aged matched control subjects. For example, platelets from AD patients have altered APP ratio (130kDa/110kDa), which results lower compared to control subjects, principally due to an increase expression and activation of β-secretase, with the consequent augmented Aβ production in plasma. Simultaneously reduced α-secretase activity has been shown in platelets from AD patients, further supporting changes in amyloidogenic APP metabolism in this pathological condition (Veitinger et al., 2014; Borroni et al., 2010; Colciaghi et al., 2004). Moreover, independent studies also established increase expression and activation of MAO-B, the enzyme responsible for neurotransmitters degradation in nervous system (Mészàros et al., 1998).

Changes in platelet morphology and functionality have been also documented, in particular AD platelets exhibit greater platelet-leukocytes complexes and platelet aggregates in circulation. In addition, P-selectin expression and integrin

$\alpha_{IIb}\beta_3$ activation were significantly increased in AD resting platelets. Finally, besides the hyperactivated state of platelets, impaired coagulation has been described in AD patients, as proved by the prothrombotic phenotype observed in AD patients (Cortes-Canteli et al., 2010).

Hence, in this moment could be relevant to define whether this pathological platelet alterations might be correlated with the onset and progression of AD. Unfortunately, the analysis of platelet functionality in AD patients is complicated by several factors, for instance, they are subjected to different pharmacological treatments. Moreover, there is enormous variability in term of ages and genetic backgrounds between the different subjects. Since all these limitations in directly examining affected human persons, several AD transgenic mice have been developed (http://www.alzforum.org/research-models). Indeed, the use of AD mouse models allows to analyse possible alterations of platelet functions in drug-free animals with an identical genetic background. Moreover, since these AD mice typically carry specific genetic mutations, it is possible to define the exact correlation between selected mutation to specific change of platelet function. Finally, the use of AD mouse models permits to monitor age-related alterations of platelet properties during the progressive phases of the disease.

The development of different animal models, carrying specific AD causative mutations have been extensively studied to investigate several aspects of the onset and progression of the pathology, but only few of these murine models have been characterized in terms of platelet and vascular alterations. A single previous study has analyzed platelet functions in a mouse model of AD, the APP23 mice. These mice carry the Swedish APP mutation under the control of the neuronal promoter. Jarre et al. demonstrated that platelets isolated from APP23 mice shown a hyperactivated state, with an increased integrin activation and degranulation (Jarre et al., 2014).

Firstly, I evaluated whether the AD pathology affected platelet function and thrombus formation using a well characterized mouse model of AD, the triple-transgenic-AD (3xTg-AD) mice, generated in a B6129SF2 background and harbouring three specific mutations associated with familial AD. In this AD mouse model, two human transgenes encoding APP with a double mutation (Swedish mutation), resulting in a substitution of two amino acids (KM670/671NL) and MAPT tau with the P301L mutation, both under the control of the mouse neuronal Thy1.2 promoter, are coinjected into a single cell embryo harvested from mice with knock-in

of PSEN1 with the PS1 M146V mutation. Translation of the overexpressed transgenes is restricted to the central nervous system, particularly in hippocampus and cerebral cortex. These mice exhibit progressive development of both plaques and tangles pathology, associated with synaptic dysfunction, traits similar to those detected in AD patients (Oddo et al., 2003).

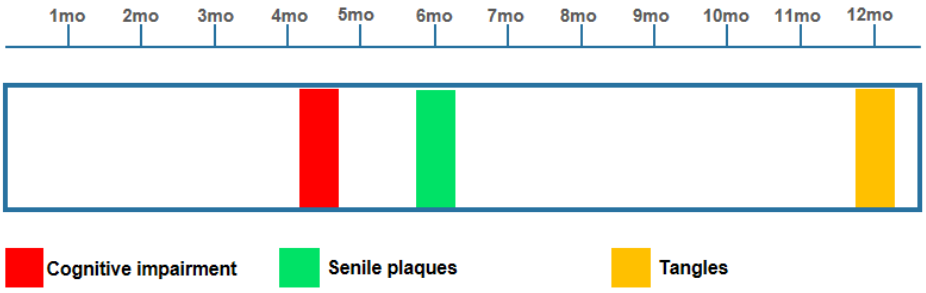

Figure 9. 3xTg-AD mice phenotype timeline (image modified by www.alzforum.org)

As reported in figure 9, 3xTg-AD mice display the gradual development of the pathology. In more details, intraneuronal Aβ deposition in hippocampus and amygdala is progressive and can be detected as early as at 3 to 4 months of age (Billings et al., 2005). Extracellular deposition of Aβ in senile plaques can be observed at 6 months in the frontal cortex and become more extensive by twelve months. Whereas, alterations in tau occur later, since aggregates of conformationally-modified and hyperphosphorylated tau are detected in the hippocampus by 12 to 15 months of age.

Moreover, 3xTg-AD mice show cognitive impairments in spatial learning and memory starting at 4 months (Stover et al., 2015).

Therefore, 3xTg-AD mice are considered a valuable mouse model of AD and have been widely used to investigate neuronal dysfunctions, but little is known about the consequences of these mutations in peripheral tissues and in particular, in circulating blood cells. In a previous study with this AD animal model, it has been demonstrated that at 12 months 3xTg-AD mice also showed a significantly higher vascular expression of Aβ, thrombin, tumor necrosis factor α, interleukin-1β, interleukin-6 and matrix metalloproteinase 9 compared to aged matched control mice, thus confirming cerebrovascular activation and chronic inflammation in 3xTg-AD

mice (Grammas et al., 2014). In addition, using the same AD mouse model, Cho and colleagues found increased Aβ plasma accumulation with age, while its concentration decreased in the cerebrospinal fluid (CSF), hence demonstrating an inverse correlation between the plasma and CSF Aβ levels in 3xTg-AD mice's brains (Cho et al., 2016).

I selected this AD mouse model principally because it summarized the progressive neuropathology of human AD, including plaques and tangles. I principally focused my attention on aged mice (18 months old) since at this age all the characteristic hallmarks of the pathology are already evident. In particular, platelets isolated from 3xTg-AD mice were characterized in term of activation (e.g. integrin $\alpha_{IIb}\beta_3$ inside-out activation, platelet aggregation and α-granules secretion) and adhesion.

RESULTS I

1. Characterization of platelets from 3xTg-AD mice

3xTg-AD mice represent a well characterized mouse model of AD, which contain three mutations associated with the familial AD: APP KM670/671NL (Swedish), tau MAPT P301L and presenilin1 PSEN1 M14V. These mutations result in overexpression of APP, overproduction of $A\beta_{42}$ and hyperphosphorylation of tau predominately in neurons (Oddo et al., 2003). In these mice, extracellular deposition of Aβ into senile plaques can be observed at 6 months; whereas changes in tau occurred later, by 12 to 15 months of age.

To verify the accuracy of my model I analysed the expression of amyloid precursor protein APP in brain as well as in isolated platelets. I used two different antibodies to recognize human and mouse APP: antibody 6E10 recognizes the first 16 amino acids of Aβ peptide of human APP and therefore is able to detect only the transgenic human APP inserted under neuronal promoter; whereas, antibody 22C11 is directed to the amino acids 66-81 of N-terminus of both human and murine APP.
Brain and platelet lysates from 3xTg-AD and control mice were prepared as previously described in methods 1 and 2, and 30 μg of total proteins were separated by 7.5 % SDS-PAGE gels and APP expression was analyzed by immunoblotting (methods 11). The immunoblotting analysis confirmed the specific neuronal expression of human APP by using antibody 6E10, since it reveals the presence of human APP only in brain but not in platelet lysates of 3xTg-AD mice. Here, human platelets have been used as positive control.

Moreover, accordingly to APP Swedish mutation (Oddo et al., 2003), it has been found that APP expression is double in the brain of 3xTg-AD mice. Indeed, immunoblotting with antibody 22C11 (that recognized human and murine APP) clearly shows that the level of APP expression in brain of 3xTg-AD mice is two/three folds higher than in control mice. Conversely, the level of APP expression in platelets is normal and comparable in both genotypes. The bottom row shows the comparable expression of tubulin in all samples (figure R1A). The figure R1A also shows that the molecular weight of APP appears slightly different between platelet and brain

samples, as indicated through the arrows. This difference is principally due to diverse APP isoforms expressed in brain and platelets: the principal neuronal APP isoform is APP_{695} (106-110 kDa), while platelets mainly express APP_{751} and APP_{770} (about 130 kDa).

3xTg-AD mice express human mutant APP exclusively under a neuronal promoter as indicated in the upper panel of figure R1A. Whereas, the immunoblotting reveals that platelets express endogenous native murine APP protein, that migrates with a similar molecular mass in both genotypes, suggesting that the progression of the pathology doesn't cause changes in the metabolism of the APP expressed in circulating platelets.

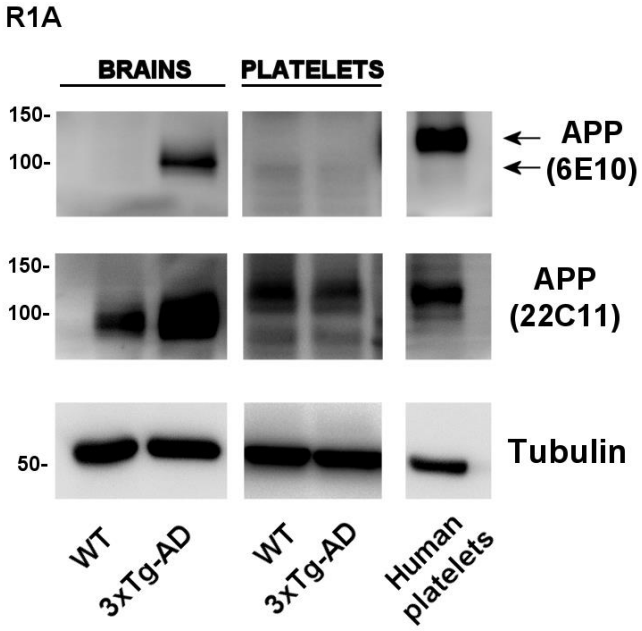

Figure R1A. Characterization of brain and platelets from 3xTg-AD mice. Analysis of human and murine APP and tubulin expression in brain and platelets from WT and 3xTg-AD mice, by immunoblotting with specific antibodies, as indicated on the right. Human platelet sample is used as positive control. 6E10 antibody recognizes human APP, whereas 22C11 antibody detects both human and murine APP. Tubulin antibody is loaded for equal loading control.

3xTg-AD mice are viable and fertile and did not manifest any evident thrombotic events or bleeding tendency over their lifespan. In addition, no significant differences in the number of circulating platelets and white blood cells were observed

between control (WT) and 3xTg-AD mice (figure R1B). We next investigate the surface expression of some major platelet glycoproteins, including Ibα (CD42b), the immunoreceptor tyrosine-based activation motif (ITAM)–coupled collagen receptor GPVI, α2 (CD49b) and α_{IIb}(CD41) integrins by flow cytometry. As indicated in figure R1C, no differences in surface expression of these platelet glycoproteins were described between the two genotypes (figure R1C).

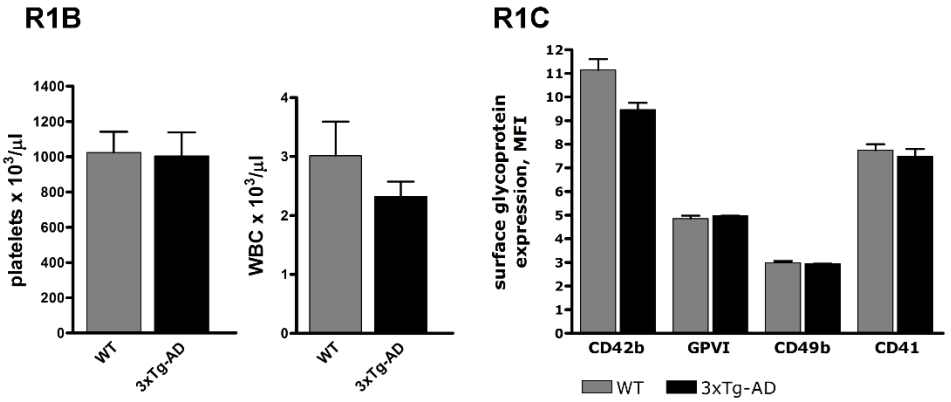

Figure R1B-C. Characterization of platelets from 3xTg-AD mice. (B) Platelet and white blood cell count from control (grey bars) and 3xTg-AD (black bars) mice. Results are the means ± SEM of determination performed in 10 different mice. **(C)** Surface expression of different platelet glycoproteins on WT (grey bars) and 3xTg-AD (black bars) mice determined by flow cytometric analysis with specific antibodies. Data are expressed as mean fluorescence intensity (MFI) ± SEM of n=6 mice/group.

Subsequently, platelet morphology was compared by electron microscopy analysis. No gross morphological alterations were observed between WT and 3xTg-AD platelets, although signs of accidental activation-induced degranulation were described. Measurement of platelet diameter and quantification of α and dense granules content are shown in the histograms in the figure R1D. This analysis revealed that platelet diameter was significantly slightly larger in platelets from 3xTg-AD mice, but the number of platelet granules was comparable to that of control platelets (figure R1D).

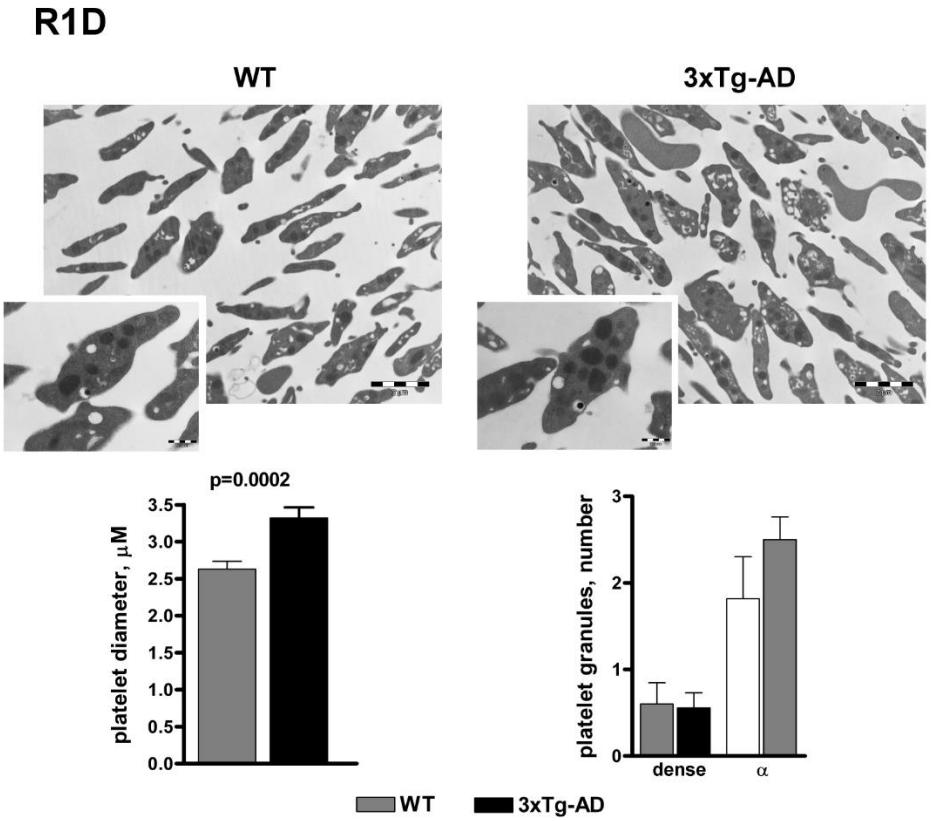

Figure R1D. Characterization of platelets from 3xTg-AD mice. Electron microscopy analysis of WT and 3xTg-AD platelets. Representative images at different magnitudes (10000x and 40000 in the insets) are reported. Measurement of platelet diameter and quantification of dense and alpha granules in WT (grey bars) and 3xTg-AD (black bars) platelets are shown. Data are expressed as means ± SEM and have been obtained from the analysis of 50 platelets from 5 different slides for each genotype (n= 5 mice/group).

2. Analysis of platelet activation and aggregation in 3xTg-AD mice

Alterations in APP isoforms and abnormalities in platelet morphology have been documented in platelets from AD patients. In addition, in a different mouse model for AD, the APP23 mice, blood platelets were found to circulate in an hyperactivated state (Jarre et al., 2014). In their study, they used aged APP transgenic mice, which carry only the APP Swedish (KM670/671NL) mutation and are known to develop amyloid β-plaques in the brain parenchyma and the microvasculature. Jarre and coworkers demonstrated that platelets isolated from these mice shown increased granules secretion, integrin activation and aggregation. To extend our knowledge beyond the observations made in this AD model, I deeply analyzed platelet activation in aged (18 months) 3xTg-AD mice, which are the best model to recapitulate all AD specific mutations.

First, I investigated platelet aggregation. Washed murine platelets (3×10^8/mL) were stimulated with different concentrations of thrombin, GPVI agonist convulxin, thromboxane analogue U46619 and $A\beta_{25\text{-}35}$ under constant stirring in the presence of 1mM extracellular Ca^{2+}. Platelet aggregation was monitored as increase of light transmission up to 5 minutes in a Born aggregometer as described in method 7. The aggregation traces are shown in figure R2A.

Platelet aggregation is not altered in 3xTg-AD platelets stimulated with different doses of thrombin (0.05 U/ml and 0.01 U/ml), convulxin (50 ng/ml), U46619 (1μM) and $A\beta_{25\text{-}35}$ (10μM) (figure R2A) compared to WT control platelets.

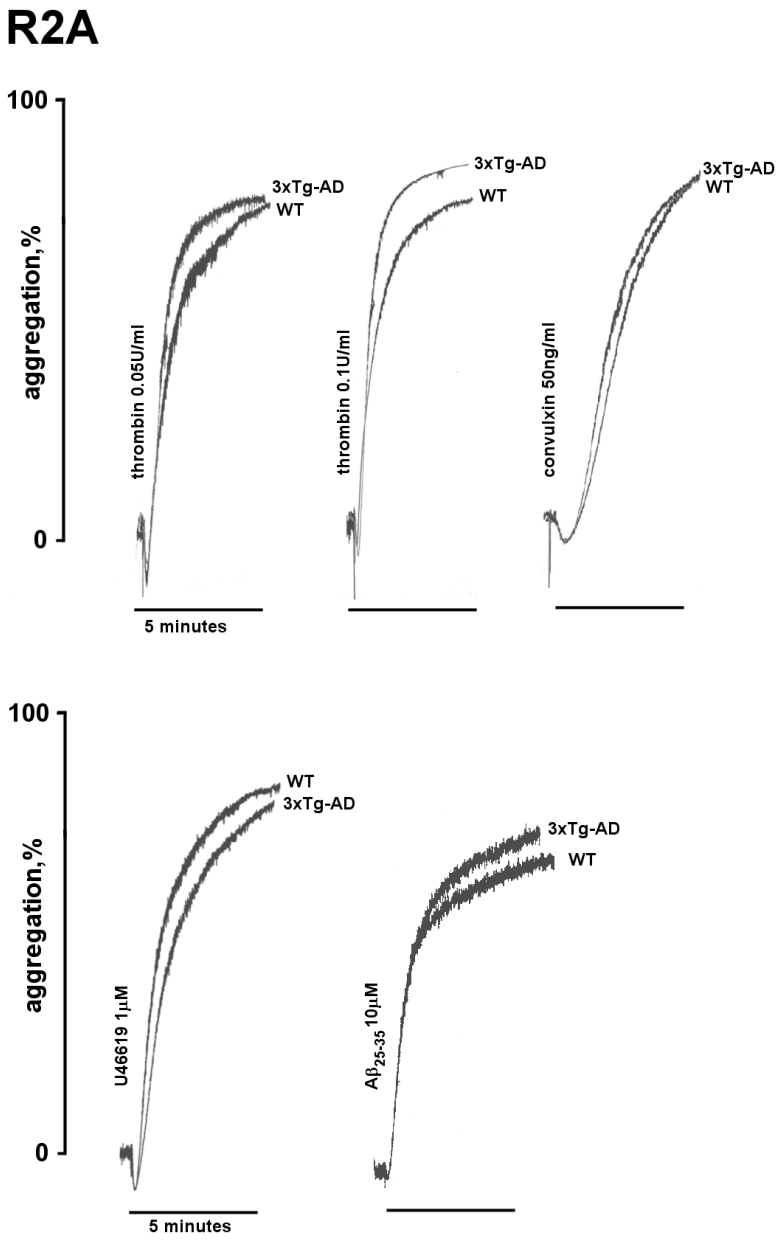

Figure R2A Normal platelet aggregation in 3xTg-AD mice. Washed platelets ($3x10^8$ /ml) from control (WT) and 3xTg-AD mice were stimulated in aggregometer with different concentrations of thrombin (0.05 U/ml and 0.01 U/ml), convulxin (50 ng/ml), U46619 (1 μM) and $A\beta_{25-35}$ (10 μM), as indicated in each panel. Aggregation was monitored as the increase of light transmission up to 5 minutes. Traces in the figure are representative of at least three different experiments. N= 3 mice/ group.

Platelet aggregation is supported by integrin $\alpha_{IIb}\beta_3$, since it is responsible of the binding of platelets to soluble fibrinogen. Integrin $\alpha_{IIb}\beta_3$ undergoes a conformational change upon platelet activation that increases the receptor affinity for fibrinogen. Thus, I analyzed the integrin $\alpha_{IIb}\beta_3$ activation induced by different platelet agonists. Here, washed platelets at $2x10^7$ were treated with HEPES buffer (none) or with 0.5mM TRAP4, 0.1U/ml thrombin, 50ng/ml convulxin, 5μM U46619 and 10μM $A\beta_{25-35}$, as reported in figure R2B. Fluorescein isothiocyanate (FITC)-conjugated fibrinogen was added to platelet suspension and incubated for 30 minutes before diluting samples with 0.5% PFA to stop the reaction (method 4). The samples were immediately analyzed by flow cytometry. Consistent with the aggregation, integrin $\alpha_{IIb}\beta_3$ inside-out activation is also comparable between 3xTg-AD platelets and control platelets (figure R2B).

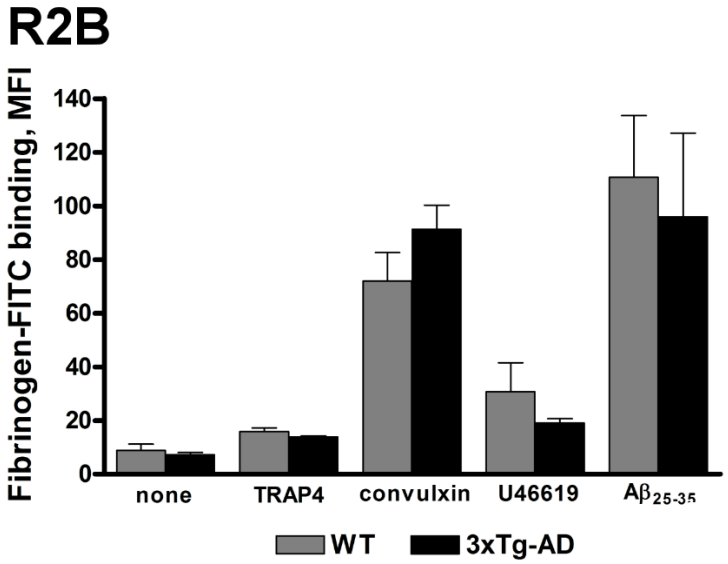

Figure R2B. Normal platelet activation in 3xTg-AD mice. Flow cytometric analysis of FITC-labelled fibrinogen binding to WT (grey bars) and 3xTg-AD (black bars) platelets resting or stimulated with TRAP4 (0.5mM), convulxin (50ng/ml), U46619 (5μM) and $A\beta_{25-35}$ (10μM), as indicated in each panel. Data are expressed as means ± SEM. N=4 mice/group.

In addition, to further assess platelet activation, I next performed the analysis of α-granules secretion in flow cytometry. α-granules secretion was evaluated by examining P-selectin (an α-granule marker) expression on plasma membrane following stimulation with agonists. Platelets were stimulated with thrombin

(0.1U/ml), convulxin (50ng/ml), U46619 (5μM) in the presence of 10μM ADP, and $A\beta_{25-35}$ (10μM), as indicated in figure R2C. No significant differences in α-granules secretion were observed between the two genotypes (figure R2C), suggesting normal platelet activation in3xTg-AD mice.

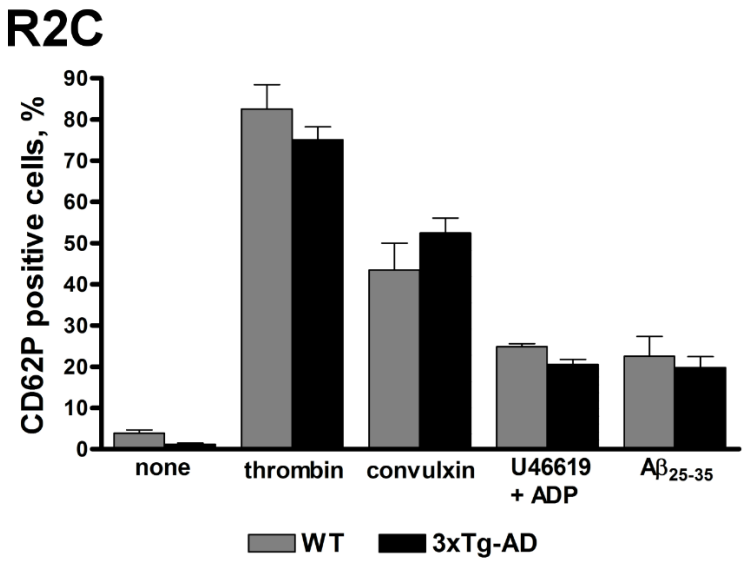

Figure R2C. Normal platelet activation in 3xTg-AD mice. Flow cytometric analysis of P-selectin expression on platelet surface either in WT (grey bars) and 3xTg-AD (black bars) platelets both in resting or upon stimulation with thrombin (0.1U/ml) convulxin (50ng/ml), U46619 (5μM) plus ADP (10μM) and $A\beta_{25-35}$ (10μM), as indicated in each panel. Data are expressed as means ± SEM. N=4 mice/group.

3. Analysis of platelet adhesion in 3xTg-AD mice

Platelets adhesion is the initial response to vascular injury during which platelets immediately adhere with different kinetics to various subendothelial extracellular matrices, such as collagen, von Willebrand factor, and fibrinogen through specific receptors. Upon adhesion, platelets extend filopodia and lamellipodia, increasing the area of adhesion and undergoing spreading. In addition, platelet rapidly undergo activation through the ability of adhesive receptors to transduce signals across the membrane.

I investigated platelet adhesion to collagen. Washed platelets ($4x10^7$/mL) isolated from 3xTg-AD and control mice were let to adhere to collagen for 60 minutes in the presence of 2mM $MgCl_2$. Subsequently, adherent platelets were fixed with 3% PFA, permeabilized with 0.25%TRITON and finally visualized in immunofluorescence after staining of actin filaments with phalloidin-TRITC. Representative images of adherent platelets over collagen coated glasses are shown in figure R3A.

Platelet adhesion to collagen (indicated as number of adherent platelets per mm^2) is significantly increased in 3xTg-AD mice compared to control mice, as confirmed by the quantitative analysis (figure R3A).

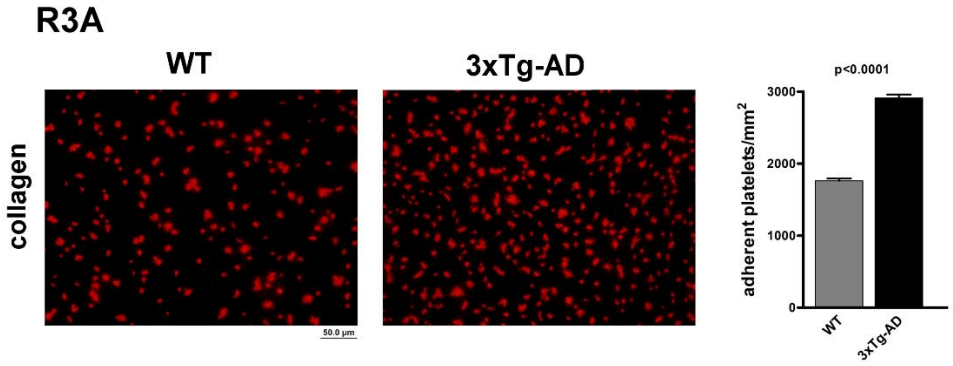

Figure R3A. Enhanced platelet adhesion on collagen of 3xTg-AD mice. 3xTg-AD and control platelets were let to adhere to dishes coated with 25µg/ml collagen in the presence of 2mM $MgCl_2$ for 60 minutes. Adherent platelets were fixed, permeabilized and stained TRITC-conjugated phalloidin. Representative images at 400x magnification of adherent platelets to collagen are shown. Quantification of platelet adhesion, evaluated as number of adherent platelets/mm^2 is reported on the right. WT (grey bars) and 3xTg-AD (black bars). N=5 mice/group.

To investigate whether the increased ability of platelets from 3xTg-AD mice to adhere to collagen also leads to an increased platelet activation of some intracellular signalling pathways, I analyzed phosphorylation of selected signalling proteins in 3xTg-AD and control platelets adherent to collagen. In these experiments, platelets were incubated on collagen in the presence of 2mM $MgCl_2$ and 1mg/ml BSA for 60 minutes and then, non-adherent cells were removed while adherent cells were solubilized by adding 0.3mL 2% SDS in HEPES buffer and then collected. The protein content in the cleared supernatant was determined by the bicinchoninic assay (method 10), and aliquots of each sample, containing the same amounts of proteins,

were used for immunoblotting analysis with the following phospho-antibodies: P-Pyk2 (Y402), P-Akt (S473), P-p38 MAPK (T180-Y182) and P-MLC (S18). I found increased phosphorylation of the focal adhesion kinase Pyk2 (Mw 112KDa), the PI3K downstream effector Akt (Mw 60KDa), mitogen activated kinase p38 MAPK (Mw 38KDa), and myosin light chain (MLC) (Mw 18KDa) in response to collagen adhesion in platelets isolated from both genotypes compared to non-adherent platelets (NA). Equal loading of samples was verified by subsequent immunoblotting with anti-tubulin (bottom row).

Moreover, focusing our attention on adherent platelets (collagen), 3xTg-AD adherent platelets shown enhanced protein phosphorylation compared to WT adherent platelets (figure R3B).

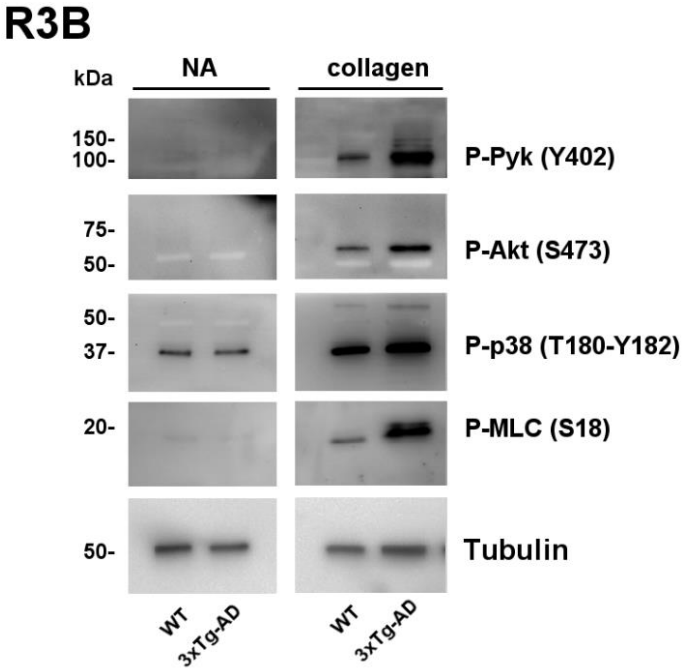

Figure R3B. Enhanced signalling in collagen adherent 3xTg-AD platelets. Aliquots (7 μg) of whole lysates from platelets adherent to collagen and non-adherent cells (NA) were analysed by immunoblotting with the following antibodies: P-Pyk2 (Y402), P-Akt (S473), P-p38 MAPK (T180-Y182) and P-MLC (S18). Tubulin was used as equal loading control.

The quantitative evaluation of protein phosphorylation is reported in figure R3C and confirmed enhanced activation of intracellular signalling pathways in 3xTg-AD adherent platelets (figure R3C).

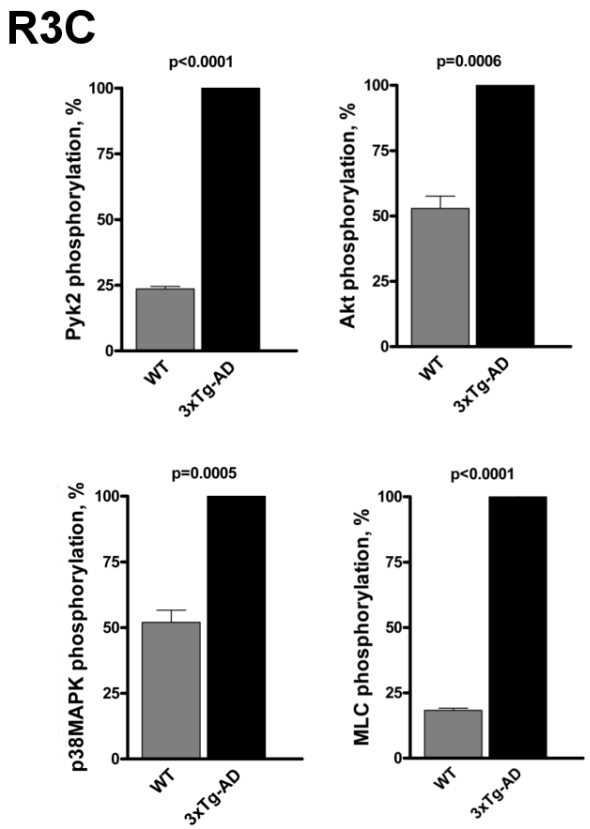

Figure R3C. Enhanced signalling in collagen adherent 3xTg-AD platelets. Quantitative evaluation of protein phosphorylation is reported in the histograms as the means ± SEM of three different experiments. WT (grey bars) and 3xTg-AD (black bars). N=3mice/ group.

Subsequently, I compared platelet adhesion to fibrinogen (100μg/mL) and to von Willebrand factor (10μM) between control and 3xTg-AD platelets. Washed platelets ($4x10^7$/mL) isolated from 3xTg-AD and control mice were let to adhere to fibrinogen in the presence of 1mM $CaCl_2$, and to vWF in the presence of brotrocetin cofactor for 60 minutes. Consistent with the previous evidence with collagen, it has been observed that the number of adherent platelets was significantly increased in

3xTg-AD compared to control over both substrates tested, as also reported in the quantitative analysis in figure R3D.

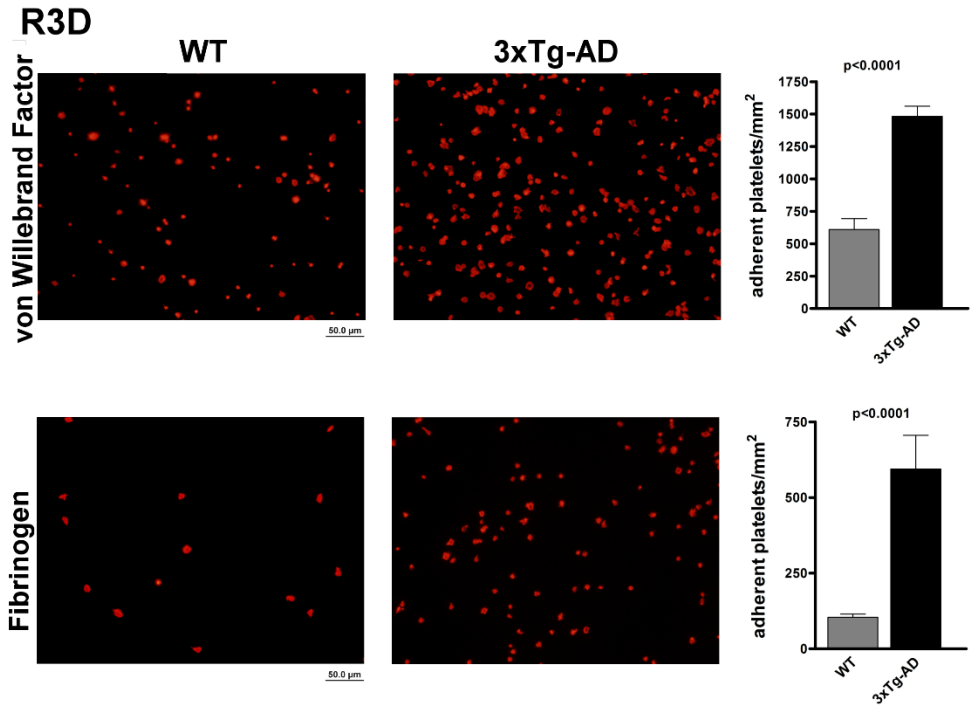

Figure R3D. Enhanced platelet adhesion on fibrinogen and vWF of 3xTg-AD mice. 3xTg-AD and control platelets were let to adhere to dishes coated with 100µg/ml fibrinogen in the presence of 1mM $CaCl_2$ and with 10µM vWF in the presence of botrocetin (5µg/ml) for 60 minutes. Adherent platelets were fixed, permeabilized and stained TRITC-conjugated phalloidin. Representative images at 400x magnification of adherent platelets are shown. Quantification of platelet adhesion, evaluated as number of adherent platelets/mm^2 is reported on the right. WT (grey bars) and 3xTg-AD (black bars). N=5 mice/ group.

Finally, since previous study of our group also demonstrated that platelets specifically adhere on different immobilized amyloid peptides ($A\beta_{25-35}$, $A\beta_{1-40}$ and $A\beta_{1-42}$) (Canobbio et al., 2013), I further investigated the ability of platelets from WT and 3xTg-AD mice to adhere to Aβ peptide, and also in this case 3xTg-AD mice shown enhanced platelet adhesion on Aβ peptide, as reported in figure R3E.

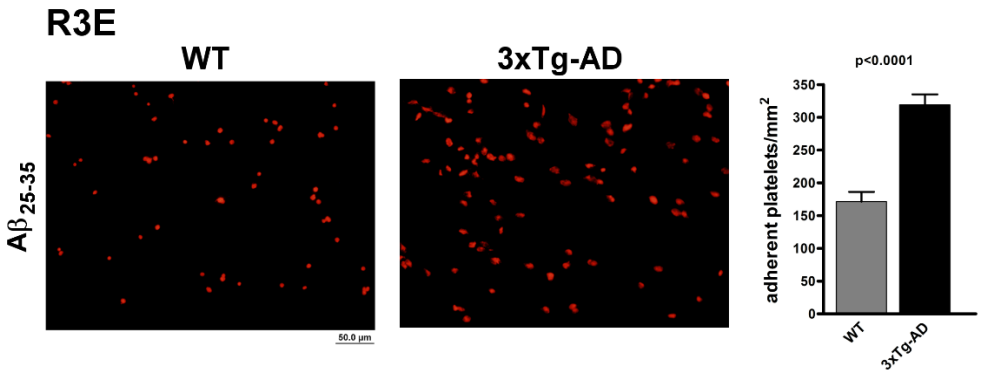

Figure R3E. Enhanced platelet adhesion on Aβ of 3xTg-AD mice. 3xTg-AD and control platelets were let to adhere to $A\beta_{25\text{-}35}$ (10µM) in the presence of 1mM $CaCl_2$ for 60 minutes. Representative images at 400x magnification are shown. Adherent cells were fixed, permeabilized and stained with phalloidin-TRITC. Quantification of adhesion (evaluated as number of adherent platelets/mm^2) was reported on the right. WT (grey bars) and 3xTg-AD (black bars). N=5 mice/ group.

Aβ peptides accumulate not only into senile plaques in the brain parenchyma but also in cerebral vessel walls, causing CAA, also observed in 3xTg-AD mice (Oddo et al., 2003). Therefore, the enhanced ability to adhere to Aβ peptide in platelets from 3xTg-AD mice suggest a possible mechanism by which Aβ deposits in cerebral vessel may worsen the AD pathology.

4. Analysis of thrombus formation on collagen in 3xTg-AD mice

Finally, I analyzed thrombus formation on collagen under arterial flow conditions. Fluorescently labelled platelets in whole blood from 3xTg-AD and control mice were perfused for 5 minutes at a shear rate of 1000/second over immobilized fibrillar collagen to favour platelet adhesion and thrombus formation. The stability of the formed thrombus formation was then evaluated after extensive perfusion with HEPES flow buffer for 10 minutes. Thrombus formation was estimated as percentage of area covered by adherent platelets. As shown in figure R4A, WT platelets are able to adhere on collagen under arterial flow condition (left panel). Interestingly, platelet adhesion and thrombus formation on collagen-coated surfaces are significantly increased in 3xTg-AD mice (right panel). The quantification of surface covered after

5 minutes of perfusion with HEPES flow buffer is reported in the histogram in figure R4B and shows that the percentage of covered area by 3xTg-AD adherent platelets is 71.77% ± 2.782%, whereas it is 50.14% ± 3.743 in control platelets.

Platelet adhesion and thrombus formation on collagen-coated surface are significantly increased in 3xTg-AD compared to control platelets (figures R4A and R4B).

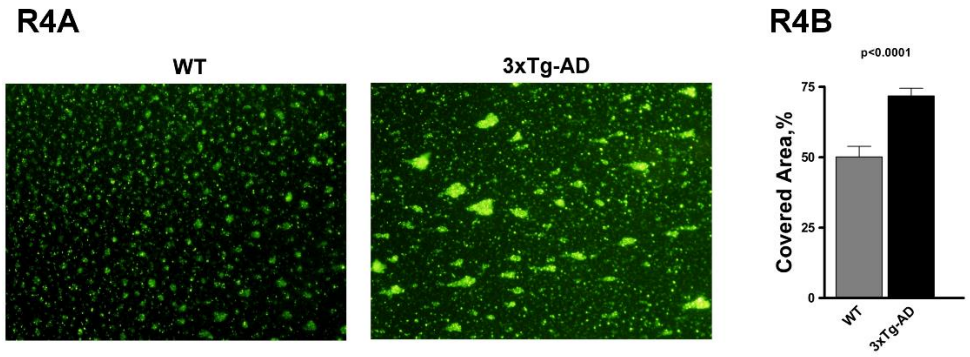

Figure R4A-B. Enhanced thrombus formation on collagen in 3xTg-AD mice under flow. (A) CFSE-labelled platelets in whole blood from control and 3xTg-AD mice were perfused over immobilized fibrillar collagen at a share rate of 1000/s for 5 minutes. Images are taken after brief rinse of the coverslips with HEPES flow buffer. (**B**) Thrombus formation was evaluated by measuring the covered area in 10 different and randomly taken microscopic fields and results were reported in histogram as percentage of covered areas. Images in the figure are representative of at least three different experiments. N=3 mice/ group.

DISCUSSION I

AD is the most common neurodegenerative cause of dementia in the elderly, affecting more than 45 million people worldwide, with a tendency to rise in the next decade (World Alzheimer Report 2015, http://www.alz.co.uk/research/world-report-2015). AD is not only a medical problem, but also an economical challenge for the health care system. Nowadays no reliable biomarkers exist and the pathology is still incurable.

Several recent evidences have led to novel vascular hypothesis for AD pathogenesis suggesting that early cerebrovascular dysfunctions impaired Aβ deposition in brain and cerebral vessels and strongly correlate with onset of AD (de la Torre et al., 2010). Indeed, vascular risk factors (aging, hypercholesterolemia, hypertension, obesity and diabetes) predispose not only to cardiovascular diseases (such as myocardial infarction, ischemic stroke and atherothrombosis) but also affect circulation in the cerebrovasculature and increase the risk of vascular dementia and AD.

Blood platelets are responsible for haemostasis and thrombosis, involved in inflammation and immunity and are major players in vascular pathologies. Moreover, platelets also have an important role in the onset and progression of AD. In fact, platelets express high amounts of amyloid precursor protein (APP), store Aβ peptides in α-granules and release them upon activation (Casoli et al., 2014; Li et al., 1994). In addition, platelet-derived Aβ peptides accumulate in cerebral as well as peripheral vessels and in pathological conditions may cross the brain-blood barrier (BBB), and deposit in the brain, determining cerebral blood flow and BBB alterations (Sonkar et al., 2014; Gowert et al., 2014). Finally, anomalies in APP metabolism and Aβ production, together with hyperactivation of circulating platelets have been documented in AD patients and in AD mouse models (Veitinger et al., 2014; Jarre et al., 2014).

All these reports strongly suggest that platelet activation is potentially able to influence the pathogenesis and progression of AD.

In this work I deeply analyzed platelet activation in a well characterised mouse model of AD: the triple transgenic mice 3xTg-AD (Oddo et al., 2003). These mice contain three mutations associated with familial AD (APP Swedish KM670/671NL, Presenilin1 M146V and MAPT P301L), which result in overexpression of APP,

overproduction of $A\beta_{1-42}$ and hyperphosphorylation of tau principally in central nervous system. 3xTg-AD mice review the progressive neuropathology of human AD, including plaques and tangles. In addition, it has been also observed signs of cerebrovascular activation, chronic inflammation and cognitive impairments in spatial learning and memory in 12 months-aged 3xTg-AD mice (Grammas et al., 2014; Stover et al., 2015).

In the present thesis, I have demonstrated that circulating platelets isolated from 3xTg-AD mice exhibited an enhanced propensity to adhere to components of the subendothelial matrix, such as collagen, vWF and fibrinogen and to form thrombi under arterial blood flow, compared to platelets from age-matched control mice. This greater adhesive tendency of platelets from AD mice may suggest a new explanation for the increased pro-thrombotic risk state described in many patients affected by AD (Stellos et al., 2010).

Several parameters were evaluated indicating a normal platelet physiology, since no significant differences in the surface expression of some major glycoproteins were observed (figure R1C) and no evident morphological alterations were shown between control and 3xTg-AD platelets (figure R1D). Occasionally, signs of activation have been described in electron microscopy analysis, since 3xTg-AD platelets appeared more prone to degranulation. Albeit the analysis of α-granules secretion revealed that P-selectin expression on plasma membrane, following platelet stimulation, was comparable in both genotypes (figure R2C), the fact that platelet boundary observed by electron microscopy clearly appears fractal suggested a forthcoming activation in 3xTg-AD mice (figure R1D). Moreover, integrin $\alpha_{IIb}\beta_3$ activation (figure R2B) and platelet aggregation (figure R2A) were also similar between WT and 3xTg-AD mice.

On the contrary, the analysis of platelet adhesion to different matrix components, such as collagen, vWF and fibrinogen revealed that platelets from aged 3xTg-AD mice displayed a greater tendency to adhere to all substrates tested compared to platelets from age-matched control mice (figures R3A and R3D).

In addition, I have also described that the increased ability of platelets from 3xTg-AD mice to adhere to collagen leads to an increased activation of selected signalling proteins, as shown by the increased phosphorylation of the tyrosine kinase

Pyk2, the Akt kinase (a PI3K downstream effector), the mitogen activated kinase p38MAPK, and the myosin light chain kinase (figures R3B and R3C).

Finally, the increased adhesive ability of 3xTg-AD platelets, together with the enhanced activation of the same adherent platelets to collagen provides a potential explanation of the increased ability of platelets from 3xTg-AD mice to form larger thrombi when flushed over immobilized collagen under arterial blood flow (figures R4A and R4B).

In the past, only one single previous study has analysed platelet functionality in a mouse model for AD, the APP23 mice, demonstrating a constitutive hyper-activated phenotype (Jarre et al., 2014). Differently from APP23, 3xTg-AD platelets undergo normal activation, albeit they showed altered platelet adhesion (Canobbio et al., 2016).

Importantly, it has been previously demonstrated by our group that the amyloidogenic β-peptide was able to support platelet adhesion and to potentiate thrombus formation when immobilized on a collagen matrix (Canobbio et al., 2013; 2015). Moreover, it has been already seen that Aβ peptides, in the circulation, were able to activate circulating platelets and to augment platelet activation induced by several agonists (Shen et al, 2008). Here it has been demonstrated that platelets isolated from 3xTg-AD mice, with a propensity to abnormally accumulate Aβ and tau proteins in the brain over time, also adhered more efficiently to Aβ peptides than control mice (figures R3E).

In this regard, my working hypothesis is that in the course of AD, activation of circulating platelets, which cause vascular dysfunctions and inflammation, may facilitate and accelerate the progression of the disease.

Indeed, the observation that platelets from 3xTg-AD mice adhere more efficiently to immobilized substrates including collagen, von Willebrand factor or fibrinogen and importantly to Aβ peptide, together with the stronger activation of adherent platelets and the enhanced thrombus formation in 3xTg-AD mice, is indicative of a marked pro-thrombotic phenotype of circulating platelets of aged 3xTg-AD mice. In addition, it is important to remember that Aβ is a platelet agonist, and essentially, Aβ peptides in the cerebral vasculature might activate circulating platelets and potentiate platelet activation induced by several agonists (Shen et al., 2008 and Gowert et al., 2014). This process leads to platelet secretion and therefore release of additional Aβ peptides, worsening the development of the pathology.

These results encourage to investigate whether such a prothrombotic phenotype may influence the progression of the pathology and conversely whether inhibition of platelet activation may have positive effects on the evolution of AD. In this regard, future studies will be required to describe in detail the modifications in platelet responses during the onset and the progression of AD.

Part II:

Amyloid Precursor Protein APP as a regulator of haemostasis and thrombosis

AIM OF THE STUDY II

Amyloid precursor protein APP is a transmembrane glycoprotein, principally studied as the precursor molecule of amyloid β-protein (Aβ), which is accumulated in senile plaques of AD patients. In humans, the APP gene is located on chromosome 21 and contains at least18 exons in 240 kilobases (Yoshikai et al., 1990). During transcription, differential splicing of APP mRNA can result in several APP splice variants. The major expressed isoforms of APP have 770, 751 or 695 amino acid residues. APP_{695} is the predominant neuronal isoform, while APP_{770} and APP_{751} are more commonly expressed in non-neuronal cells, such as leukocytes, fibroblasts, and at high amount in platelets.

APP is anchored in the membrane through a single transmembrane domain, followed by a cytosolic domain which contains transduction and internalization signals. APP contains an N-terminal globular domain in the extracellular side which includes binding site for heparin, zinc and copper. This is connected through an unstructured acidic domain followed by Kunitz protease inhibitor (KPI) domain (which is an active domain that inhibits the function of protease), the OX-2 domain and a large glycosylated domain that may be involved in homo- and hetero-dimerization. The structure of APP suggests that it may act as a cell-surface receptor or as a growth factor. Moreover, APP has been reported to influence cell proliferation, differentiation, neurite outgrowth, cell adhesion and synaptogenesis. Despite these data, the exact physiological role of APP has not been fully elucidated.

APP can be proteolytically processed by specific proteases, termed α-, β- and γ- secretases, which cleave APP in different sites. Two alternative metabolic pathways of APP have been identified depending on the type of secretase involved: non-amyloidogenic pathway (α- and γ- secretases) and amyloidogenic pathway (β- and γ-secretases) (Allison et al., 2003; Vassar et al., 1999). The two pathways are mutually exclusive. In most peripheral cells APP is processed through the non- amyloidogenic pathway, while the amyloidogenic pathway is predominant in neuronal cells and originates amyloid β-peptide (Aβ). Aβ is the major protein component of amyloid plaques in the AD brain.

Among the different peripheral cells expressing APP, platelets have the highest APP levels (Van Nostrand et al., 1990). Additionally, platelets express all the enzymatic machinery responsible for APP metabolism. The predominant isoforms of APP expressed in platelets are APP_{770} and APP_{751}, which contain the additional KPI

domain and therefore these isoforms might influence wound repair by regulating blood clotting serine proteases, including factor XIa, factor IXa, factor Xa and tissue factor-factor:VIIa (Van Nostrand et al., 1991). Moreover, previous studies have reported that this KPI domain inhibit the clotting plasma *in vitro* and *in vivo*. All these regards suggest a role of APP in the maintenance of haemostasis.

Furthermore, platelets provide a circulating source of APP that can be releases upon platelet activation.

The aim of this work is to provide a complete characterization of the role of APP expressed on platelets. I investigated whether these platelet APP may contribute to haemostasis and thrombosis by regulating platelet functionality. To address this question, I used APP knockout (KO) mice. These mice have been generated and provided by Dr. Ulrike Müller, from University of Heidelberg, Germany.

APP KO mice were generated through the inactivation of the endogenous mouse APP gene by replacing a 3.8 kb sequence encoding the promoter and the exon 1 with a neomycin resistance cassette, determining a complete deficiency for APP at mRNA and protein levels (Müller et al., 1994). Homozygous APP KO mice were viable and fertile. They are slightly smaller, with a reduced body weight of 15-20% and reduced brain weight compared with that of wild-type (WT), aged-matched, mice (Zheng et al., 1995). Recently, Xu and collaborators have demonstrated that APP deficient mice displayed a significant increase in cerebral thrombosis *in vivo*. In contrast, transgenic mice overexpressing APP both in platelets and in brain showed an anti-thrombotic phenotype with a reduced cerebral thrombosis (Xu et al 2005; Xu et al 2007). These results suggested that APP may regulate cerebral thrombosis.

In this study, I have characterized platelets from APP KO mice and analyzed their functionality through *in vitro* and *in vivo* experiments to clarify the role of APP in regulating platelet biology. Ex vivo aggregation, secretion and integrin $\alpha_{IIb}\beta_3$ inside out activation induced by different platelet agonists were investigated together with the ability of APP KO platelets to adhere over several subendothelial matrices (collagen, fibrinogen, von Willebrand factor) and Aβ peptides. Analysis of *in vivo* arterial and venous thrombosis were also performed.

RESULTS II

1. Characterization of platelets from APP KO mice

APP KO mice are viable and fertile and do not manifest any evident physical abnormalities. The body weight of both male and female homozygous animals is 15-20% less at all ages compared with that of WT aged matched mice (Zheng et al., 1995). These mice were generated and kindly provided by Dr. U. Müller from University of Heidelberg, Germany.

To confirm APP deficiency in APP KO platelets, platelet samples ($5x10^8$/mL, 0.1mL) isolated from WT and APP KO mice according to method 1 were separated by 7.5% SDS-PAGE and analyzed for APP expression using antibody 22C11, which specifically recognized both human and murine APP. Tubulin was used for equal loading control. The immunoblotting analysis confirmed the absence of APP in platelets from APP KO mice (figure R1A).

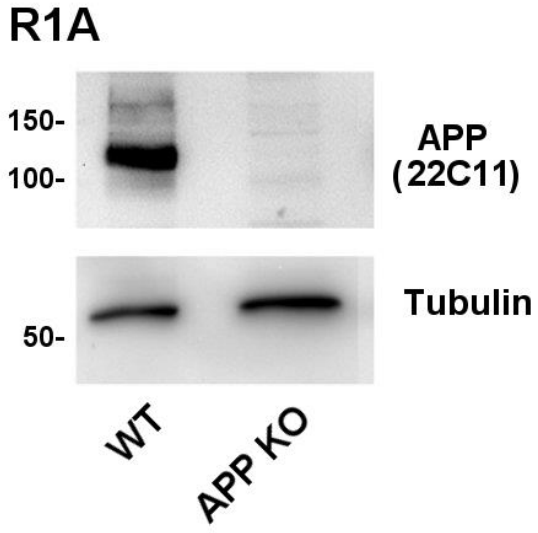

Figure R1A. Characterization of platelets from APP KO mice. Analysis of APP and tubulin expression in platelets from WT and APP KO mice by immunoblotting analysis with specific antibody as indicated on the right**.**

Subsequently, I analyzed in flow cytometry the surface expression of some major platelet glycoproteins using specific antibodies, as reported in the figure R1B. I observed the expression GPIbα (CD42b) and GPV of the complex GPIb-V-IX, the main vWF receptor; CD9 (tetraspannin) which modulates other platelet receptors; integrin $\alpha_{IIb}\beta_3$ (CD41/CD61) which specifically binds to fibrinogen and GPVI and α_2 subunit of integrin $\alpha_2\beta_1$ (CD49b) that represents the principal collagen receptors. No differences in the expression of all these platelet glycoproteins were observed between WT and APP KO mice (figure R1B).

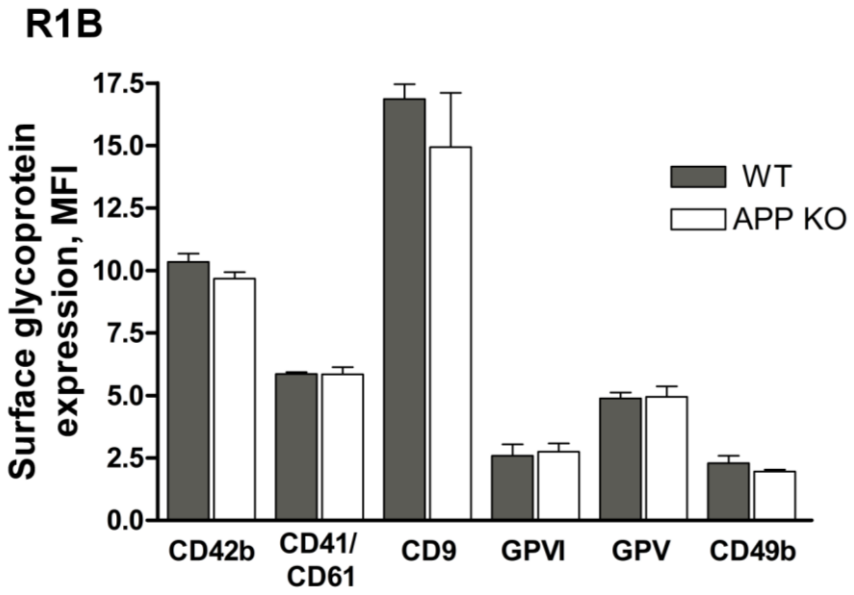

Figure R1B. Characterization of platelets from APP KO mice. Surface expression of different glycoproteins including CD42b (GPIbα), CD41/61 (integrin $\alpha_{IIb}\beta_3$), CD9, GPVI, GPV and CD49b (integrin α_2) on WT (grey bars) and APP KO (white bars) mice was determined by flow cytometric analysis with specific antibodies. N= 7 mice /group.

I have investigated whether the absence of APP might cause abnormalities in platelets and white blood cells count. I found that the number of platelets from APP-deficient mice (818± 88 $x10^3/\mu L$) was significantly lower to that of platelets from WT (1095± 73 $x10^3/\mu L$), whereas no significant differences in the number of circulating white blood cells were observed between the two genotypes (figure R1C).

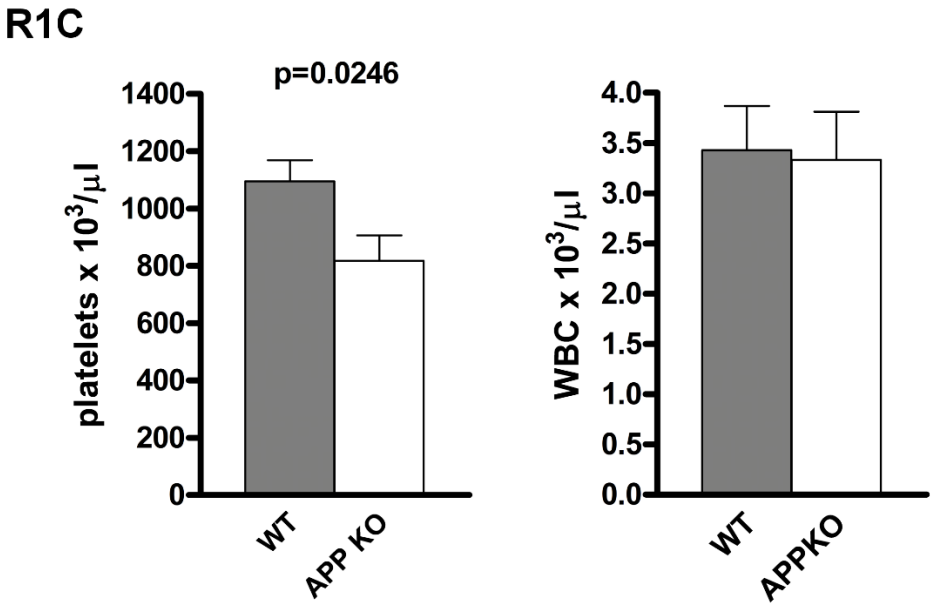

Figure R1C. Characterization of platelets from APP KO mice. Platelet and white blood cell count in the whole blood in WT (grey bars) and APP KO (white bars) mice**.** N= 4 mice /group.

To unravel the reason of the reduced platelet count in APP KO mice I analyzed platelet life span and in this set of experiments mice were first *in vivo* injected with anti-GPIX antibody conjugated with Alexa Fluor 488 to stain platelets. Then, after 24 hours from the injection, whole blood was drawn and was incubated with PE-conjugated anti-GPIbα antibody. Finally, samples were analyzed in flow cytometry and the ratio between Alexa Fluor-positive to PE-positive platelets was determined. The results demonstrated that the significant reduction observed in platelet count of APP deficient mice was not due to a faster platelet clearance, because the life span of circulating platelets was not altered in the absence of APP (figure R1D).

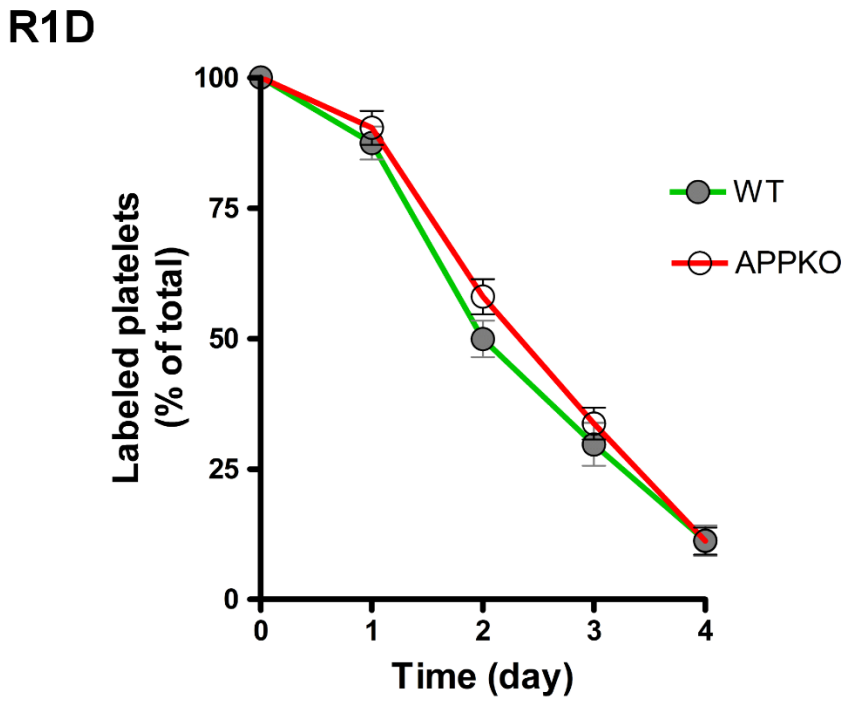

Figure R1D. Characterization of platelets from APP KO mice. Blood was withdrawn from WT and APP KO mice at the indicated points after injection of AlexaFluor488-labeled antibodies to GPIX, and the fraction of labelled to unlabelled platelets was determined. N= 4 mice /group.

Platelet morphology was analyzed in electron microscopy. Figure R1E shows representative images of WT and APP KO platelets at 5600X magnitude (upper panel) and at 28000X magnitude (lower panel). The electron microscopy analysis revealed an overall normal platelet morphology in APP deficient mice, with a comparable number of α- and dense granules between WT and APP KO platelets (figure R1E).

Nevertheless, it has been observed that platelets size was increased in APP KO mice compared to aged matched WT mice. Indeed, precise measurement of platelet diameter (longitudinal axis) revealed that APP KO platelet diameter was 2.74± 0.29μm (n=4 APP KO), whereas WT platelet diameter was 1.84± 0.22μm (n=4 WT), and this difference resulted statistically significant. Consequently, platelet from APP KO mice were slightly but significantly larger than those from WT control mice.

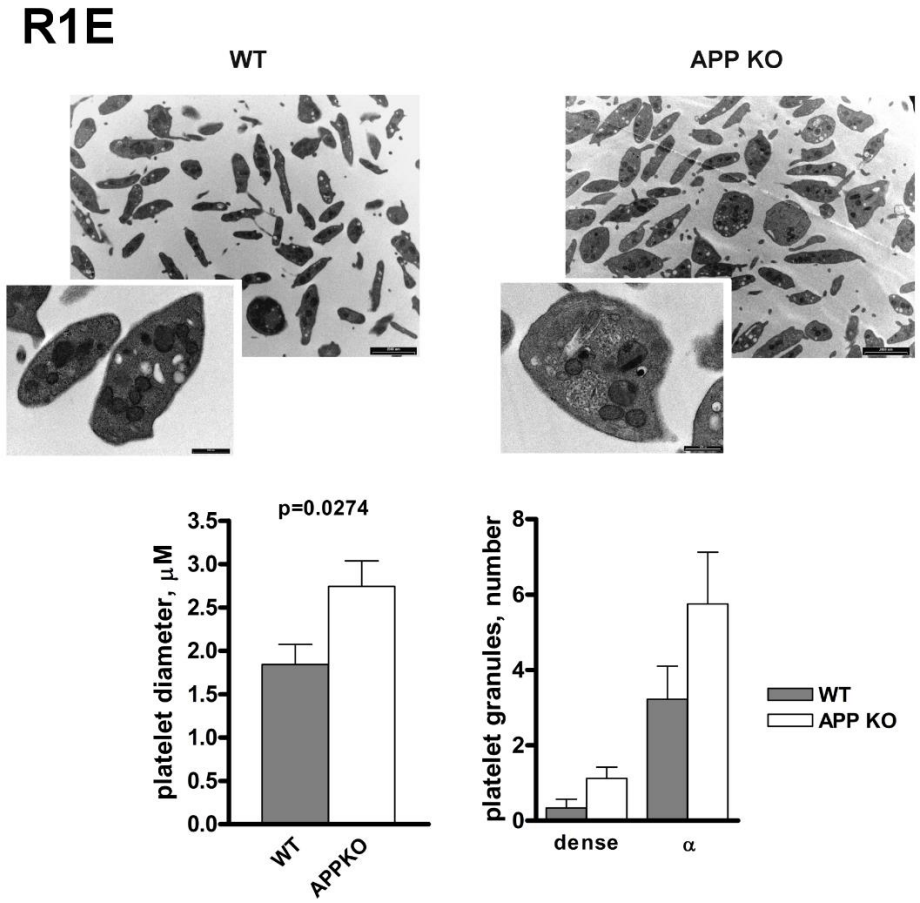

Figure R1E. Characterization of platelets from APP KO mice. (E) Electron microscopy analysis of platelet morphology. Representative images at different magnitude (5600X, upper; and 28000X, lower). Quantification of the mean platelet diameter and number of internal α and dense granules is reported in the histograms. WT (grey bars) and APP KO (white bars) mice. Data have been obtained from the analysis of 50 different platelets from 5 different slides. N= 4 mice /group.

This result suggested a possible alteration of platelet formation in the absence of APP. Therefore, I investigated platelet production from bone marrow megakaryocytes.

Although, the number of mature megakaryocytes differentiated from bone marrow cells was similar in both genotypes, I found a greater percentage of bone-marrow megakaryocytes protruding proplatelets in APP KO mice (figure R1F).

Overall these results suggested that APP may regulate platelet release. In particular, the abnormally proplatelets formation might result in a premature platelet

release and this could explain why I found a reduced number of platelets in circulation in APP KO mice. Unfortunately, I couldn't explain exactly the reasons of the abnormalities found in platelet number and size, which deserve further investigations.

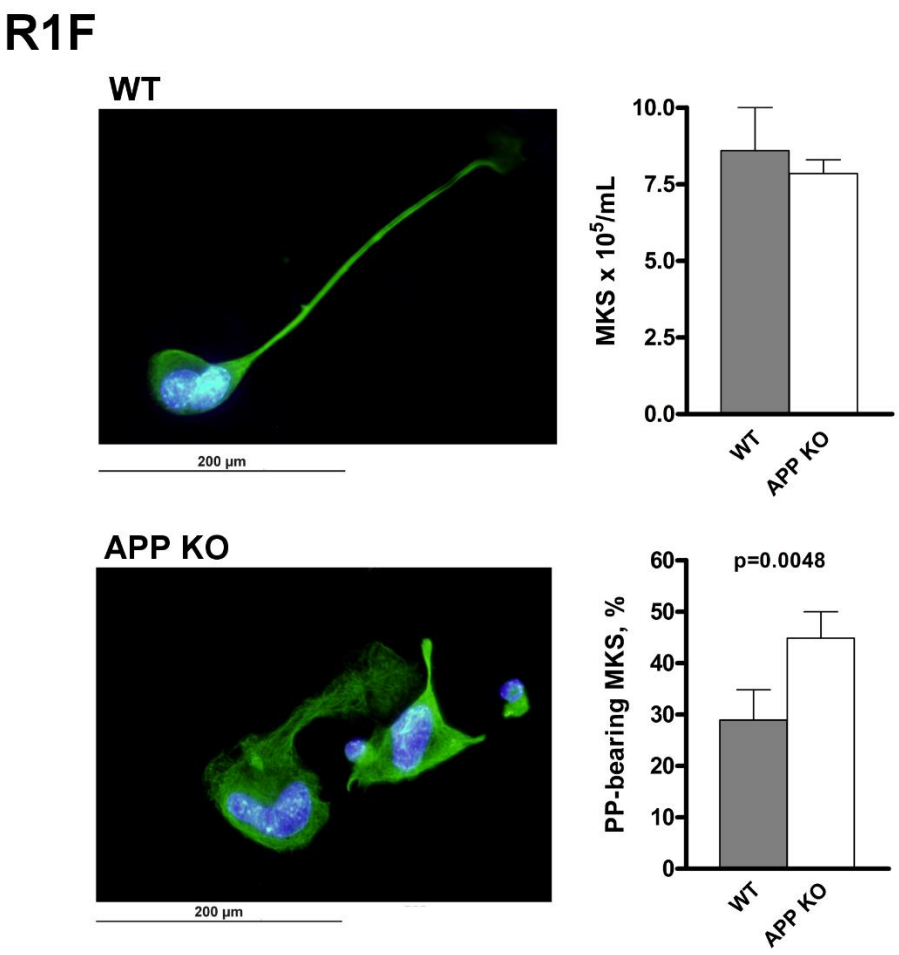

Figure R1F. Characterization of platelets from APP KO mice. Analysis of megakaryocytes and proplatelets formation. Representative images of proplatelets forming megakaryocytes from WT and APP KO mice on staining with anti-tubulin antibody (green) and with Hoechst (blue). Quantification of total megakaryocytes (MKs) and percentage of cells protruding proplatelets (PP) is reported in the histograms. WT (grey bars) and APP KO (white bars) mice. Images are representative of 4 different experiments. N= 4 mice/ genotypes.

2. Analysis of platelet function in APP KO mice

The overall hemostatic process in WT and APP KO mice was evaluated by comparing tail bleeding time. The time required for bleeding cessation (panel i), as well as the amount of blood lost indicated as the amount of hemoglobin (panel ii) were not affected by the absence of APP (figure R2A).

R2A

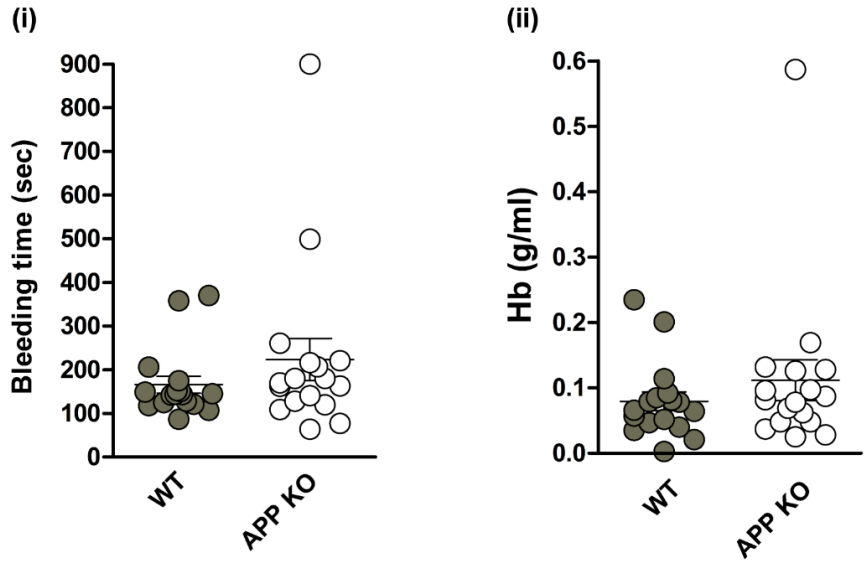

Figure R2A. Analysis of **t**ail bleeding time determined in groups of 17 mice for each genotype and expressed as time required for bleeding cessation **(i)** and amount of blood haemoglobin lost **(ii)**. Each symbol represents 1 animal. WT (grey dot) and APP KO (white dot).

One parameter of platelet activation is the aggregation. Washed platelets from WT and APP KO mice ($3x10^8$/mL) were stimulated with different doses of the most common soluble platelets agonists, including thrombin receptor activated peptide TRAP4, convulxin, thromboxane analogue U46619 and ADP, at the concentration indicated in the figure R2Bi. Platelet aggregation was continuously monitored over 5

minutes and representative traces are reported in the figure R2Bi. APP null platelets displayed normal aggregation.

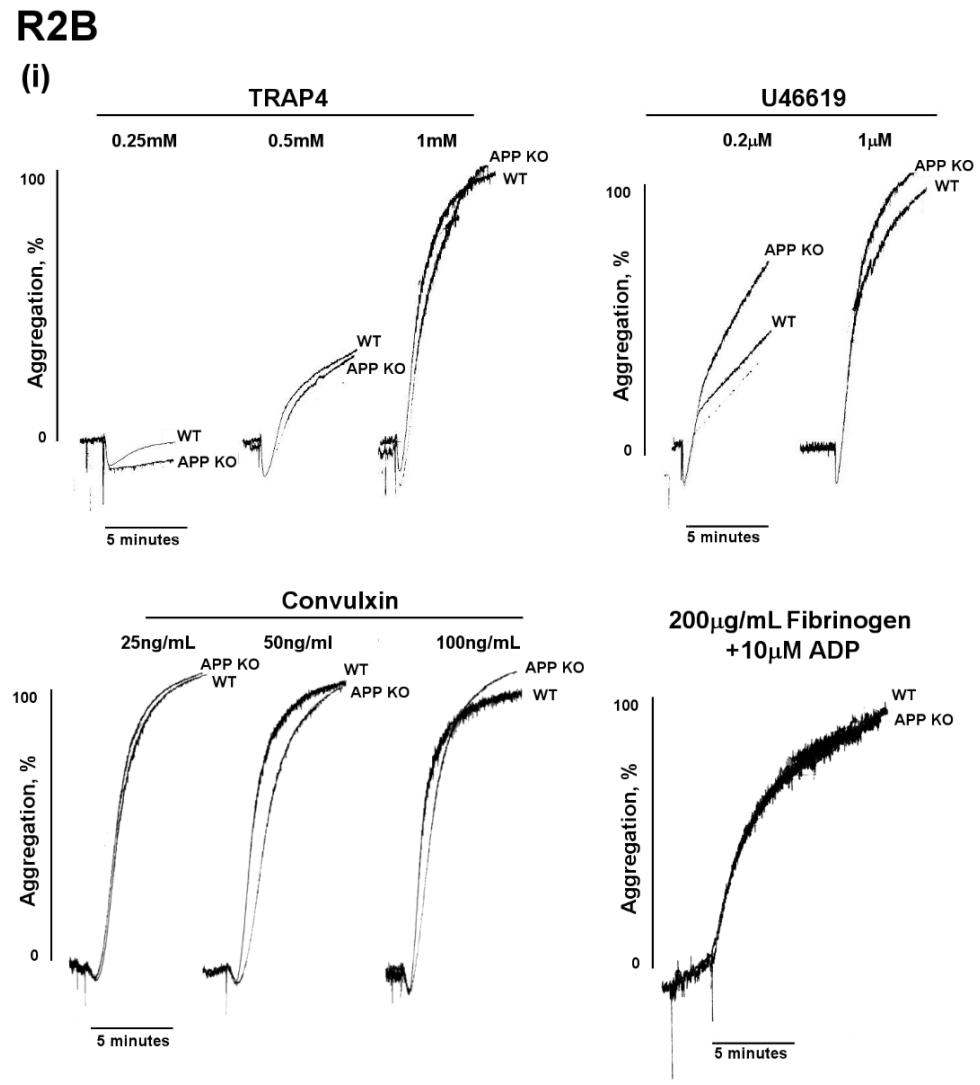

Figure R2B. Analysis of platelet aggregation. (i) Washed platelets ($3x10^8$/mL, 0.25mL) from WT and APP KO mice were stimulated in aggregometer with different concentrations of TRAP4 (0.25mM, 0.5mM, 1mM), U46619 (0.2μM and 1μM), convulxin (25ng/mL, 50ng/mL, 100ng/mL), and ADP (10μM) measured on addition of purified fibrinogen (200μg/mL) as indicated. Aggregation was monitored as increase light transmission up to 5 minutes. Traces in the figure are representative of four different experiments. N= 4 mice/group.

Since previous study in my lab demonstrated that Aβ peptides are able to trigger platelet aggregation (Canobbio et al., 2014), I analyzed platelet aggregation induced by different Aβ peptides: the synthetic $A\beta_{25-35}$ peptide and the two physiological peptides, $A\beta_{1-40}$ and $A\beta_{1-42}$. $A\beta_{25-35}$ is a synthetic peptide corresponding to the 11 amino acids located in the intermembrane domain of APP (Kang et al. 1987), which corresponds to a fragment of $A\beta_{1-40}$ and $A\beta_{1-42}$ peptides and is often selected as a model for full-length Aβ because it retains both its physical and biological properties (Kaminsky et al., 2010).

Here it has been observed that platelet aggregation induced by 10μM of each Aβ peptides was comparable in WT and APP KO platelets (figure R2Bii).

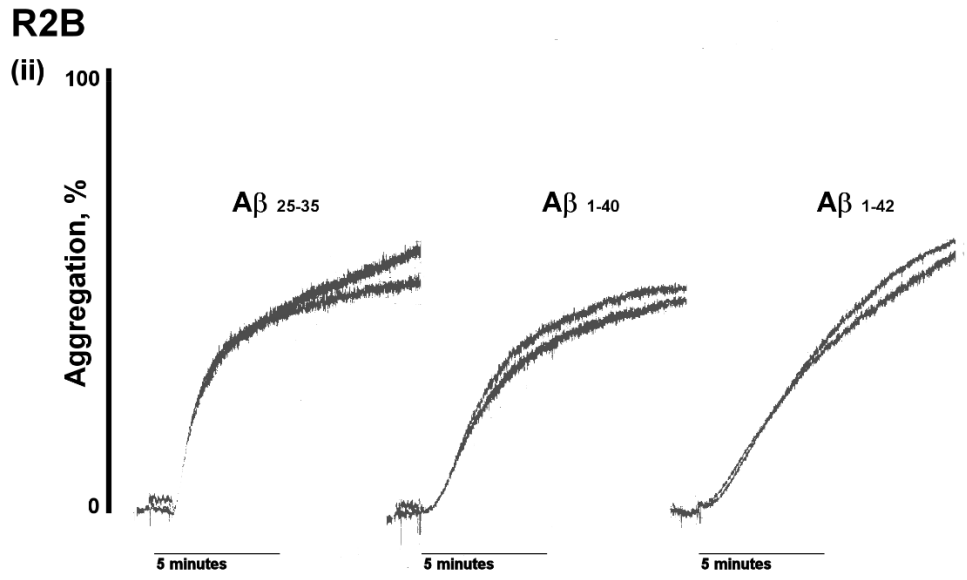

Figure R2B. Analysis of platelet aggregation. (ii) Aggregation of washed platelets ($3x10^8$/mL, 0.25mL) from WT and APP KO mice induced by 10μM of Aβ peptides: $A\beta_{25-35}$, $A\beta_{1-40}$ and $A\beta_{1-42}$. Aggregation was monitored as increased light transmission up to 5 minutes. Traces in the figure are representative of three different experiments. N= 3 mice/group.

Consistent with this result, integrin $\alpha_{IIb}\beta_3$ inside-out activation, measured as the ability of integrin to bind FITC-fibrinogen, was comparable in resting and stimulated APP KO platelets compared to WT platelets (figure R2C).

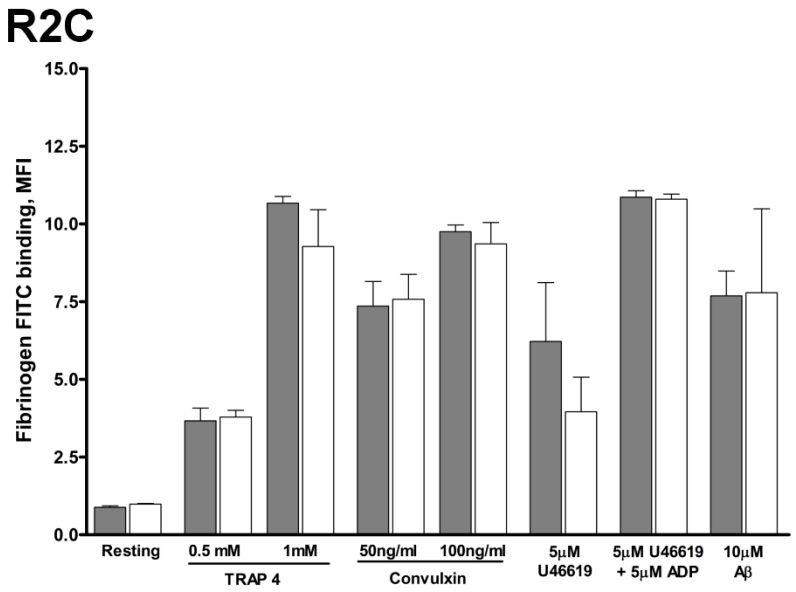

Figure 2C. Analysis of platelet function. Flow cytometric analysis of agonist-induced integrin $\alpha_{IIb}\beta_3$ activation, measured as binding of fluorescein isothiocyanate-labelled fibrinogen to WT (grey bars) and APP KO (white bars) platelets resting or stimulated with TRAP4 (0.5mM and 1mM), convulxin (50ng/mL and 100ng/mL), U46619 (5μM), ADP (5μM) and $A\beta_{25-35}$ (10μM), as indicated in each panel. Data are expressed as means ± SEM. N= 4 mice/group.

I also investigate α-granules secretion, analyzing P-selectin (CD62P) exposure on platelet plasma membrane in resting platelets or upon stimulation with different agonists, including thrombin, convulxin and $A\beta_{25-35}$. As shown in the figure R2D, α-granules secretion occurred normally in the absence of APP, as P-selectin expression was comparable in WT and APP KO mice, either in resting and activated cells (figure R2D).

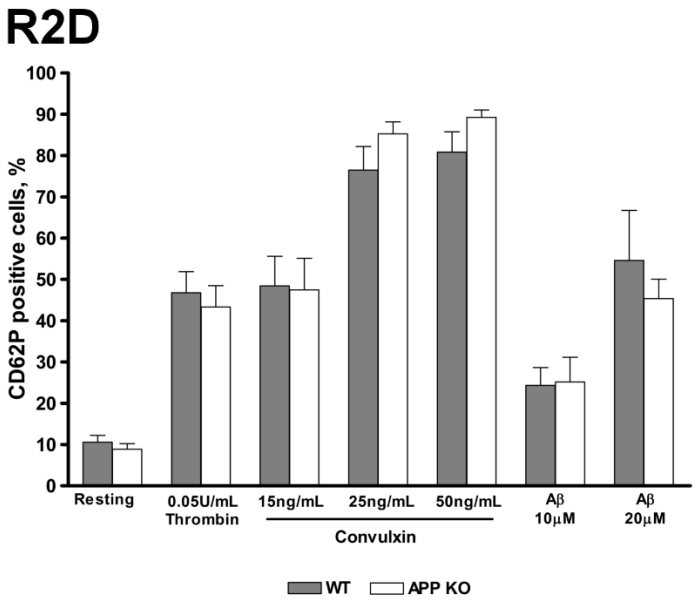

Figure 2D. Analysis of platelet function. Flow cytometric analysis of P-selectin expression on platelet surface either in WT (grey bars) and APP KO (white bars) platelets both in resting or upon stimulation with thrombin (0.05U/ml), convulxin (15ng/mL, 25ng/mL and 50ng/mL), and $A\beta_{25-35}$ (10μM and 20μM), as indicated in each panel. Results are the means ± SEM. N= 4 mice/group.

Overall these results demonstrated that APP deficiency did not significantly affect platelet activation.

3. Investigation of the role of APP in platelet adhesion

A role for APP in cell adhesion is supported by biochemical interaction of APP with extracellular matrix proteins, such as heparin, and heparan sulphate proteoglycans via its heparin binding domain HBD. In addition, APP also engages other proteins like laminin, glypican and F-spondin (Müller et al., 2017).

I analysed the ability of platelets isolated from both genotypes to adhere to heparin. Washed platelets isolated from WT and APP KO mice were let to adhere to heparin for 60 minutes in the presence of 1mM $CaCl_2$. Subsequently, adherent platelets were fixed with 3% PFA, permeabilized with 0.25%TRITON and then visualized in immunofluorescence after staining of actin filaments with phalloidin-TRITC. Representative images of heparin adherent platelets are shown in figure R3A. I measured platelet adhesion (as number of adherent platelet per mm^2) and as expected I found that APP null platelets were unable to adhere to heparin (figure R3A). In addition, also the analysis of the mean platelet area, which is indicative of platelet spreading was significantly reduced in APP KO platelets, further confirming the role of APP in mediating the adhesion to heparin.

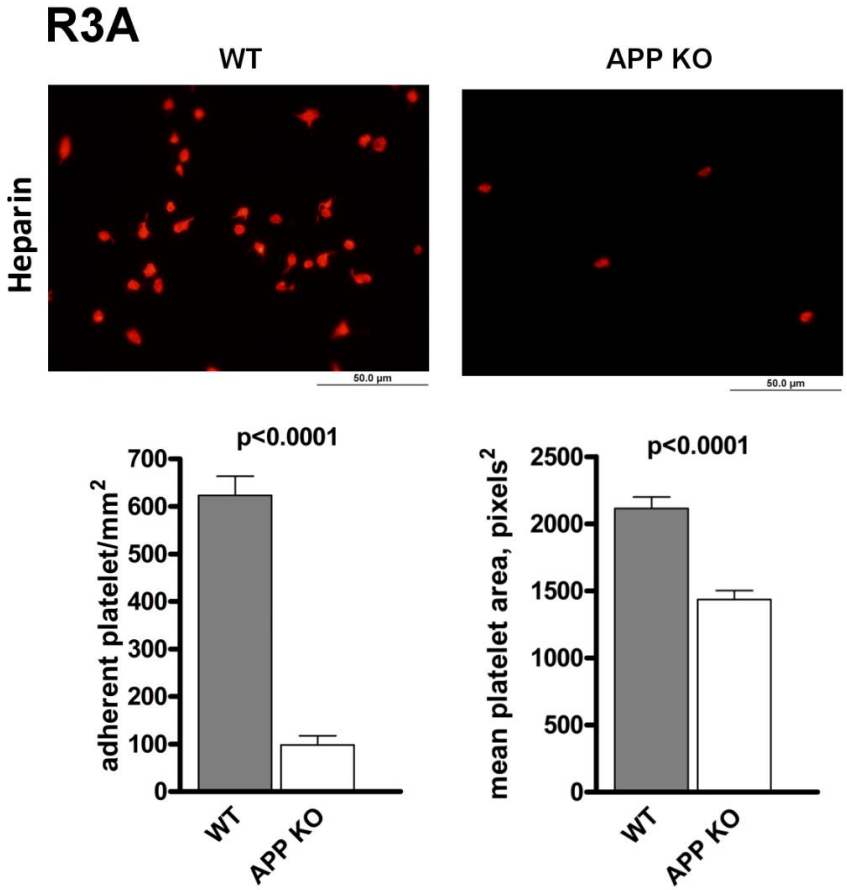

Figure R3A. Analysis of platelet adhesion to heparin. APP KO and control platelets were let to adhere to dishes coated with 10U/mL heparin in the presence of 1mM $CaCl_2$ for 60 minutes. Adherent platelets were fixed, permeabilized and stained TRITC-conjugated phalloidin. Representative images at 1000x magnification of adherent platelets to heparin are shown. Quantification of platelet adhesion (evaluated as number of adherent platelets/mm^2) and spreading (measured as mean platelet area/$pixels^2$) are reported on the right. WT (grey bars) and APP KO (white bars). Images in the figure are representative of four different experiments.

Subsequently, I analysed the ability of APP KO platelets to adhere to collagen in static condition (figure R3B) as well as under arterial shear stress (figure R3C). In the first case, WT and APP KO platelets ($4x10^7$/mL) were allowed to adhere to immobilized fibrillar collagen for 60 minutes. Adherent cells were permeabilized and stained with TRITC-phalloidin. Adhesion (as number of adherent platelet/mm^2) and spreading (as mean platelet area/$pixels^2$) were evaluated as described in method 8. No

differences in term of platelet adhesion and spreading were observed between WT and APP KO platelets adherent to collagen in static experiment (figure R3B).

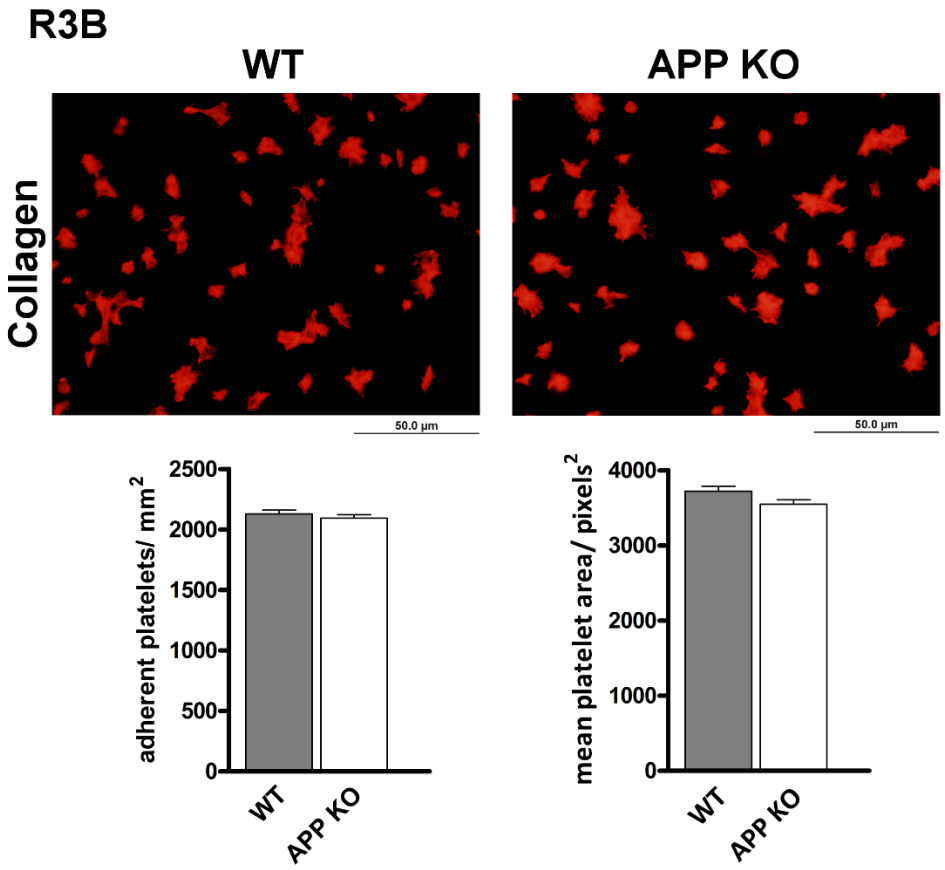

Figure 3B. Analysis of platelet adhesion to collagen. WT and APP KO platelets ($4x10^7$/mL) were let to adhere to dishes coated with 25µg/ml collagen in the presence of 2mM $MgCl_2$ for 60 minutes. Adherent platelets were fixed, permeabilized and stained TRITC-conjugated phalloidin. Representative images at 1000x magnification of adherent platelets to collagen are shown. Quantification of platelet adhesion and spreading, evaluated as number of adherent platelets/mm^2 and mean platelet area/$pixels^2$ respectively, are reported on the right reported on the right. WT (grey bars) and APP KO (white bars). Images in the figure are representative of four different experiments. N= 4 mice/group.

Correspondingly, the ability of platelet to adhere to collagen and to form microthrombi in arterial flow condition (1000/s) was essentially similar using WT and APP KO whole blood (figure R3C). In these experiments, fluorescently labelled platelets in whole blood from WT and APP KO mice were perfused over immobilized

fibrillar collagen at a shear rate of 1000/second for 5 minutes. Platelet adhesion and thrombus formation was then evaluated after additional perfusion with HEPES flow buffer for 10 minutes. Thrombus formation was measured as percentage of area covered by adherent platelets. As shown in figure R3C WT and APP KO platelets were able to adhere on collagen under arterial flow condition similarly, as also confirmed by the quantification of surface covered reported in the histogram.

Therefore, I conclude that platelet adhesion and thrombus formation on collagen-coated surface resulted comparable between WT and APP KO mice (figure R3C).

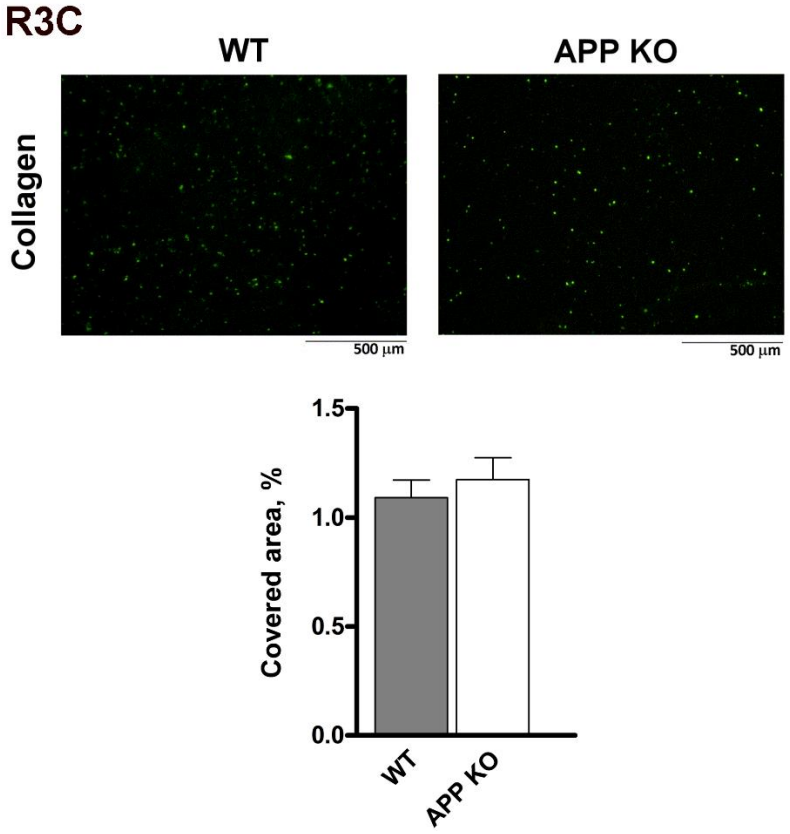

Figure 3C. Analysis of thrombus formation on collagen under flow. CFSE-labelled platelets in whole blood from WT and APP KO mice were perfused over immobilized fibrillar collagen (50µg/mL) at a share rate of 1000/s for 5 minutes. Images are taken after brief rinse of the coverslips with HEPES flow buffer. Thrombus formation on the coverslips was evaluated by measuring the covered area in 10 different and randomly taken microscopic fields and results were reported in histogram as percentage of covered areas. Images in the figure are representative of three different experiments. N= 3 mice/group.

APP is known to localize with integrin on the surface of axon and at sites of adhesion in neuronal cells and to participate in integrin-mediated cell adhesion (Young-Pearse TL et al., 2008). To assess the role of APP in integrin outside-in signalling in platelets, I allowed control and APP-null platelets to adhere on fibrinogen, and I found that adhesion to fibrinogen was similar between the two genotypes (figure R3Di) either in term of number of adherent platelets and of mean area of spreading. Similarly, platelets were let to adhere to vWF in the presence of botrocetin cofactor for 60 minutes and no differences in adhesion and spreading to vWF were reported between WT and APP KO platelets (Figure R3Dii).

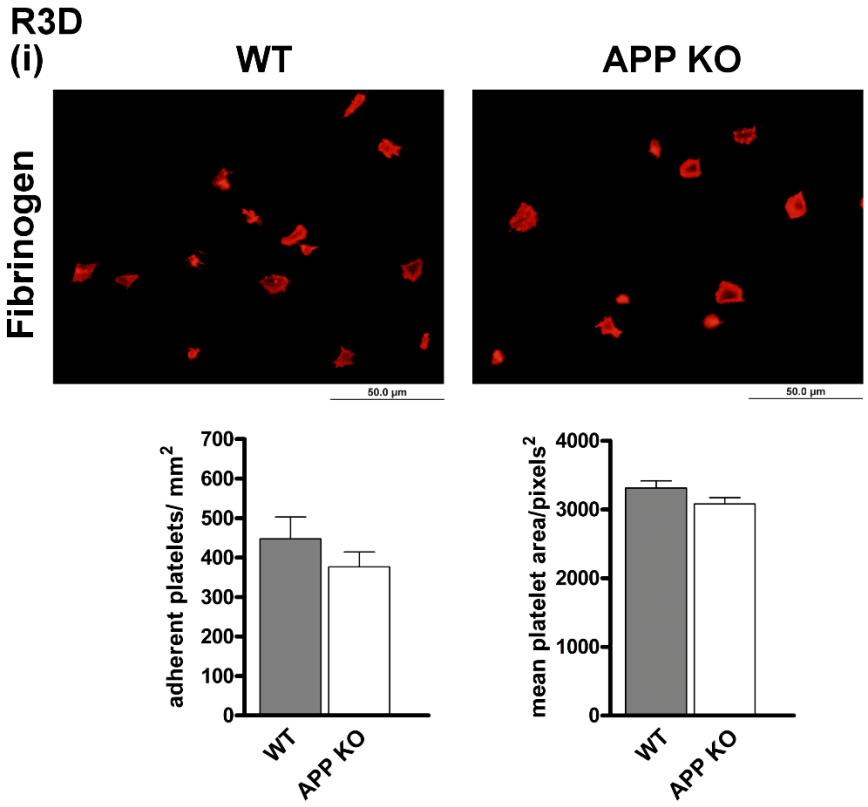

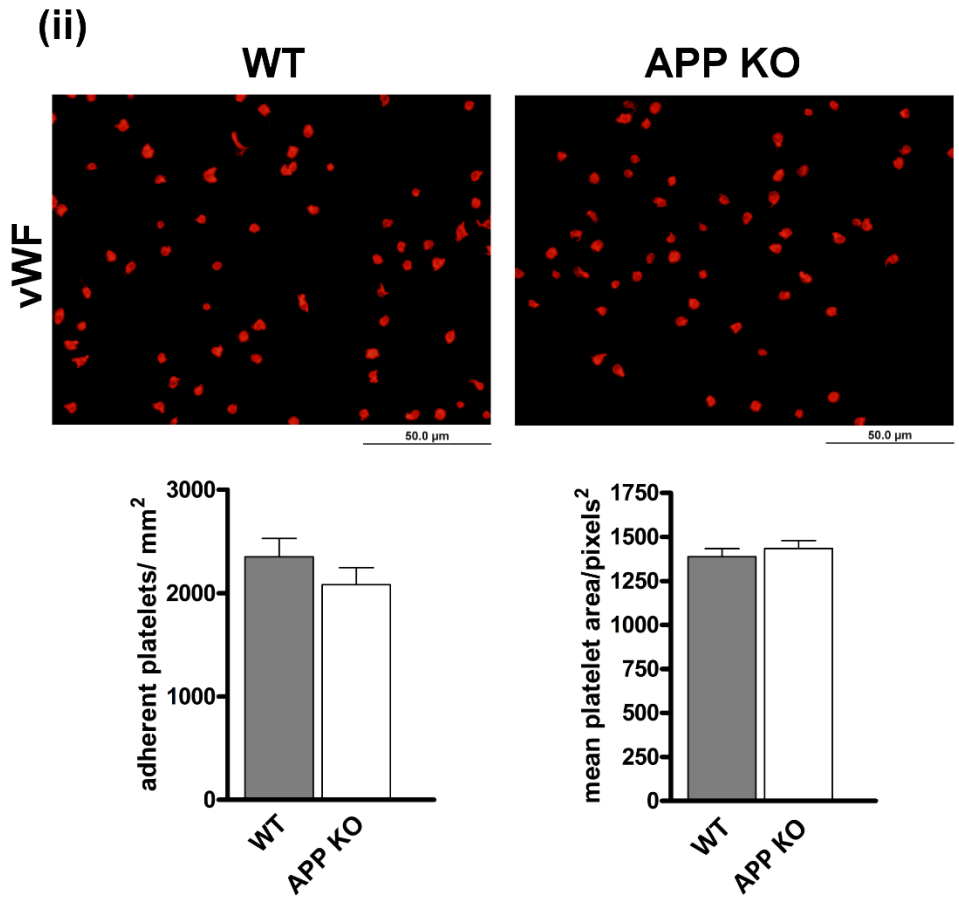

Figure R3D. Analysis of platelet adhesion. WT and APP KO platelets were let to adhere to dishes coated with 100µg/ml fibrinogen in the presence of 1mM $CaCl_2$ (panel **i**) and to 10µM vWF in the presence of botrocetin (5µg/ml) (panel **ii**) for 60 minutes. Adherent platelets were fixed, permeabilized and stained TRITC-conjugated phalloidin. Representative images at 1000x magnification of adherent platelets are shown. Quantification of platelet adhesion was evaluated as number of adherent platelets/mm^2 whereas platelet spreading was measured as mean platelet area/$pixels^2$. WT (grey bars) and APP KO (white bars). Images in the figure are representative of four different experiments. N= 4 mice/group.

It has been previously demonstrated that platelets adhere to immobilized Aβ peptides in static conditions. Canobbio and collaborators analyzed adhesion of human platelets to Aβ peptides by using three different peptides: the physiological $Aβ_{1-40}$ and $Aβ_{1-42}$ and the synthetic $Aβ_{25-35}$ that retains the biological properties of the entire Aβ peptide (Canobbio et al., 2013).

Moreover, there is a large body of evidences to indicate that APP can form homo- and hetero- complexes (Soba et al., 2005) suggesting that APP might be involved in adhesion processes, and in particular, Yankner and colleagues reported that Aβ is a candidate ligand for APP (Lorenzo et al., 2000).

To investigate this hypothesis platelets isolated from WT and APP KO mice were let to adhere to Aβ peptides for 60 minutes and adherent platelets were visualized by immunofluorescence after staining of actin filament with phalloidin-TRITC.

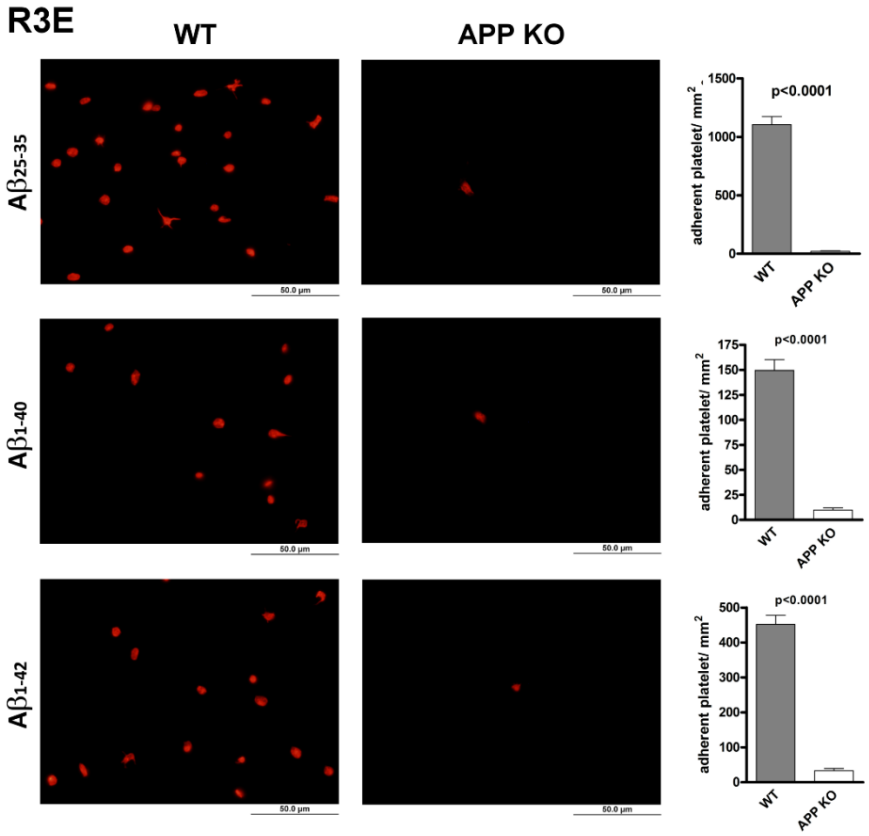

Figure R3E. Analysis of platelet adhesion to immobilized Aβ peptides. WT and APP KO platelets ($4x10^7$/mL) were let to adhere to dishes coated with 10μM $Aβ_{1-40}$ and $Aβ_{1-42}$ and the synthetic $Aβ_{25-35}$ in the presence of 1mM $CaCl_2$ for 60 minutes. Adherent platelets were fixed, permeabilized and stained TRITC-conjugated phalloidin. Representative images at 1000x magnification of adherent platelets to collagen are shown. In the histograms was reported the quantification of platelet adhesion (as number of adherent platelets/mm^2) of WT (grey bars) and APP KO (white bars) mice. Images in the figure are representative of four different experiments. N= 4 mice/group.

I found that in addition to human platelets, also WT platelets were able to adhere over all Aβ peptides, even though with different kinetics. On the contrary, APP null platelets were unable to adhere to immobilized Aβ peptides (figure R3E).

To further validate this result, I investigated the ability of cells constitutively expressing increased amount of APP to adhere to immobilized Aβ peptides. I used three different cellular models: Human Embryonic Kidney cells that express endogenous APP level (HEK293), HEK293 cells stably transfected with endogenous APP751 (HEK293/APP751) (Cenini et al., 2010) and malignant human breast cancer cells MDA-MB-231, that have been shown to significantly overexpress APP (Lim et al., 2014). Initially, I verified the expression APP in the three cellular models by immunoblotting with antibody 22C11 that specifically recognized the murine and human APP (figure R3Fi). Equal loading of the samples was proved by subsequent immunoblotting with anti-tubulin antibody. Moreover, platelet sample was loaded as positive control. Densitometric analysis revealed that APP expression is approximately 6.35 fold in HEK293/APP751 and 17.33 fold in MDA-MB-231 compared to HEK293 (figure R3Fii).

Same number of cells ($5x10^5$/mL) were let to adhere to $A\beta_{1-40}$ for 60 minutes and adhesion was evaluated by staining of nuclei of adherent cells with Hoechst. I found that HEK293/APP751 and MDA-MB-231 cells adhered more efficiently than HEK293 cells. As shown in figure R3Fiii the number of adherent cells seem to increase proportionally with APP expression level, confirming the hypothesis that Aβ may be a ligand for APP (figure R3Fiii).

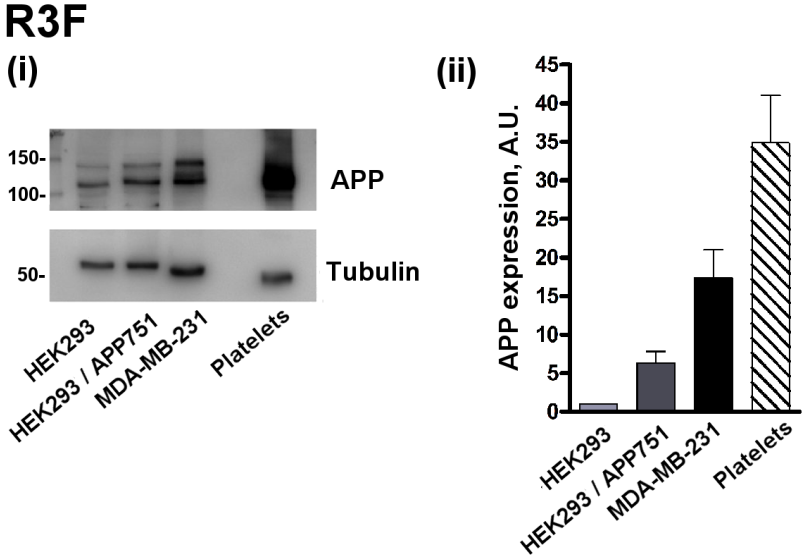

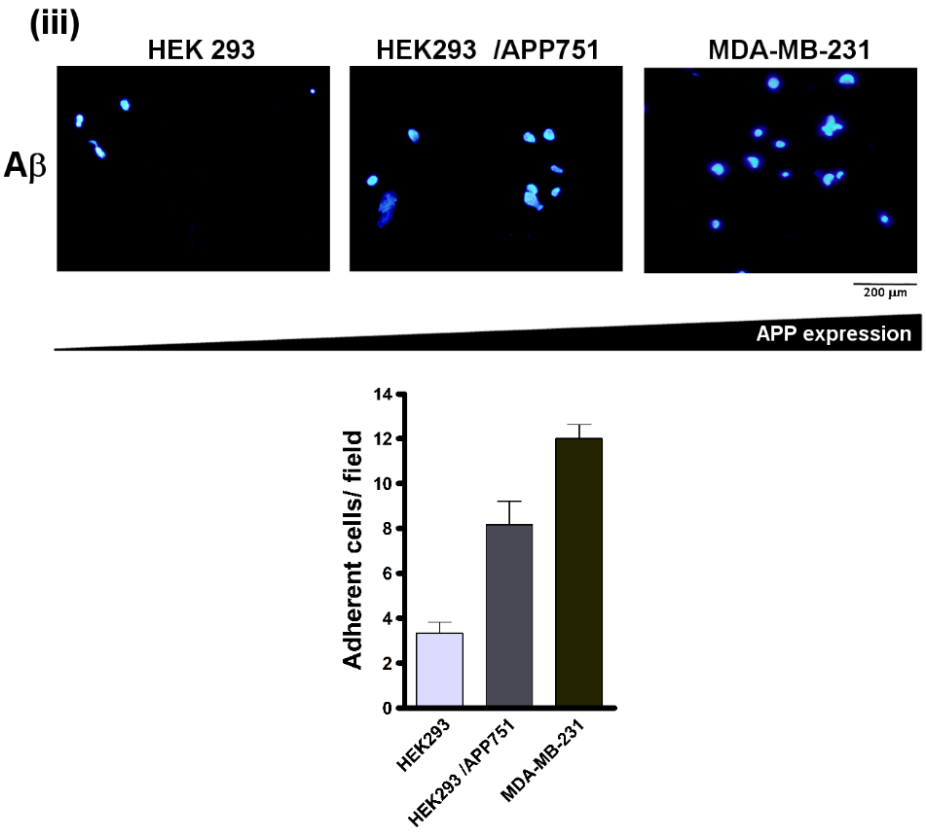

Figure R3F. Study of cell adhesion to Aβ $_{1-40}$. (i) Analysis of APP and tubulin expression in three different cellular models: HEK293, HEK293 stably transfected with APP751 (HEK293/APP751) and MDA-MB-231 by immunoblotting with specific antibodies as indicated on the right. Platelet sample was used as positive control. **(ii)** The histogram shows the quantitative evaluation of APP expression in the three different cell types and in platelets, according to the densitometric analysis of the immunoblotting reported in panel i. **(iii)** Cells were allowed to adhere to $A\beta_{1-40}$ (10µM) for 60 minutes and then stained with Hoechst. Representative images at 100X magnification (right panel) are shown. Analysis of cell adhesion (indicated as adherent cells/field) was reported in the histogram.

Since, it has been previously observed that Aβ increased the ability of human platelets to adhere to collagen under flow condition (Canobbio et al., 2015), I decided to analyzed thrombus formation on collagen also in the presence of Aβ peptides during coating.

In these set of experiments, whole blood drawn from WT and APP KO mice was incubated with CFSE to label platelets and then perfused for 5 minutes under

arterial shear stress (1000/second) over immobilized fibrillar collagen alone or in the presence of $A\beta_{25-35}$ and $A\beta_{1-42}$ peptides. The firmness of formed thrombus was then assessed after secondary perfusion with HEPES flow buffer for other 5 minutes. I found that the presence of Aβ together with collagen increase thrombus formation under flow in WT whole blood (figure R3Gi), confirming the previous results obtained with human platelets.

Although previously it has been observed that platelet adhesion and thrombus formation on collagen under flow in APP KO resulted similar to WT control animals (figure R3C and figure R3Gi upper panels), here, I found that the absence of APP on platelets eliminate the increase of platelet adhesion to collagen in the presence of Aβ observed in WT mice (figure R3Gi lower panels and figure R3Gii). Indeed, the statistical analysis in figure R3G iii showed that WT platelets were able to adhere on collagen under flow, and platelet adhesion and thrombus formation was significantly increased by coincubation of collagen with both Aβ peptides. On the contrary, the presence of Aβ peptides together with collagen does not increase thrombus formation in APP KO whole blood. In line with the result shown in static conditions, also in flow conditions it has been demonstrated that APP binds to Aβ.

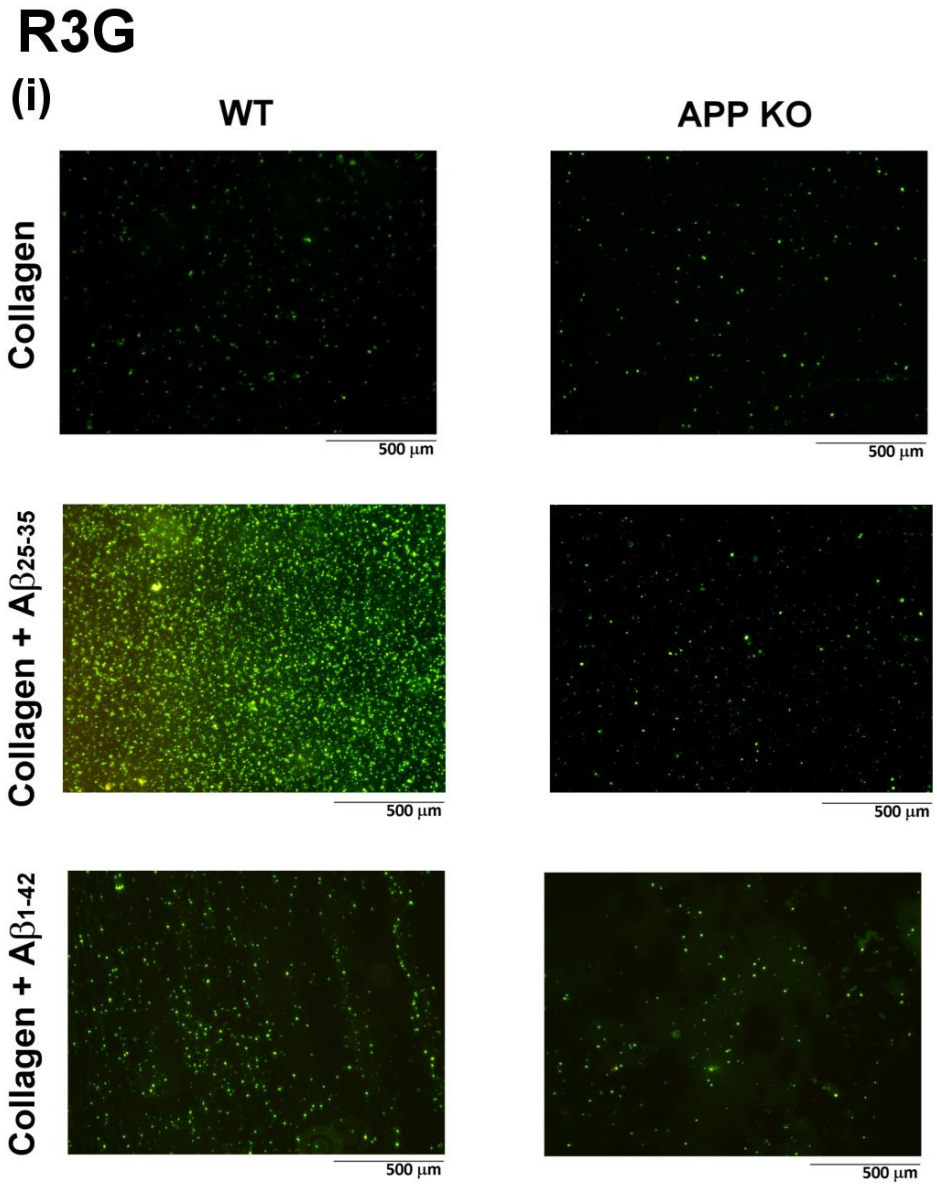
R3G
(i)
WT
APP KO
Collagen
Collagen + Aβ25-35
Collagen + Aβ1-42
500 μm
500 μm
500 μm
500 μm
500 μm
500 μm

(ii)

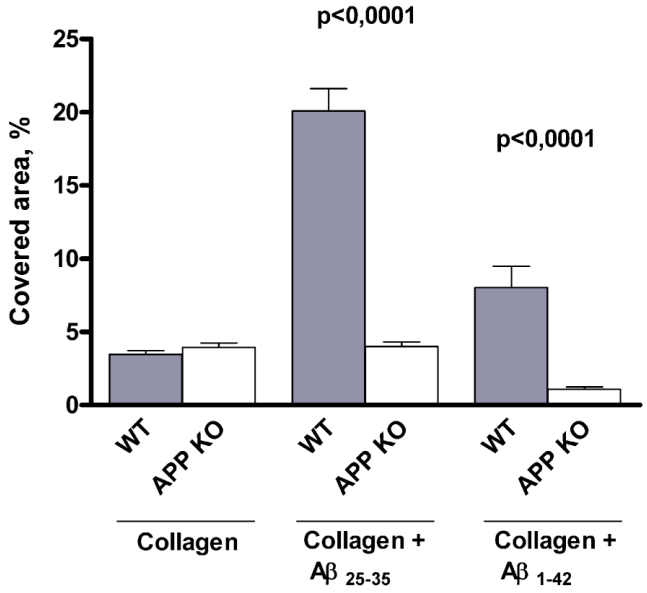

Figure 3G. Analysis of thrombus formation in WT and APP KO mice. (i) CFSE-labelled platelets in whole blood from WT control and APP KO mice were perfused over immobilized fibrillar collagen (50μg/ml) alone or in the presence of $A\beta_{25-35}$ and $A\beta_{1-42}$ peptides (10μM) at a share rate of 1000/s for 5 minutes. Images are taken after brief rinse of the coverslips with HEPES flow buffer. **(ii)** Thrombus formation was evaluated by measuring the covered area in 10 different and randomly taken microscopic fields and results were reported in histogram as percentage of covered areas. WT (grey bars) and APP KO (white bars) mice. Images in the figure are representative of three different experiments. N= 3 mice/group.

4. Analysis of *in vivo* thrombus formation

Xu and co-workers have reported that transgenic mice with specific overexpression of APP in both brain and platelets shown a reduced thrombotic capacity and in contrast APP KO mice displayed a significant increase in thrombosis (Xu et al., 2005; Xu et al., 2007). These studies supported a role for APP in regulating cerebral thrombosis.

However, the potential contribution of APP in regulating peripheral thrombosis has never been tested. Therefore, in collaboration with Dr.ssa Stefania Momi and Prof. Paolo Gresele from the Department of Internal Medicine of University of Perugia we performed *in vivo* thrombosis models. We analyzed arterial thrombosis, deep vein thrombosis and pulmonary thromboembolism.

To unravel the contribution of APP in **arterial thrombosis**, we analyzed a model of photochemical induced femoral artery thrombosis in mice infused with rose Bengal, as described in method 18. The formation of an occlusive thrombus was monitored by measuring the blood flow on the exposed artery with a laser Doppler probe. Figure R4A shows that blood flow cessation (indicated as time needed for complete artery occlusion) was comparable in WT and APP KO mice, indicating that APP is not involved in peripheral artery thrombosis (Figure R4A).

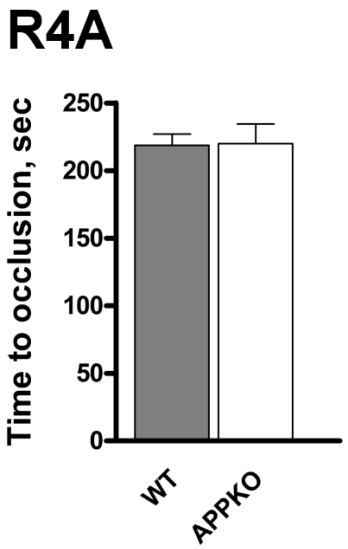

Figure R4A. Study of arterial thrombosis in WT and APP KO mice. Photochemical-induced arterial thrombosis evaluated as time required for occlusion of femoral artery measured by laser Doppler in WT (grey bars) and APP KO (white bars) mice. Data are the mean ± SEM of measurements performed on 5 animals for both genotypes.

Deep vein thrombosis was analyzed using the inferior vena cava (IVC) stenosis model (method 18). In these experiments, ligation of IVC caudal to the renal veins was performed. Only a needle was used to create stenosis and was removed during the course of the procedure, creating a reduction of blood flow of approximately 80%, without endothelial damage in the area of ligation. After 24 and 48 hours from surgery, animals were euthanized, and the formed thrombi were isolated and measured. It has been observed that, as expected, ligation of IVC produced the formation of occlusive thrombi in WT mice. Interestingly, as shown in panel i of figure R4B, APP KO mice developed clearly larger thrombi than WT mice, with a significant increase of both the length and the weight of collected venous thrombi both after 24 and 48 hours from IVC ligation (figure R4B i e ii).

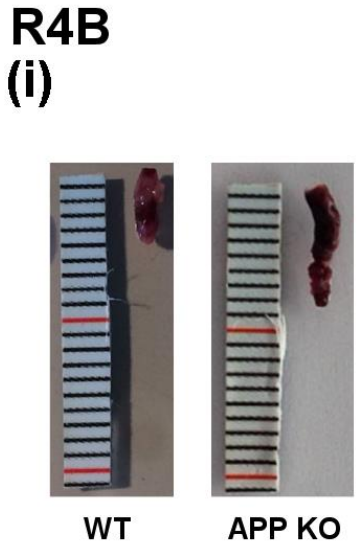

Figure R4B. Analysis of deep vein thrombosis in WT and APP KO mice. Thrombus formation in the IVC was induced by vein ligation. Thrombi were isolated 24 or 48 hours after surgery. **(i)** Representative image showing the different size of thrombi from WT and APP KO mice after 24 hours of ligation.

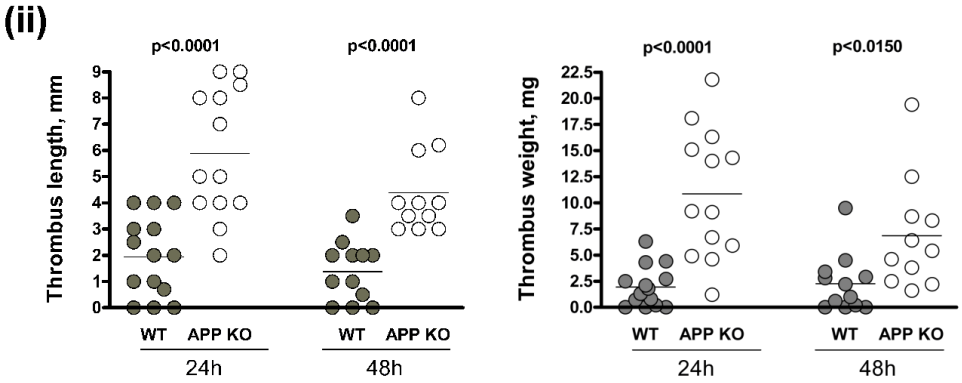

Figure R4B. Analysis of deep vein thrombosis in WT and APP KO mice. Thrombus formation in the IVC was induced by vein ligation. Thrombi were isolated 24 or 48 hours after surgery from WT and APP KO mice. **(ii)** Quantification of thrombus length and weight at 24 and 48 hours of ligation. Each symbol represents one animal. Grey symbols, WT platelets; white symbols, APP KO platelets.

After 48 hours from IVC ligation a slightly reduced size of thrombi was observed in both genotypes, and it could be explained as the result of thrombus embolization.

To verify this hypothesis, we collected the lung after 48 hours from IVC ligation and prepared different sections then stained with phosphotungstic acid-hematoxylin (PTAH), that specifically recognized fibrin deposits. As shown in the figure R4C APP deficiency results in an enhanced fibrin deposition into the lung vessels, as indicated by the arrows. The quantification of the occluded vessels demonstrated a significant increase of the percentage of occluded vessels in APP KO mice (figure R4C).

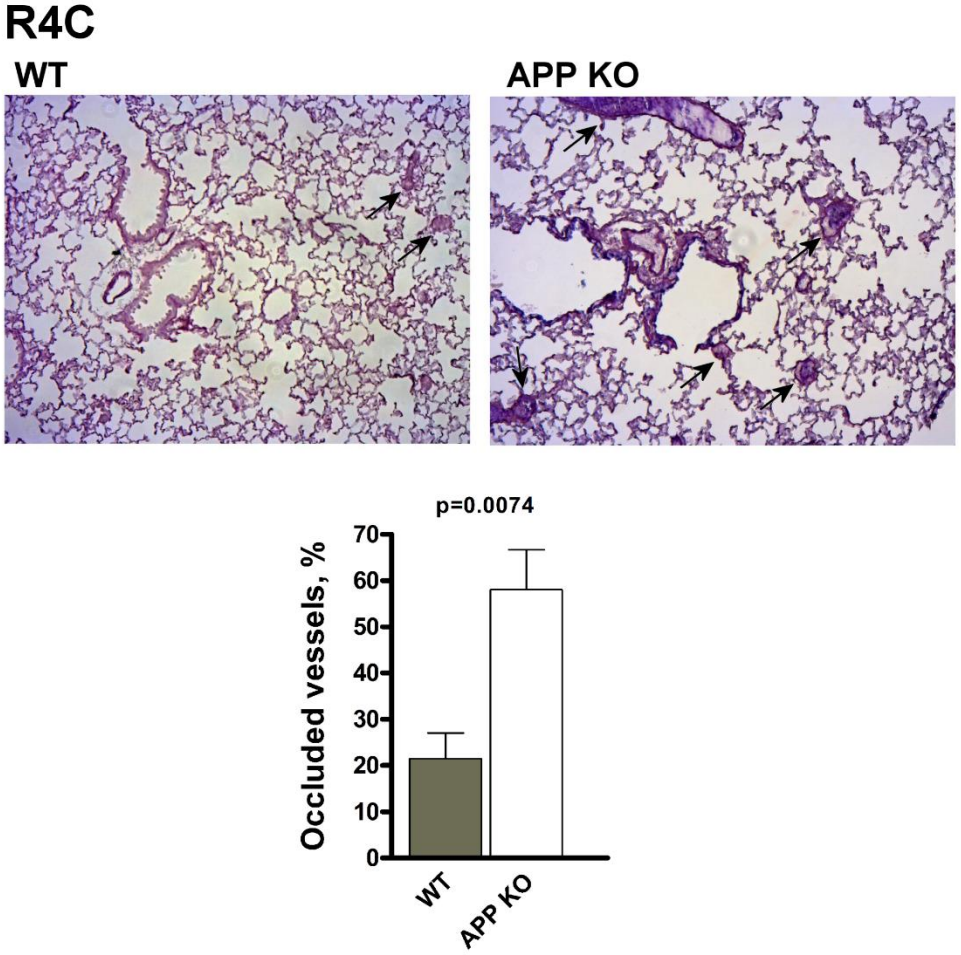

Figure R4C. Analysis of thrombus embolization. Staining of lung sections from WT or APP KO with phosphotungstic acid-hematoxylin. Samples were prepared 48 hours after IVC ligation. Fibrin-occluded vessels are indicated by the arrows. Analysis of the percentage of occluded vessel observed in the 2 genotypes was reported in the histogram. WT (grey bar) and APP KO (white bar). Data are presented as mean ± SEM. N =5.

In contrast to arterial thrombosis, that relies principally on platelet function, deep vein thrombosis is a complex process resulting from the contribution of both blood cells and vascular endothelium, as extensively illustrated in the introduction of this PhD thesis. Therefore, to verify the role of blood derived APP in DVT we compared venous thrombosis in WT mice transplanted with bone marrow cells from APP KO mice (shown as $WT^{APP\ KO}$) and WT mice transplanted with bone marrow

cells from WT mice (indicated as WT^{WT}), as also described in method 19. Although the size and weight of venous thrombi were overall reduced in all chimeric mice, transplantation of bone marrow cells from APP KO mice into recipient WT mice induced the formation of thrombi significantly larger than those observed in WT mice transplanted with WT bone marrow cells (figure R4D). These results are perfectly in line with the previous analysis of DVT in WT and APP KO mice, and in addition demonstrated the importance of blood cells-derived APP in the protection from venous thrombosis.

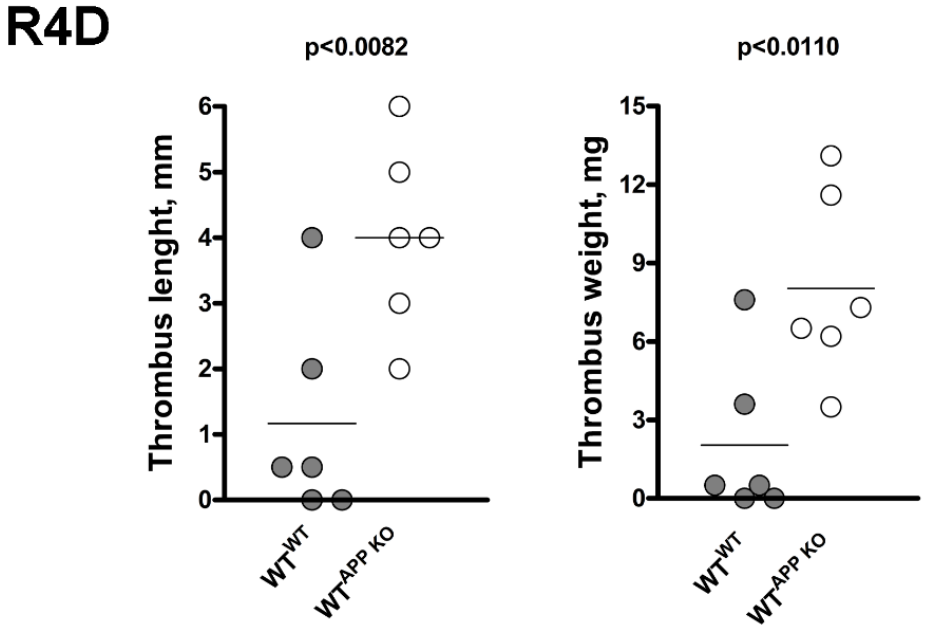

Figure R4D. Analysis of venous thrombosis after bone marrow transplantation. Comparison of venous thrombosis in WT mice transplanted with bone marrow cells from WT animals (WT^{WT}, grey symbols) and in WT mice transplanted with bone marrow cells from APP-KO mice ($WT^{APP\ KO}$, white symbols). Thrombus length and thrombus weight of thrombi collected after 24 hours from IVC ligation were assessed.

Subsequently, the enhanced tendency of APP KO mice to develop vein thrombosis was confirmed by the analysis of **pulmonary thromboembolism**. Here, thromboembolism was induced by the injection of thrombin in one of the tail veins. After 15 minutes, mice were euthanized, and lungs were collected, fixed and lung sections were prepared for histological analysis by labelling with hematoxylin and

eosin (H&E) to reveal platelet rich thrombi and with PTAH to show fibrin deposits. Even though the number of occluded vessels was comparable between the two genotypes, the average diameter of occluded vessels in APP KO mice was significantly larger than those in WT control animals (figure 4E i and ii), indicating the formation of bigger occlusive thrombi in the absence of APP.

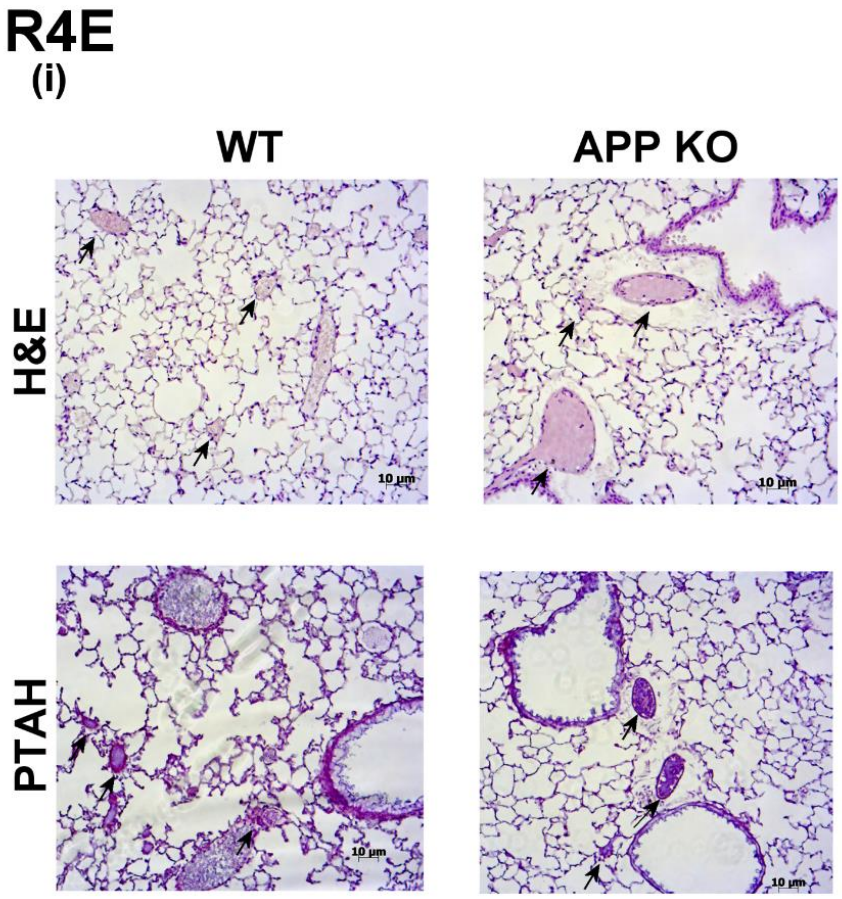

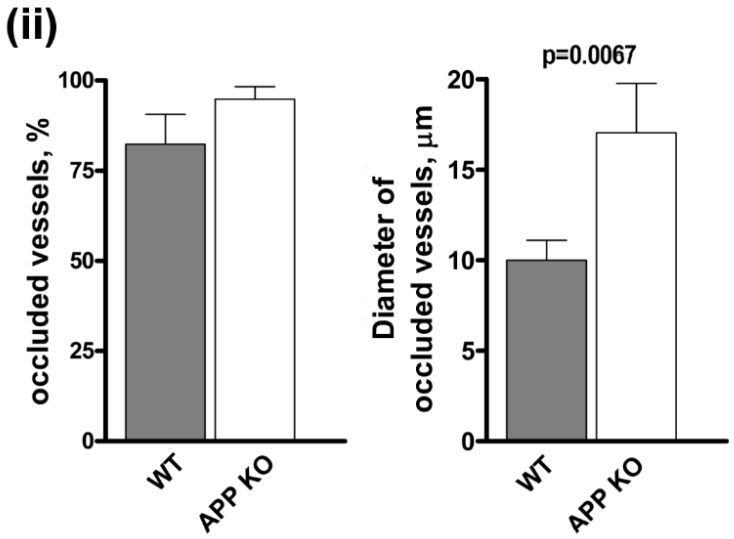

Figure R4E. Analysis of pulmonary thromboembolism. (i) Representative lung histology images staining with hematoxylin/eosin (H&E) and phosphotungstic acid–hematoxylin (PTAH). Arrows indicate occluded vessels. **(ii)** Quantification of the percentage of occluded vessels and analysis of the mean diameter of occluded vessels. Data have been collected by examining 10 microscopic fields for each lung section, prepared from 5 different animals, and were presented as mean ±SEM. N= 5 mice/group.

5. Study of blood coagulation in APP KO mice

One of the major triggers for venous thrombosis is the activation of blood coagulation cascade. Moreover, platelets express the APP isoforms containing the KPI domain (APP_{770} e APP_{751}), which is known to inhibit different serine proteases of the coagulation cascade (Van Nostrand et al., 1989).

Therefore, I analysed blood coagulation and coagulation factors in APP KO mice.

I first quantify the level of plasma fibrinogen in the two genotypes and as shown in the figure R5A WT and APP KO mice possessed comparable amount of circulating fibrinogen (figure R5A).

R5A

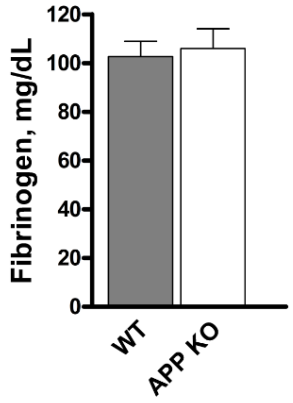

Figure R5A. Quantification of the level of plasma fibrinogen in WT and APP KO mice. Fibrinogen content was measured in WT (grey bar) and APP KO (white bar) plasma by the Clauss method in a Coagulab MJ coagulometer (Ortho Diagnostic Systems), using bovine thrombin. N= 6 mice/group.

Fibrin formation was then explored by evaluating both the extrinsic and intrinsic coagulation pathways through two different commercially available assays: the prothrombin time (PT) and the activated partial thromboplastin time (APTT) assays, respectively.

The prothrombin time (PT) is a one stage test through which it is possible to measure the activity of the extrinsic pathway of coagulation as time required to form clot after the addition of thromboplastin, phospholipid and calcium. The investigation of the extrinsic pathway of coagulation revealed that no significant differences in the

time required for clot formation were observed between WT and APP KO mice when measurements were performed in platelet poor plasma or PPP (panel i) or in the presence of platelets, using PRP (panel ii) (figure R5B).

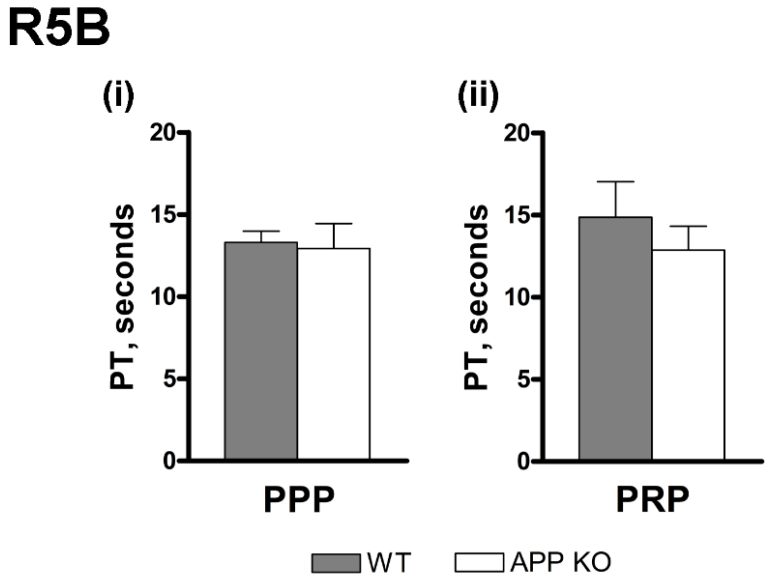

Figure R5B. Prothrombin assay. PT was measured in PPP **(i)** and PRP **(ii)** in WT (grey bar) and APP KO (white bar) plasma. N= 6 mice/group.

The analysis of the intrinsic pathway was performed using the APTT assay. PRP or PPP were incubated at 37°C and then phospholipid and contact activator were added, followed by calcium. Addition of calcium initiates clot formation. APTT time represented the time required to fibrin clot formation after the addition of calcium. This analysis showed that when measurements were performed in the presence of platelets (using PRP), the APTT time was significantly shortened in the APP KO mice (figure R5Cii). By contrast, APTT time still remained comparable in PPP of both genotypes (figure R5Ci). These results suggested a possible contribution of platelet APP in the intrinsic pathway.

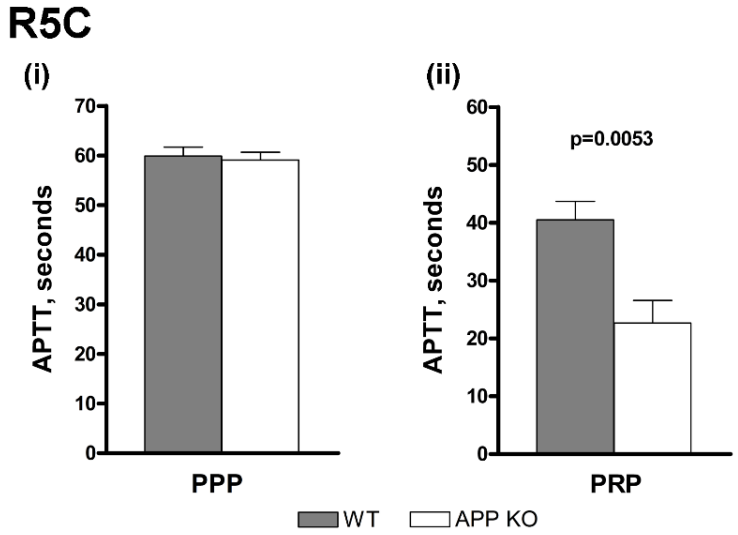

Figure R5C. Activated partial thromboplastin time (APTT) assay. APTT was measured in PPP **(i)** and PRP **(ii)** in WT (grey bar) and APP KO (white bar) plasma. N= 6 mice/group.

To further confirm the role of platelet APP in the intrinsic pathway of coagulation I measured the APTT time in samples resulting from reconstitution experiments. The addition of platelets from APP KO mice to PPP from WT mice was able to significantly shorten the APTT time, compared to the opposite situation in which WT platelets were added to PPP from APP KO mice (figure R5D).

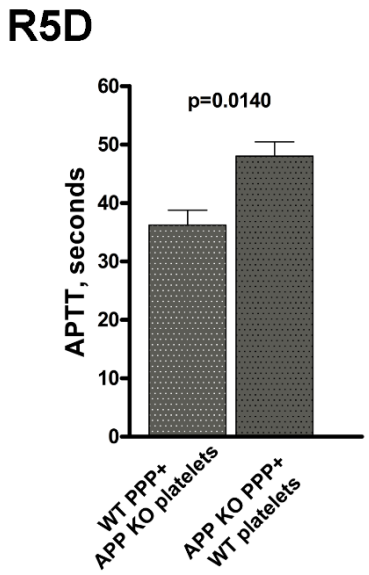

Figure R5D. APTT assay in reconstitution experiments. Measurement of APTT in reconstituted samples obtained by mixing PPP from one genotype with washed platelets from the other genotype, as indicated in the histogram. N= 6 mice/group.

Altogether these results demonstrated that APP expressed on platelet negatively regulates fibrin formation through the intrinsic coagulation pathway.
Finally, to identify the probable target of APP in the coagulation cascade, I principally focalized my attention to two coagulation factors: factor XIIa and factor XIa. Factor XIIa was known to be involved in the initiation of DVT (von Brühl et al., 2012), whereas factor XIa was referred as the major substrate for the KPI inhibitory domain of APP (Smith et al.,1990). I simply measured the activity of both coagulation factors in PRP condition and I found that only the activity of factor Xia (panel i, figure R5E), but not that of factor XIIa(panel ii, figure R5E), was significantly higher in the APP KO than WT mice, showing factor XIa as feasible target of APP in the intrinsic coagulation pathway.

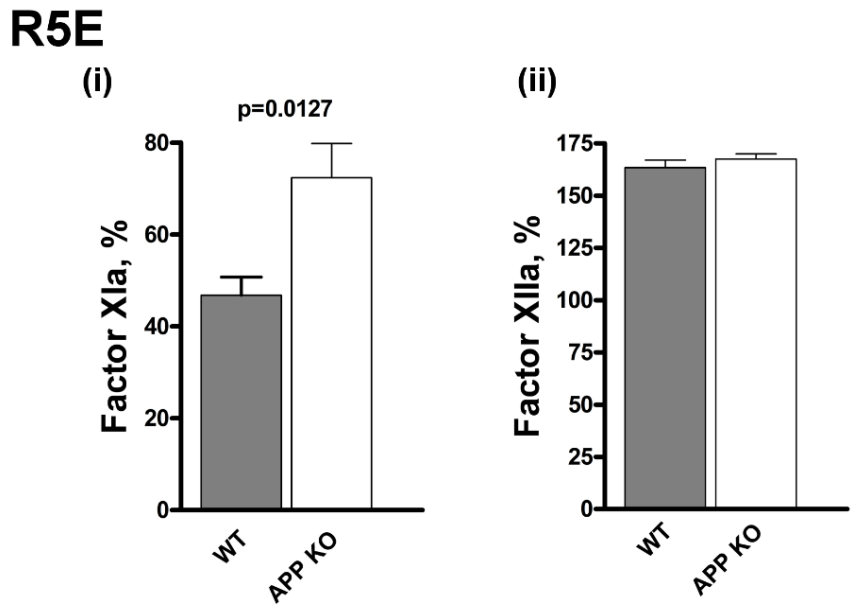

Figure R5E. Quantification of the activity of FXIa e FXIIa. Measurement of the activity of FXIa **(i)** and FXIIa **(ii)** in PRP from WT (grey bars) and APP KO (white bars) mice. N= 6 mice/group.

6. Analysis of NETs formation by neutrophils from WT and APP KO mice

In addition to the activation of blood coagulation cascade, previous studies have described that also neutrophils are involved in propagating DVT principally through the extrusion of neutrophil extracellular traps or NETs (Kimball et al., 2016). Therefore, I examined NETs formation in APP KO mice.

Neutrophils were isolated from bone marrow (method 6) and were left unstimulated or treated with phorbol myristate acetate (PMA, 100nM). Cells were citospun, followed by fixation and permeabilization and finally were labelled with a NETs specific marker, the citrullinated histone H3. Neutrophils were counterstained for DNA with Hoechst.

Figure R6A shows that neutrophils from APP KO mice spontaneously protruded a greater amount of NETs compared to WT neutrophils. As expected, PMA stimulation strongly induced NETs formation by neutrophils from both genotypes, but did not further increased NETosis by unstimulated APP KO neutrophils (figure R6A panel i and panel ii).

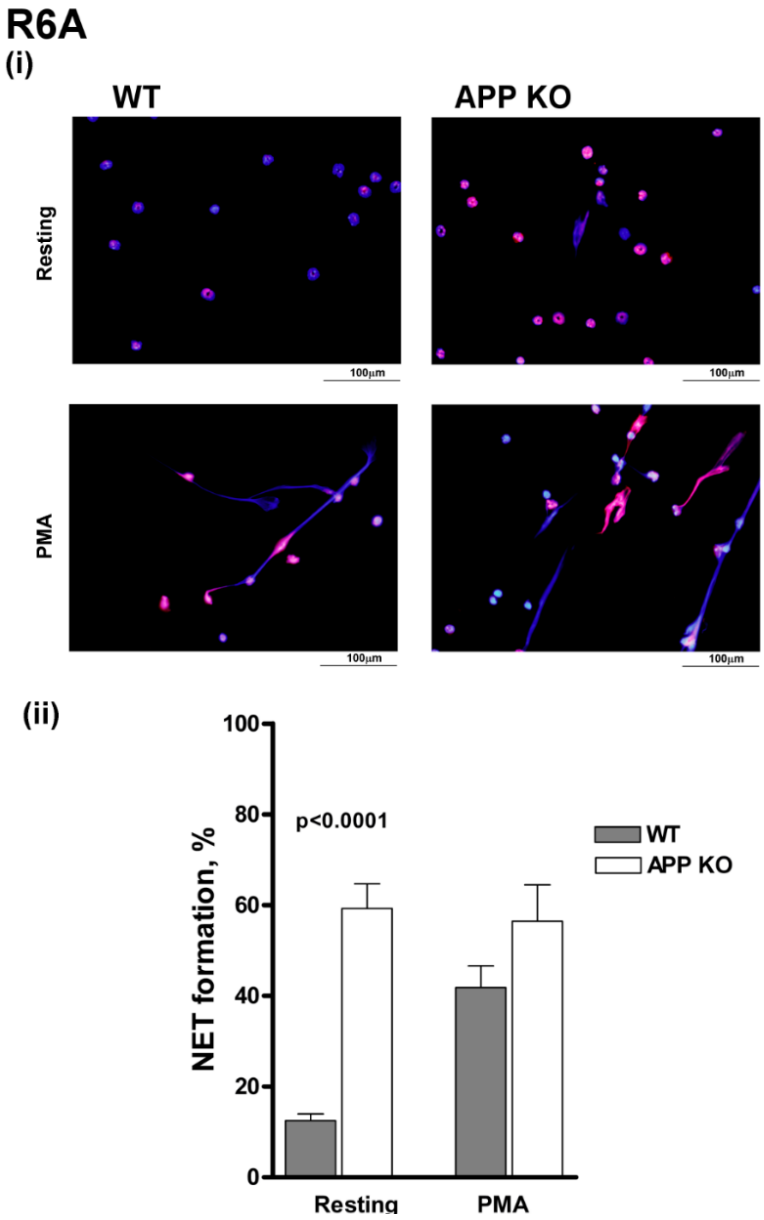

Figure R6A: Analysis of NETS formation. (i) NETs formation in purified neutrophils from WT and APP KO mice was visualized by staining for DNA with Hoechst (blue) and for citrullinate Histone H3 (red). Representative images at 400X magnification of resting and PMA-stimulated neutrophils are representative of five different experiments. **(ii)** Quantification of NETs formation expressed as percentage of neutrophils extruding NETs is reported in the histogram. Grey bars refer to WT mice, and white bars to APP KO mice. Data are expressed as mean ± SEM. N= 5 mice/group.

Since it has been already documented that platelets play an important role in the regulation of NETs formation (Fuchs et al., 2010; Brill et al., 2012), I stimulated neutrophils isolated from WT and APP KO mice with platelets from both genotypes. Figure R6B shows that both WT and APP-null platelets were equally able to stimulate neutrophils from either WT or APP KO mice to extrude NETs (figure R6B). Thus, platelets can stimulate NETosis independently of APP expression on platelet surface.

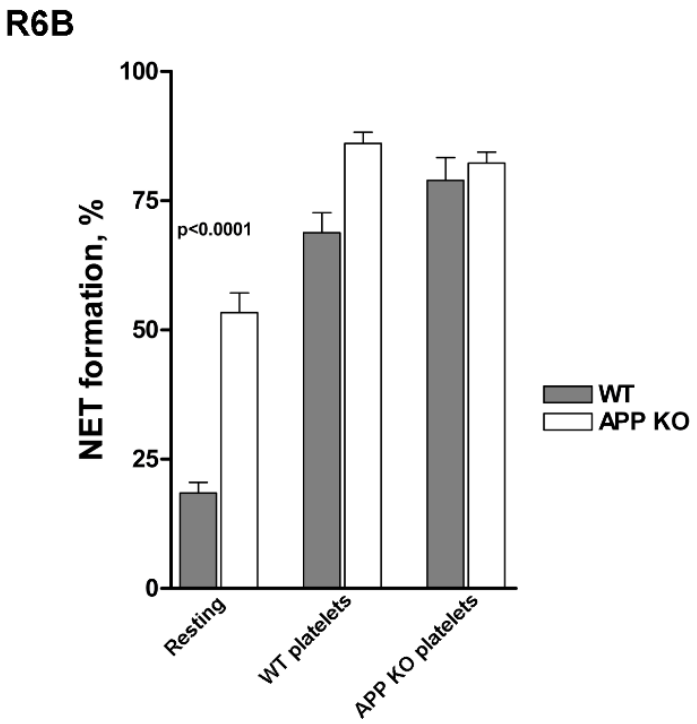

Figure R6B. Analysis of platelet-induced NETosis. Analysis of NETs formation triggered by incubation of WT and APP KO neutrophils with WT platelets, APP KO platelets, or no cells (resting), as indicate in the bottom. NETs formation is expressed as percentage of neutrophils extruding NETs. Grey bars refer to WT mice while white bars to APP KO mice. Data are expressed as mean ± SEM. N=5 mice/ group.

The association between NETs formation and venous thrombosis has been further proved through the histochemical analysis of collected venous thrombi to reveal NETs incorporation.

The formed thrombi were extracted and stained with two NETs-specific markers, CRAMP and citrullinated histone H3, as indicated in the panel i of the figure R6C. The quantification of positive cells to both markers shown a significantly

stronger incorporation of NETs into venous thrombi from APP KO compared to WT mice (figure R6Cii).

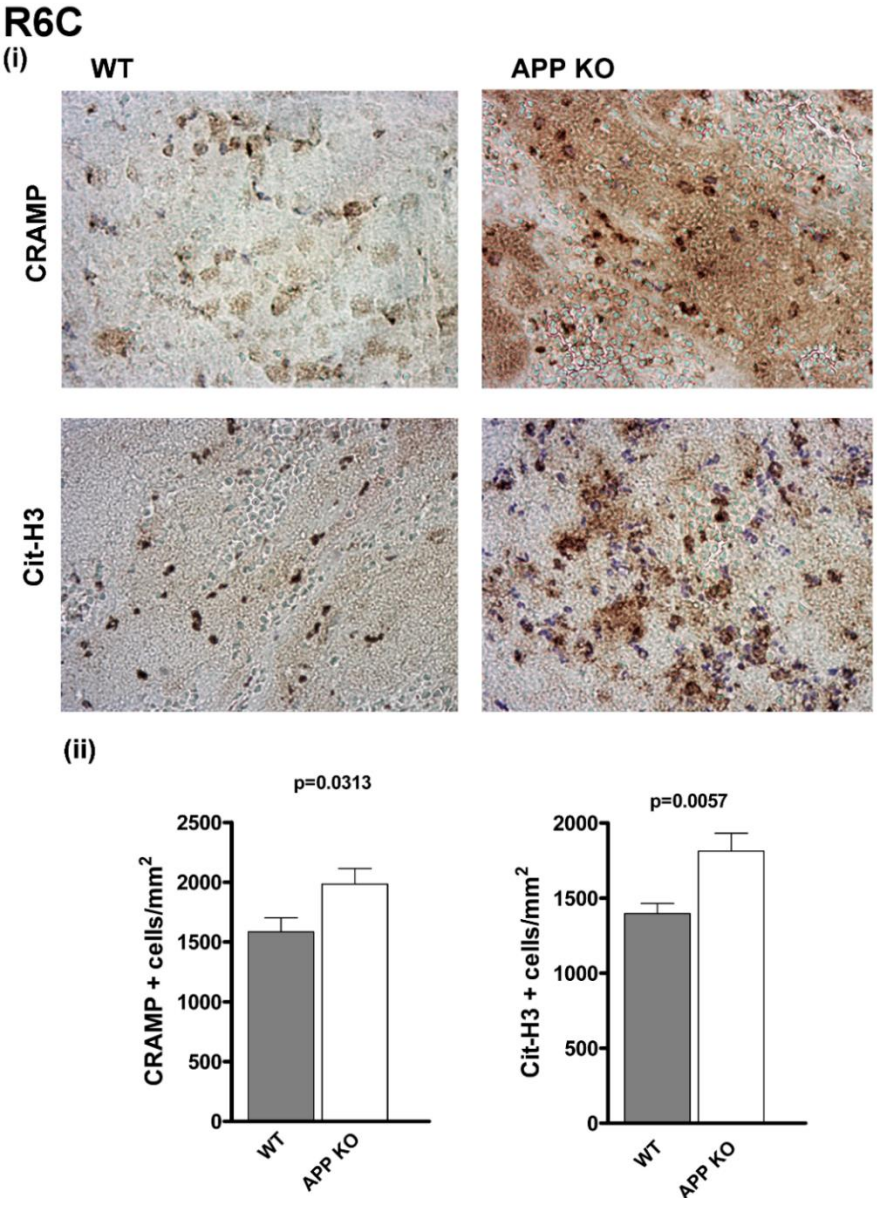

Figure R6C. Analysis of NETs in venous thrombi. (i) Representative images of venous thrombi isolated from WT and APP KO mice 24 hours after IVC ligation, and stained for the NETs-related markers CRAMP and citrullinated histone H3 (Cit-H3), as indicated. **(ii)** Quantification of the positive cells to both markers are counted. Data have been collected by examining 10 microscopic fields for each thrombi section, prepared from 5 different animals, and were presented as mean ±SEM. N= 5 mice/group.

Since NETosis is strongly associated with inflammation, I searched for platelet-leukocyte aggregates in flow cytometry. Indeed, the formation of platelet-leukocyte aggregates (PLAs) is increased in several inflammatory and thrombotic conditions. Remarkably, I found that the number of circulating platelet-leukocyte aggregates in circulation was significantly higher in APP KO than in control mice and stimulation with thrombin further increased the formation of these complexes in both genotypes (figure R6D).

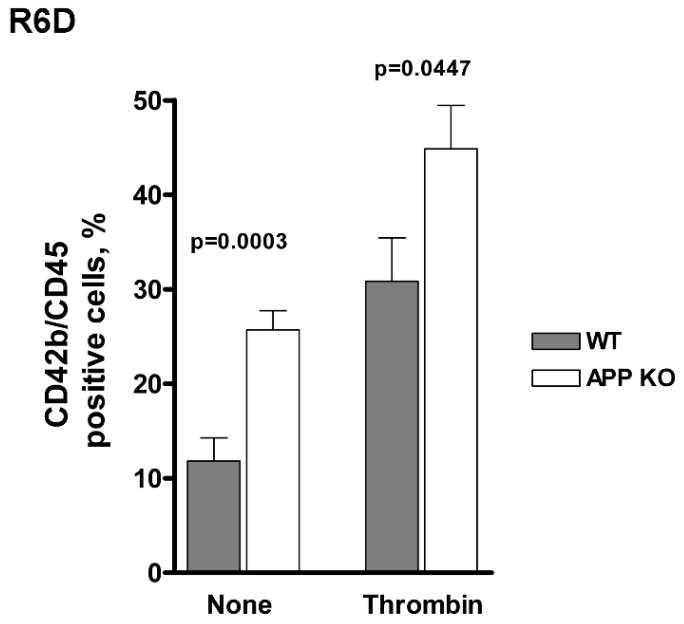

Figure R6D. Investigation of platelet–leukocyte aggregates. Flow cytometry analysis of circulating platelet-leukocyte aggregates in blood from WT (grey bar) and APP KO (white bar) mice untreated (none) or upon stimulation with 0.5 U/mL thrombin, as indicated. N=6 mice/ group.

Altogether, these results may suggest that the absence of APP determined an enhanced constitutive interaction of platelets with neutrophils, related with the strong NETs formation previously observed.

DISCUSSION II

Amyloid precursor protein APP is a transmembrane glycoprotein that belongs to a family of evolutionary and structurally related proteins. APP is highly expressed in neurons and is principally known as the precursor molecule of Aβ peptides whose accumulation in brain parenchyma is correlated with AD. Beyond its pathological role associate to AD pathogenesis, APP functions in the central nervous system are related to synaptogenesis, neurons migration and cell-cell, cell-substrates adhesion.

Platelets represent the second source of APP after neurons. APP isoforms expressed in platelets, APP_{751} and APP_{770}, contain the KPI domain that is known to inhibit serine protease activity (Schmaier et al.,1993; Mahdi et al., 1995; Mahdi et al., 2000). Platelet APP is mainly metabolized by α- and γ-secretases to produce soluble fragments (sAPPα) that are release in the circulation upon platelet activation. Previous studies described that either intact APP expressed on plasma membrane and released sAPPα regulated cerebral thrombosis (Xu et al., 2005) but despite all these reports, the exact role of APP in circulating blood platelets has not been fully elucidated.

In this PhD thesis I have studied the physiological function of platelet APP through the utilization of APP deficient mice. APP KO mice are viable and fertile and are generated and provided by Dr. U. Müller (University of Heidelberg, Germany).

I first validate my model confirming that platelet isolated from APP KO mice do not express APP (figure R1A). To provide a complete characterization of the role of APP in platelet physiology, I performed a comparative analysis of the functional responses of platelets from APP KO mice and platelets from WT matched littermates.

Several parameters were evaluated, and the results showed that APP deficient platelets aggregate and activate normally in response to several soluble agonists, including thrombin, thromboxane analogue U46619, GPVI agonists convulxin and ADP, demonstrating that APP does not significantly participate in agonist-induced platelet aggregation (figure R2Bi). In addition, integrin $\alpha_{IIb}\beta_3$ inside out activation as well as α-granules secretion resulted unaffected by the absence of APP (figure R2C-D). All these data demonstrated that APP is dispensable for platelet activation and aggregation. Considering that besides APP, platelets express, albeit at a lower level, the APP-like protein 2 (APLP2, 2000 copy number/platelets), therefore APP deficiency may be balanced by the presence of a functional APLP2 that may compensated slight differences in term of activation.

APP is important in mediating cell adhesion in neurons, where it localizes together with integrin β_1 at adhesion complexes and seem to be involved in the regulation of integrin-based cell adhesion and migration. Since some peculiar properties of APP supports its role in cell-cell and cell-substratum adhesion, I have analysed the role of APP in platelet adhesion by performing cell adhesion assay to investigate whether platelets isolated from APP KO mice were able to adhere on different subendothelial components. No differences in platelet adhesion over fibrinogen and collagen were detected demonstrating that APP was dispensable in integrin-mediated adhesion (figures R3B and R3Di). These results were also confirmed in a recent study of Elvers and collaborators that shown unaltered thrombus formation on collagen and fibrinogen coated capillaries in APP deficient platelets compared to WT platelets (Gowert et al., 2017). Moreover, adhesion to vWF occurred normally in the absence of APP (R3Dii). These results were consistent with the comparable surface expression of the principal platelet glycoproteins receptors described in both genotypes (figure R1B).

Nevertheless, APP is involved in platelet adhesion to immobilized Aβ peptides. Previous studies have identified a high affinity binding site for fibrillar Aβ between residues 95 to 118 of APP (Van Nostrand et al., 2002) and others have proposed Aβ as a potential ligand for APP (Lorenzo et al., 2000).
Here I demonstrated for the first time that APP specifically interacts with Aβ peptides. Indeed, APP KO platelets fails to adhere to all Aβ peptides tested ($A\beta_{25-35}$, $A\beta_{1-40}$ and $A\beta_{1-42}$ peptides) (figure R3E). Conversely, cell adhesion on Aβ peptides increased proportionally with APP expression level. In these experiments, cells overexpressing APP751 (HEK293/APP751) adhered more on Aβ coated surfaces, compared with cells that expressed low level of APP (figure R3F). Moreover, it has been observed that the increased adhesion and thrombus formation of WT platelets under arterial flow condition on collagen in the presence of Aβ peptides is completely suppressed in APP KO platelets (figure R3G). All together these results demonstrated that immobilized Aβ peptide is a ligand for platelet APP.

It is important to keep in mind that in cerebral amyloid angiopathy (CAA) deposits of Aβ peptides in the cerebral vessels may cause platelet activation and haemorrhagic or ischemic stroke. Therefore, platelets can bind to Aβ deposits in cerebral vessels promoting platelet adhesion and activation to further induce thrombus formation (Gowert et al., 2014). Considering these new evidences, APP expressed on

platelets may be somehow involved in platelet adhesion to immobilized Aβ peptides in cerebral vessels.

On the contrary, Aβ peptides seem to be not a ligand for APP if platelets were stimulated *in vitro*. Indeed, no differences were observed in platelet aggregation, integrin $\alpha_{IIb}\beta_3$ activation and α-granules secretion between WT and APP KO platelets when Aβ peptides were used as stimulus (figure R2B, R2C and R2D).

Despite APP KO platelets undergo normal activation, they showed some abnormalities in term of number and size of platelets, as reported in the electron microscopy analysis (figure R1E) suggesting a possible role for APP in haematopoiesis. In addition, platelet count is slightly but significantly reduced in APP KO mice (figure R1C). However, this reduction does not impact platelet functionality and/or support bleeding tendency. The lower platelet number may be compensated by a little increase in platelet size observed in APP KO platelets.

Although the analysis of platelet clearance was normal and comparable between the two genotypes (figure R1D), I demonstrated an enhanced percentage of megakaryocytes protruding proplatelets in APP KO mice (figure R1F). The molecular mechanism of these abnormalities is not clear and deserves further investigations.

Previous studies have documented that APP regulates cerebral thrombosis (Xu et al., 2009). Xu and co-workers assessed a role of APP in reducing cerebral thrombosis through an intracerebral haemorrhage model as well as in a carotid artery thrombosis assay (Xu et al., 2005). Differently from what they described in the carotid artery model, here photochemical-induced thrombosis in the femoral artery occurred normally in the absence of APP. This discrepancy may be related to the different vascular districts exploited in the two models, carotid artery and femoral artery, respectively.

This observation is also supported by the fact that arterial thrombosis is strictly dependent on platelet activation and I have shown that platelet activation is unaffected in APP KO mice, thus confirming that APP is not involved in peripheral arterial thrombosis (figure R4A).

Also, lack of APP did not affect the tail bleeding time (figure R2A), indicating that the overall platelet-dependent haemostatic response is well preserved in APP KO mice. Again, the existence of APLP2 in platelets may explain why APP deficiency could be overcome.

In addition to peripheral arterial thrombosis, I have also investigated peripheral venous thrombosis, that is principally dependent on coagulation cascade, utilizing a model of flow restriction of inferior vena cava. Unexpectedly, APP KO mice developed significantly larger thrombi than WT control littermates after 24h and 48h of IVC ligation, with a significant increase in both length and weight of collected venous thrombi (figure R4B). These bigger thrombi seem to be unstable since after 48 hours of IVC ligation I observed a slightly reduction in their size. Probably these thrombi break free and can travel around the bloodstream. In fact, I found significant increase in lung occluded vessels in APP KO mice after 48 hours of stenosis (figure R4C).

Moreover, another evidence of the role of APP in peripheral venous thrombosis derived from the analysis of pulmonary thromboembolism. In this model, thrombin injection triggered a massive fibrin deposition in pulmonary arteries, and even if the number of occluded vessels was similar between the two genotypes, the average diameter occluded vessels in APP KO mice was significantly greater compared to controls, indicating again the formation of bigger occlusive thrombi in APP KO mice (figure R4E).

To confirm the role of blood derived-APP in venous thrombosis chimeric mice were generated by transplantation of bone marrow from both genotypes into WT recipient mice and then IVC ligation was performed. After 24 hours from procedure, I observed the formation of larger venous thrombi in chimeric mice transplanted with bone marrow cells from APP KO mice compare to chimeric mice transplanted with WT bone marrow cells, clearly demonstrating the direct involvement of blood derived APP in the regulation of venous thrombosis (figure R4C).

Since venous thrombosis is more dependent on the activation of the coagulation cascade than arterial thrombosis, which is principally related to platelet function, I decide to explore the role of APP in blood coagulation.

Differently from the neuronal isoform, APP expressed in platelets carries a KPI domain, which is a potent inhibitor of serine proteases (Van Nostrand et al., 1989). Purified or recombinant KPI domain containing APP fragments have been deeply characterized in vitro and it has been found to potently affect many coagulation factors, including FIXa, FXa, FVII:tissue factor complex, and, particularly, FXIa (Smith et al., 1990; Schmaier et al.,1993; Mahdi et al., 1995; Mahdi et al., 2000).

Here, platelet APP displayed an important inhibitory action on the intrinsic coagulation pathway, as I demonstrated a reduction in APTT time both in PRP from

APP KO mice and in WT PPP in the presence of platelets from APP KO (figure R5Cii and R5D). Therefore, APP expressed on platelets negatively regulated fibrin formation through the intrinsic pathway, possibly thanks to its KPI domain. Subsequently, I analysed the activity of some coagulation factors also involved in deep vein thrombosis, including FXIa e FXIIa and my results suggested that one possible target of APP could be FXI, whose activity resulted increased in APP KO mice (figure R5Ei). Therefore, I propose that lack of APP in platelets accelerates fibrin formation through the intrinsic pathway, and this may be responsible for the formation of larger occlusive thrombi observed upon vein flow restriction.

Besides blood coagulation, it is well recognised that circulating neutrophils actively contribute to the onset and the propagation of DVT (Von Brüll et al., 2012; Kimball et al., 2016). Indeed, neutrophils induce thrombosis *in vitro* and *in vivo* by releasing neutrophil extracellular DNA and proteins known as neutrophil extracellular traps (NETs) (Massberg et al., 2010). Neutrophils from APP KO mice released a higher amount of NETs than neutrophils from WT animals even in the absence of specific stimulation (figure R6A). In addition, it has been observed an increased amount of NETs incorporated into venous thrombi collected from APP KO mice (figure R6C), supporting the correlation between venous thrombosis and NETs formation.

Moreover, a significant greater number of platelet-leukocyte aggregates in circulation was detected in APP KO mice, and stimulation with thrombin further increased the formation of these complexes (figure R6D), indicating that APP may negatively controls platelet-leukocyte interaction.

The constitutive interaction between neutrophils and platelets found in APP KO mice induced a strong release of NETs, which could be considered an additional possible mechanism supporting the greater venous thrombosis in APP KO mice.

To conclude, the absence of APP on platelets seems to be responsible of the increased number of platelet- leukocytes aggregates in circulation, which are indicative of a pro-inflammatory state. This constitutively enhanced interaction between platelets and neutrophils leads to a strong NETs formation and predispose to venous thrombosis. In addition, the absence of APP on platelet surface, with its KPI domain, accelerated clot formation through the intrinsic pathway, justifying why APP KO mice developed larger thrombi upon vein flow restriction.

CONCLUSIONS

This PhD thesis analyses the multiple roles of amyloid precursor protein (APP) in platelets especially its involvement in peripheral manifestations of Alzheimer's disease (AD).

AD is one of the major social and health emergency worldwide and many efforts are devoted to search for a cure in very early phase of disease. A number of recent evidences suggest that the onset of AD is related to alterations of the vascular system and is associated to vascular disorders. Studying the circulatory system represents one of the most promising approach in the definition of an early marker. Therefore, circulating blood platelets may be a reliable and accessible source to study AD pathology and may represent a useful biomarker for prognosis of the disease. In addition, although platelets and neurons have different embryological origin, many proteins especially expressed in neurons are also present at high amount in platelets. For instance, amyloid precursor protein APP. In central nervous system APP has neurotrophic and neuroprotective action, but little is known on its physiological function in circulation.

This PhD thesis could provide important information in this regard and opens up broad research avenues for AD related topics. In particular, two different aspects have been investigated: i) the interrelation between platelets and AD by analysing platelet adhesion and thrombus formation in a mouse model of AD, the 3xTg-AD mice, also carrying a mutation in transgenic human APP gene, and ii) APP role in circulation by exploiting APP KO mice.

The principal findings are the enhanced adhesion to different substrates and the increased thrombus formation in platelets from AD mouse model, suggesting a novel mechanism that may contribute to vascular complication associated with AD pathology. Therefore, the outcome of this research study has greatly improved our knowledge about the molecular mechanism of these aging-related pathologies and may explain the prothrombotic phenotype described in many AD patients.

In addition, this study reveals altered haemostatic and thrombotic characteristics of platelets from APP KO mice, primarily demonstrating a novel role of APP *in vivo* and a possible contribution in thromboembolism through multiple

mechanisms, including the regulation of both coagulation cascade and neutrophil extracellular trap formation.

Moreover, the fact that APP acts as a receptor to mediate adhesion to Aβ peptide may suggest a possible involvement in pathological situations, as CAA. In particular, platelet APP may facilitate platelet adhesion to the site of Aβ accumulation in cerebral vessel wall and the subsequent thrombus formation, contributing to vessel damage and AD progression.

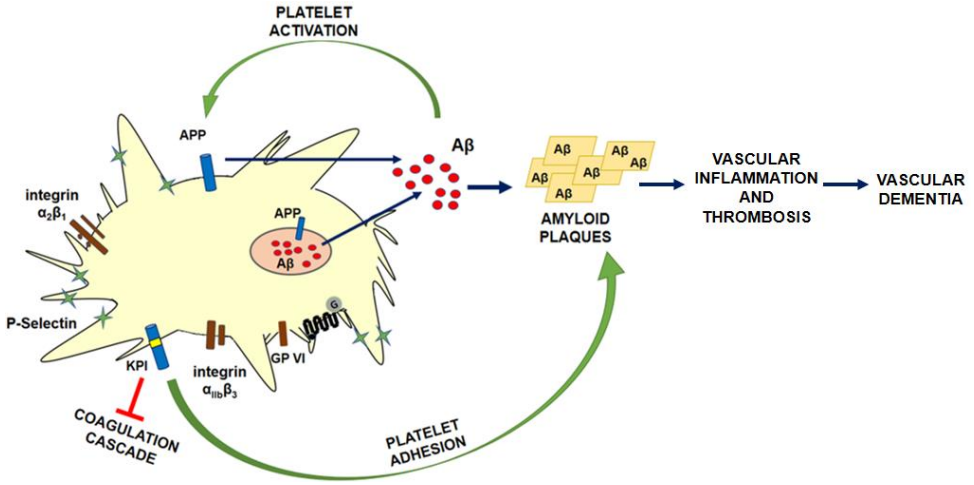

Figure 9. Schematic overview of my PhD study.

REFERENCES

Akaaboune M., Allinquant B., Farza H., Roy K., Magoul R., Fiszman M., Festoff B.W., Hantaï D. "Developmental regulation of amyloid precursor protein at the neuromuscular junction in mouse skeletal muscle". *Mol Cell Neurosci*. 15(4):355-67. 2000.

Allison T.M., Parkin E.T., Turner A.J., Hopper N.M. "ADAMs family members as amyloid precursor protein alpha-secretases".*J. Neurosci*. 74: 342-352. 2003.

Ando K., et al: "Role of phosphorylation of Alzheimer's amyloid precursor protein during neuronal differentiation". *J Neurosci*. 19(11):4421-7. 1999.

Ariëns R.A., Philippou H., Nagaswami C., Weisel J.W., Lane D.A., Grant P.J. "The factor XIII V34L polymorphism accelerates thrombin activation of factor XIII and affects cross-linked fibrin structure". *Blood*. 96(3):988-95. 2000.

Asazuma N., Ozaki Y., Satoh K., Yatomi Y., Handa M., Fujimura Y., Miura S., Kume S. "Glycoprotein Ib von Willebrand factor interactions activate tyrosine kinases in human platelets*".Blood*. 90:4789- 98. 1997.

Barrett P.J., Song Y., Van Horn W.D., Hustedt E.J., Schafer J.M., Hadziselimovic A., Beel A.J., Sanders C.R. "The amyloid precursor protein has a flexible transmembrane domain and binds cholesterol". *Science*. Jun 1;336(6085):1168-71. 2012.

Beher D., Hesse L., Masters C.L., Multhaup G. "Regulation of amyloid precursor protein (APP) binding to collagene and mapping of the binding sites on APP and collagen type I".*Biol. Chem*. 271: 1613-1620. 1996.

Barnham K.J., McKinstry W.J., Multhaup G., Galatis D., Morton C.J., Curtain C.C., Williamson N.A., White A.R., Hinds M.G., Norton R.S., Beyreuther K., Masters C.L., Parker M.W., Cappai R. "Structure of the Alzheimer's disease amyloid precursor protein copper binding domain. A regulator of neuronal copper homeostasis". *J Biol Chem*. May. 278(19):17401-7. 2003.

Berndt M.C., Shen Y., Dopheide S.M., Gardiner E.E., Andrews R.K. "The vascular biology of glycoprotein Ib-IX-V complex". *Thromb Haemost*. 86:178-188. 2001.

Berridge M.J. "Neuronal calcium signalling". *Neuron*. 21(1):13-26. Review. 1998.

Billings et al.,. "Intraneuronal Abeta causes the onset of early Alzheimer's disease-related cognitive deficits in transgenic mice". Neuron.45:675-88. 2005.

Blennow K., Hampel H., Weiner M., Zetterberg H. "Cerebrospinal fluid and plasma biomarkers in Alzheimer disease". *Nat Rev Neurol*. 6(3):131-44. 2010.

Blobel C.P. "ADAMs: key components in EGFR signalling and development".
Nat Rev Mol Cell Biol. 6(1):32-43. Review. 2005.

Borroni B., Akkawi N., Martini G., Colciaghi F., Prometti P., Rozzini L., Di Luca M., Lenzi G.L., Romanelli G., Caimi L., Padovani A. "Microvascular damage and platelet abnormalities in early Alzheimer's disease". *J. Neurol. Sci.*; 203-204: 189-193. 2002.

Borroni B., Perani D., Broli M., Colciaghi F., Garibotto V., Paghera B., Agosti C., Giubbini R., Di Luca M, Padovani A. "Pre-clinical diagnosis of Alzheimer disease combining platelet amyloid precursor protein ratio and rCBF spect analysis". *J Neurol.* 252(11):1359-62. 2005.

Borroni B., Agosti C., Marcello E., Di Luca M., Padovani A. "Blood cell markers in Alzheimer Disease: Amyloid Precursor Protein form ratio in platelets".*Exp Gerontol.* Jan;45(1):53-6. Review. 2010.

Brill A., Fuchs T.A., Chauhan A.K., Yang J.J., De Meyer S.F., Köllnberger M., Wakefield T.W., Lämmle B., Massberg S., Wagner D.D. "von Willebrand factor-mediated platelet adhesion is critical for deep vein thrombosis in mouse models". *Blood*. 117(4):1400-7. 2011.

Brill A., Fuchs T.A., Savchenko A.S., Thomas G.M., Martinod K., De Meyer S.F., Bhandari A.A., Wagner D.D. "Neutrophil extracellular traps promote deep vein thrombosis in mice". *J Thromb Haemost*. 10(1):136-44. 2012.

Brinkmann V., Reichard U., Goosmann C., Fauler B., Uhlemann Y., Weiss D.S., Weinrauch Y., Zychlinsky A. "Neutrophil extracellular traps kill bacteria". *Science*. 303(5663):1532-5. 2004.

Brill A., Fuchs T.A., Savchenko A.S., Thomas G.M., Martinod K., De Meyer S.F., Bhandari A.A., Wagner D.D. "Neutrophil extracellular traps promote deep vein thrombosis in mice*". J Thromb Haemost*. 10(1):136-44. 2012.

Brinkmann V., Zychlinsky A. "Neutrophil extracellular traps: is immunity the second function of chromatin?". *J Cell Biol*. 198(5):773-83. 2012.

Broos K., Feys H.B., De Meyer S.F., Vanhoorelbeke K., Deckmyn H. "Platelets at work in primary haemostasis*". Blood Rev*. 25(4): 155-67. 2011.

Burkhart J.M., Vaudel M., Gambaryan S., Radau S., Walter U., Martens L., Geiger J., Sickmann A., Zahedi R.P. "The first comprehensive and quantitative analysis of human platelet protein composition allows the comparative analysis of structural and functional pathways". *Blood*. 120(15):e73-82. 2012.

Bush A., Martins R.N., Rumble B., Moir R., Fuller S., Milward E., Currie J., Ames D., Weidemann A., Fischer P., et al. "The amyloid precursor protein of Alzheimer's disease is released by human platelets". *J Biol Chem*. Sep 15;265(26):15977-83. 1990.

Bush A.I., Multhaup G., Moir R.D., Williamson T.G., Small D.H., Rumble B., Pollwein P., Beyreuther K., Masters C.L. "A novel zinc(II) binding site modulates the function of the beta A4 amyloid protein precursor of Alzheimer's disease". *J Biol Chem*. 268(22):16109-12. 1993.

Canobbio I., Catricalà S., Balduini C., Torti M. "Calmodulin regulates the non-amyloidogenicmatabolism of amyloid precursor protein in platelets". *Biochim. Biophys. Acta.*; 1813: 500-506. 2011.

Canobbio I., Catricalà S., Di Pasqua L.G., Guidetti G., Consonni A., Manganaro D., Torti M. "Immobilized amyloid Aβ peptides support platelet adhesion and activation". *FEBS Lett*. 587(16):2606-11. 2013.

Canobbio I., Guidetti G.F., Oliviero B., Manganaro D., Vara D., Torti M., Pula G. "Amyloid β-peptide-dependent activation of human platelets: essential role for Ca^{2+} and ADP in aggregation and thrombus formation". *Biochem J*. 462(3):513-23. 2014.

Canobbio I., Abubaker A.A., Visconte C., Torti M., Pula G. "Role of amyloid peptides in vascular dysfunction and platelet dysregulation in Alzheimer's disease".

Front Cell Neurosci. 9:65. doi: 10.3389/fncel.2015.00065. eCollection 2015. Review. 2015.

Canobbio I., Visconte C., Oliviero B., Guidetti G., Zarà M., Pula G., Torti M. "Increased platelet adhesion and thrombus formation in a mouse model of Alzheimer's disease". *Cell Signal*. 28 (12):1863-1871. 2016.

Catricala S., Torti M., Ricevuti G. "Alzheimer disease and platelets: how's that relevant".
Immun Ageing. 9(1):20. doi: 10.1186/1742-4933-9-20. 2012.

Casoli T., Di Stefano G., Giorgetti B., Grossi Y., Balietti M., Fattoretti P., Bertoni-Freddari C."Release of beta-amyloid from high-density platelets: implications for Alzheimer's disease pathology". *Ann N Y Acad Sci*. 1096:170-8. 2007.

Casoli T., Di Stefano G., Balietti M., Solazzi M., Giorgetti B., Fattoretti P. "Peripheral inflammatory biomarkers of Alzheimer's disease: the role of platelets". *Biogerontology*. 11:627–633. 2010.

Cenini G., Cecchi C., Pensalfini A., Bonini S.A., Ferrari-Toninelli G., Liguri G., Memo M., Uberti D. "Generation of reactive oxygen species by beta amyloid fibrils and oligomers involves different intra/extracellular pathways". *Amino Acids*. 38(4):1101-6. 2010.

Chi N.F., Chien L.N., Ku H.L., Hu C.J., Chiou H.Y. "Alzheimer disease and risk of stroke: a population-based cohort study". *Neurology*. 80(8):705-11. 2013.

Cho S.M., Lee S., Yang S.H., Kim H.Y., Lee M.J., Kim H.V., Kim J., Baek S., Yun J., Kim D., Kim Y.K., Cho Y., Woo J., Kim T.S., Kim Y. "Age-dependent inverse correlations in CSF and plasma amyloid-β(1-42) concentrations prior to amyloid plaque deposition in the brain of 3xTg-AD mice". *Sci Rep*.6:20185. 2016

Cimmino G., Golino P. "Platelet biology and receptor pathways". *J Cardiovasc Transl Res*. 6(3):299-309. 2013.

Cipolla L., Consonni A., Guidetti G., Canobbio I., Okigaki M., Falasca M., Ciraolo E., Hirsch E., Balduini C., Torti M. "The proline-rich tyrosine kinase Pyk2 regulates platelet integrin αIIbβ3 outside-in signalling". *J Thromb Haemost*. 11(2):345-56. 2013.

Clarris H.J., Cappai R., Heffernan D., Beyreuther K., Masters C.L., Small D.H. "Identification of heparin-binding domains in the amyloid precursor protein of Alzheimer's disease by deletion mutagenesis and peptide mapping". *J Neurochem*. 68(3):1164-72. 1997.

Clemetson K.J., Clemetson J.M. "Platelet GPIb-V-IX complex. Structure, function, physiology, and pathology". *Semin Thromb Hemost*. 21(2):130-6. 1995.

Clemetson J.M, Polgar J., Magnenat E., Wells T.N., Clemetson K.J. "The platelet collagen receptor glycoprotein VI is a member of the immunoglobulin superfamily closely related to FcalphaR and the natural killer receptors". *J Biol Chem*. 274:29019–29024. 1999.

Colciaghi F., Marcello E., Borroni B., Zimmermann M., Caltagirone C., Cattabeni F., Padovani A., Di Luca M. "Platelet APP, ADAM 10 and BACE alterations in the early stages of Alzheimer disease". *Neurology*. 62(3):498-501. 2004.

Consonni A., Cipolla L., Guidetti G., Canobbio I., Ciraolo E., Hirsch E., Falasca M., Okigaki M., Balduini C., Torti M. "Role and regulation of phosphatidylinositol 3-kinase β in platelet integrin α2β1 signaling". *Blood*. 119(3):847-56. 2012.

Cortes-Canteli M., Paul J., Norris E.H., Bronstein R., Ahn H.J., Zamolodchikov D., Bhuvanendran S., Fenz K.M., Strickland S. "Fibrinogen and beta-amyloid association alters thrombosis and fibrinolysis: a possible contributing factor to Alzheimer's disease". *Neuron*. 66(5):695-709. 2010.

Coulson E.J., Paliga K., Beyreuther K., Masters C.L. "What the evolution of the amyloid protein precursor supergene family tells us about its function". *Neurochem Int*. 36(3):175-84. 2000.

Covic L., Gresser A.L., Kuliopulos A. "Biphasic Kinetics of Activation and Signaling for PAR1 and PAR4 Thrombin Receptors in Platelets". *Biochemistry*. 39(18): p. 5458-5467. 2000.

Dahlbäck B. "Blood coagulation". *Lancet*. 355(9215):1627-32. Review. 2000.

Dahms S.O., Könnig I., Roeser D., Gührs K.H., Mayer M.C., Kaden D., Multhaup G.,Than M.E. "Metal binding dictates conformation and function of the amyloid precursor protein (APP) E2 domain". *J Mol Biol*. 416(3):438-52. doi: 10.1016/j.jmb.2011.12.057. 2012.

Davies T.A., Drott D., Weil G.J., Simons E.R. "Flow cytometric measurement of cytoplasmic changes in human platelets". *Cytometry*. 9: 138-142. 1988.

Dawkins E., Small D.H. "Insights into the physiological function of the β-amyloid precursor protein: beyond Alzheimer's disease". *J Neurochem*. Jun;1(5):756-69. doi: 10.1111/jnc.12675. Epub 2014 Mar 7. Review. 2014.

Dawson G.R., Seabrook G.R., Zheng H., Smith D.W., Graham S., O'Dowd G., Bowery B.J., Boyce S., Trumbauer M.E., Chen H.Y., Van der Ploeg L.H., Sirinathsinghji D.J. "Age-related cognitive deficits, impaired long-term potentiation and reduction in synaptic marker density in mice lacking the beta-amyloid precursor protein". *Neuroscience*. 90(1):1-13. 1999.

de la Torre J.C., Mussivand T. "Can disturbed brain microcirculation cause Alzheimer's disease?" *Neurol Res*. 15(3):146-53). 1993.

de la Torre J.C. "Vascular risk factor detection and control may prevent Alzheimer's disease". *Ageing Res Rev*. 9(3):218-25. Review. 2010.

De Meyer S.F., Deckmyn H., Vanhoorelbeke K. "von Willebrand factor to the rescue". *Blood*. 113(21):5049-57. Review. 2009.

De Strooper B., Annaert W. "Proteolytic processing and cell biological functions of the amyloid precursor protein". *J Cell Sci*.113 (Pt 11):1857-70. 2000.

Di Luca M., Colciaghi F., Pastorino L., Borroni B., Padovani A., Cattabeni F. "Platelets as a peripheral district where to study pathogenic mechanisms of alzheimer's disease: the case of amyloid precursor protein". *Eur. J. Pharmacol*. 405: 277-283. 2000.

Esch F.S., Keim P.S., Beattie E.C., Blacher R.W., Culwell A.R., Olterdorf T., McClure D., Ward P.J. "Cleavage of amyloid beta peptide during constitutive processing of its precursor". *Science*. 248: 1122-1124. 1990.

Esmon C.T., Owen W.G. "Identification of an endothelial cell cofactor for thrombin-catalyzed activation of protein C". *Proc Natl Acad Sci U S A*. 78(4):2249-52. 1981.

Esmon C.T. "Extracellular histones zap platelets". *Blood*. 118(13):3456-7. 2011.

Evin G., Weidemann A. "Biogenesis and metabolism of Alzheimer's disease Abeta amyloid peptides". *Peptides*. 23: 1285-1297. 2002.

Falati S., Edmead C.E., Poole A.W. "Glycoprotein Ib-V-IX, a receptor for von Willebrand factor, couples physically and functionally to the Fc receptor gamma-chain, Fyn, and Lyn to activate human platelets". *Blood*. 94: 1648-56. 1999.

Falati S., Gross P., Merrill-Skoloff G., Furie B.C., Furie B. "Real-time in vivo imaging of platelets, tissue factor and fibrin during arterial thrombus formation in the mouse". *Nat Med*. 8(10):1175-81. 2002.

Franchini M., Mannucci P.M. "Venous and arterial thrombosis: different sides of the same coin? " *Eur J Intern Med*. 19(7):476-81. Review. 2008.

Fulcher C.A., Gardiner J.E., Griffin J.H., Zimmerman T.S. "Proteolytic inactivation of human factor VIII procoagulant protein by activated human protein C and its analogy with factor V". *Blood*. 63(2):486-9. 1984.

Fluhrer R., Capell A., Westmeyer G., Willem M., Hartung B., Condron M.M., Teplow D.B., Haass C., Walter J. "A non-amyloidogenic function of BACE-2 in the secretory pathway". *J Neurochem*. 81(5):1011-20. 2002.

Furie B. "Pathogenesis of thrombosis". *Hematology Am Soc Hematol Educ Program*. Review. 2009.

Fuchs T.A., Abed U., Goosmann C., Hurwitz R., Schulze I., Wahn V., Weinrauch Y., Brinkmann V., Zychlinsky A. "Novel cell death program leads to neutrophil extracellular traps". *J Cell Biol.* 176(2):231-41. 2007.

Fuchs T.A., Brill A., Duerschmied D., Schatzberg D., Monestier M., Myers D.D. Jr., Wrobleski S.K., Wakefield T.W., Hartwig J.H., Wagner D.D. "Extracellular DNA traps promote thrombosis". *Proc Natl Acad Sci U S A.* 107(36):15880-5. 2010.

Fuchs T.A., Bhandari A.A., Wagner D.D. "Histones induce rapid and profound thrombocytopenia in mice". *Blood*. 118(13):3708-14. 2011.

Fuchs T.A., Brill A., Wagner D.D. "Neutrophil extracellular trap (NET) impact on deep vein thrombosis". *Arterioscler Thromb Vasc Biol*. 32(8):1777-83. 2012.

Fuchs T.A., Alvarez J.J., Martinod K., Bhandari A.A., Kaufman R.M., Wagner D.D. "Neutrophils release extracellular DNA traps during storage of red blood cell units". *Transfusion*. 53(12):3210-6. 2013.

Gandy S. "The role of cerebral amyloid beta accumulation in common forms of Alzheimer disease". *J Clin Invest*. 115:1121-9. 2005.

Gawaz M., Langer H., May A.E. "Platelets in inflammation and atherogenesis". *J. Clin. Invest.* 115: 3378-3384. 2005.

Gerrard J.M., White J.G., Peterson D.A. "The platelet dense tubular system: its relationship to prostaglandin synthesis and calcium flux". *Thromb Haemost*. 40(2): 224-31. 1978. Review.

Ghiso J., Rostagno A., Gardella J.E., Liem L., Gorevic P.D., Frangione B. "A 109-amino-acid C-terminal fragment of Alzheimer's-disease amyloid precursor protein contains a sequence, -RHDS-, that promotes cell adhesion". *Biochem J*. 15;288 (Pt 3):1053-9. 1992.

Goedert M. "Tau protein and the neurofibrillary pathology of Alzheimer's disease". *Trens Neusosci*.16:460-465. 1993.

Gouras G.K., Xu H., Jovanovic J.N., Buxbaum J.D., Wang R., Greengard P., Relkin N.R., Gandy S. "Generation and regulation of beta-amyloid peptide variants by neurons".
J Neurochem.71(5):1920-5. 1998.

Gowert N.S., Donner L., Chatterjee M., Eisele Y.S., Towhid S.T., Münzer P., Walker B., Ogorek I., Borst O., Grandoch M., Schaller M., Fischer J.W., Gawaz M., Weggen S., Lang F., Jucker M., Elvers M. "Blood platelets in the progression of Alzheimer's disease". PLoS One. 9(2):e90523. 2014.

Gowert N.S., Krüger I., Klier M., Donner L., Kipkeew F., Gliem M., Bradshaw N.J., Lutz D., Köber S., Langer H., Jander S., Jurk K., Frotscher M., Korth C., Bock H.H., Elvers M. "Loss of Reelin protects mice against arterial thrombosis by impairing integrin activation and thrombus formation under high shear conditions".*Cell Signal*. 40:210-221. 2017.

Grammas P., Martinez J.M. "Targeting thrombin: an inflammatory neurotoxin in Alzheimer's disease". *J Alzheimers Dis*. Review. 2014.

Grammas P., Martinez J., Sanchez A., Yin X., Riley J., Gay D., Desobry K., Tripathy D., Luo J., Evola M., Young A. "A new paradigm for the treatment of Alzheimer's disease: targeting vascular activation". *J Alzheimers Dis*. 40(3):619-30. 2014.

Greenberg S.M., Qiu W.Q., Selkoe D.J., Ben-Itzhak A., Kosik K.S. "Amino-terminal region of the beta-amyloid precursor protein activates mitogen-activated protein kinase". *Neurosci Lett.* 198(1):52-6. 1995.

Gresele P., Momi S., Berrettini M., Nenci G.G., Schwarz H.P., Semeraro N., Colucci M. "Activated human protein C prevents thrombin-induced thromboembolism in mice. Evidence that activated protein c reduces intravascular fibrin accumulation through the inhibition of additional thrombin generation". *J Clin Invest.* 101(3):667-76. 1998

Grimm M.O., Rothhaar T.L., Hartmann T. "The role of APP proteolytic processing in lipid metabolism*". Exp Brain Res*. 217(3-4):365-75. Review. 2012.

Guinto E.R., Esmon C.T. "Loss of prothrombin and of factor Xa-factor Va interactions upon inactivation of factor Va by activated protein C". *J Biol Chem*. 259(22):13986-92. 1984.

Haas C. "Strategies, development, and pitfalls of therapeutic options for Alzheimer's disease*". J Alzheimers Dis*.28(2):241-81. Review. 2012.

Hartwig J.H., Barkalow K., Azim A., Italiano J. "The elegant platelet: signals controlling actin assembly". *Thromb Haemost*. 82(2):392-8. Review. 1999.

Herczenik E., Bouma B., Korporaal S.J., Strangi R., Zeng Q., Gros P., Van Eck M., Van Berkel T.J., Gebbink M.F., Akkerman J.W. "Activation of human platelets by misfolded proteins". *Arterioscler Thromb Vasc Biol*. 27(7):1657-65. 2007.

Hesse L., Beher D., Masters C.L., Multhaup G. "The beta A4 amyloid precursor protein binding to copper". *FEBS Lett*. 349(1):109-16. 1994.

Honig L.S., Tang M.X., Albert S., Costa R., Luchsinger J., Manly J., Stern Y., Mayeux R. "Stroke and the risk of Alzheimer disease".Arch Neurol.60(12):1707-12. 2003.

Honjo K., Black S. E., Verhoeff N. P. L. G. "Alzheimer's Disease, Cerebrovascular Disease, and the β-amyloid Cascade". *Can J Neurol Sci*. 39: 712-728. 2012.

Huse J.T., Liu K., Pijak D.S., Carlin D., Lee V.M., Doms R.W. "Beta-secretase processing in the trans-Golgi network preferentially generates truncated amyloid

species that accumulate in Alzheimer's disease brain". *J Biol Chem*. 277(18):16278-84. 2002.

Iijima K., et al: "Neuron-specific phosphorylation of Alzheimer's beta amyloid precursor protein by cyclin-dependent kinase 5". *J Neurochem*. 75(3):1085-91. 2000.

Italiano J.E. Jr, Lecine P., Shivdasani R.A, Hartwig J.H. "Blood platelets are assembled principally at the ends of proplatelet processes produced by differentiated megakaryocytes". *J Cell Biol*. 147(6):1299-312. 1999.

Iwatsubo T. "The gamma-secretase complex: machinery for intramembrane proteolysis." *Curr Opin Neurobiol*. 14(3):379-83. Review. 2004.

Jackson S.P., Schoenwaelder S.M., Yuan Y.P., Rabinowitz I., Salem H.H., Mitchell C.A. "Adhesion receptor activation of phosphatidylinositol 3-kinase – Von-Willebrand-factor stimulates the cytoskeletal association and activation of phosphatidylinositol 3-kinase and Pp60(C-Src) in human platelets". *J Biol Chem*. 269:27093-99. 1994

Jackson S.P. "Arterial thrombosis--insidious, unpredictable and deadly". *Nat Med*. 17(11):1423-36. doi: 10.1038/nm.2515. 2011.

Jarre A., Gowert N.S., Donner L., Münzer P., Klier M., Borst O., Schaller M., Lang F., Korth C., Elvers M. "Pre-activated blood platelets and a pro-thrombotic phenotype in APP23 mice modeling Alzheimer's disease". *Cell Signal*. 26(9):2040-50. 2014.

Jarrett J.T., Berger E.P., Lansbury P.T. Jr. "The carboxy terminus of the β amyloid protein is critical for the seeding of amyloid formation: Implications for the pathogenesis of Alzheimer's disease". *Biochemistry*. 32, 4693–4697. 1993.

Jellinger K. A. "Alzheimer disease and cerebrovascular pathology: an update". *J Neural Transm*. 109(5-6): 813- 836. 2002.

Jorch S.K., Kubes P. "An emerging role for neutrophil extracellular traps in noninfectious disease". *Nat Med*. 23(3):279-287. 2017.

Kahn M.L., Zheng Y.W., Huang W., Bigornia V., Zeng D., Moff S., Farese R.V.Jr, Tam C., Coughlin S.R. "A dual thrombin receptor system for platelet activation". *Nature*.. 394:690–694. 1998.

Kaminsky Y.G., Marlatt M.W., Smith M.A., Kosenko E.A. "Subcellular and metabolic examination of amyloid-beta peptides in Alzheimer disease pathogenesis: evidence for Abeta(25-35) ". *Exp Neurol.* 221(1):26-37. 2010.

Kang J., Lemaire H.G., Unterbeck A., Salbaum J.M., Masters C.L., Grzeschik K.H., Multhaup G., Beyreuther K., Müller-Hill B. "The precursor of Alzheimer's disease amyloid A4 protein resembles a cell-surface receptor". *Nature*. 325(6106):733-6. 1987.

Kasirer-Friede A., Cozzi M.R., Mazzucato M., De Marco L., Ruggeri Z.M., Shattil S.J. "Signaling through GP Ib-IX-V activates alpha IIb beta 3 independently of other receptors". *Blood*. 103:3403–3411. 2004.

Kehrel B., Wierwille S., Clemetson K.J., Anders O., Steiner M., Knight C.G., Farndale R.W., Okuma M., Barnes M.J. "Glycoprotein VI is a major collagen receptor for platelet activation: it recognizes the platelet-activating quaternary structure of collagen, whereas CD36, glycoprotein IIb/IIIa, and von Willebrand factor do not" *Blood.* 91(2):491-9. 1998.

Kimball A.S., Obi A.T., Diaz J.A., Henke P.K. "The emerging role of NETs in venous thrombosis and immunothrombosis". *Front Immunol.*7:236. 2016.

Kimberly W.T., Zheng J.B., Guenette S.Y., Selkoe D.J. "The intracellular domain of the beta-amyloid precursor protein is stabilized by Fe65 and translocates to the nucleus in a notch like manner". *J Biol Chem*. 276: 40288–40292. 2001.

Kimberly W.T., et al: "Physiological regulation of the beta-amyloid precursor protein signaling domain by c-Jun N-terminal kinase JNK3 during neuronal differentiation". *J Neurosci*. 25(23):5533-43. 2005.

Kirchhofer D., Nemerson Y. "Initiation of blood coagulation: the tissue factor/factor VIIa complex". *Curr Opin Biotechnol*. 7(4):386-91. Review. 1996.

Kitaguchi N., Takahashi Y., Tokushima Y., Shiojiri S., Ito H. "Novel precursor of Alzheimer's disease amyloid protein shows protease inhibitory activity". *Nature*. 331 530–532. 1988.

Kokjohn T.A., Van Vickle G.D., Maarouf C.L., Kalback W.M., Hunter J.M., Daugs I.D., Luehrs D.C., Lopez J., Brune D., Sue L.I., Beach T.G., Castaño E.M., Roher A.E. "Chemical characterization of pro-inflammatory amyloid-beta peptides

in human atherosclerotic lesions and platelets". *Biochim Biophys Acta*. 1812(11):1508-14. 2011.

Komiyama Y, Murakami T, Egawa H, Okubo S, Yasunaga K, Murata K. "Purification of factor XIa inhibitor from human platelets". *Thromb Res*. 66(4):397-408. 1992.

Koo E. H., Squazzo S. L., Selkoe D. J., Koo C. H. "Trafficking of cell-surface amyloid β-protein precursor. 1. Secretion, endocytosis and recycling as detected by labeled monoclonal antibody". *J. Cell Sci*. 109: 991-998. 1996.

Lane D.A., Philippou H., Huntington J.A. "Directing thrombin". *Blood*. 106(8):2605-12. Epub 2005 Jun 30. Review. 2005.

Lee M.S., et al: "APP processing is regulated by cytoplasmic phosphorylation*". J Cell Biol* 163(1):83-95. 2003.

Leissring M.A., Murphy M.P., Mead T.R., Akbari Y., Sugarman M.C., Jannatipour M., Anliker B., Muller U., Saftig P., De Strooper B., Wolfe M.S., Golde T.E., LaFerla F.M. "A physiologic signalling role for the gamma-secretase-derived intracellular fragment of APP". *Proc Natl Acad Sci USA*. 99: 4697–4702. 2002.

Leshner M., Wang S., Lewis C., Zheng H., Chen X.A., Santy L., Wang Y. "PAD4 mediated histone hypercitrullination induces heterochromatin decondensation and chromatin unfolding to form neutrophil extracellular trap-like structures". *Front Immunol*. 3:307. 2012.

Leslie M. "Cell biology. Beyond clotting: the powers of platelets". *Science*. 30;328(5978):562-4. 2010.

Li Q. X., Berndt M. C., Bush A. I., Rumble B., Mackenzie I., Friedhuber A., Beyreuther K., Masters C. L. "Membrane-associated form of beta A4 amyloid protein precursor of Alzheimer's disease in human platelets and brain: surface expression on the activated human platelet". *Blood*. 84: 133-42. 1994.

Li Q.X., Cappai R., Evin G., Tanner J. E., Gray C.W., Beyreuther K., Masters C.I. "Products of the Alzheimer's disease amyloid precursor protein generated by b-secretase are present in human platelets, and secreted upon degranulation". *Am. J. Alzheimer's Dis.* 13: 236-244. 1998.

Li Z., Zhang G., Feil R., Han J., Du X. "Sequential activation of p38 and ERK pathways by cGMP-dependent protein kinase leading to activation of the platelet integrin alphaIIb beta3". Blood. 107:965–972. 2006.

Li Z., Delaney M.K., O'Brien K.A., Du X. "Signaling during platelet adhesion and activation". *Arterioscler Thromb Vasc Biol*. 30(12):2341-9.2010 Review.

Lim S., Yoo B.K., Kim H.S., Gilmore H.L., Lee Y., Lee H.P., Kim S.J., Letterio J., Lee H.G. "Amyloid-β precursor protein promotes cell proliferation and motility of advanced breast cancer". *BMC Cancer*. 14:928. 2014.

Ling Y., Morgan K., Kalsheker N. "Amyloid precursor protein (APP) and the biology of proteolytic processing: relevance to Alzheimer's disease*". Int. J. Biochem. Cell Biol.* 35: 1505-1535. 2003.

Lorenzo A., Yuan M., Zhang Z., Paganetti P.A., Sturchler-Pierrat C., Staufenbiel M., Mautino J., Vigo F.S., Sommer B., Yankner B.A. "Amyloid beta interacts with the amyloid precursor protein: a potential toxic mechanism in Alzheimer's disease*".Nat Neurosci*. 3(5):460-4. 2000.

Mackman N. "Triggers, targets and treatments for thrombosis". *Nature*. 451(7181):914-8. Review. 2008.

Mackman N. "New insights into the mechanisms of venous thrombosis". *J Clin Invest*. 122(7):2331-6. 2012.

Mahdi F., Van Nostrand W.E., Schmaier A.H. "Protease nexin-2/amyloid ß-protein precursor inhibits factor Xa in the prothrombinase complex". *J. Biol. Chem*. 270 23468–23474. 1995.

Mahdi F., Rehemtulla A., Van Nostrand W.E., Bauer K.A., Schmaier A.H. "Protease nexin-2/amyloid ß-protein precursor inhibits factor VIIa-tissue factor in the tenase complex". *Thromb. Res*. 99 267–276. 2000.

Manly D.A., Boles J., Mackman N. "Role of tissue factor in venous thrombosis". *Annu Rev Physiol*. 73:515-25. 2011.

Marambaud P., Robakis N.K. "Genetic and molecular aspects of Alzheimer's disease shed light on new mechanisms of transcriptional regulation". *Genes Brain Behav*. 4(3):134-46. Review. 2005.

Marshall S.J., Asazuma N., Best D., Wonerow P., Salmon G., Andrews R.K., Watson S.P. "Glycoprotein IIb-IIIa-dependent aggregation by glycoprotein Ibalpha is reinforced by a Src family kinase inhibitor (PP1)-sensitive signalling pathway." *Biochem J*. 361(Pt 2):297-305. 2002.

Martinod K., Wagner D.D. "Thrombosis: tangled up in NETs". *Blood*.123(18):2768-76. doi: 10.1182/blood-2013-10-463646. Epub 2013 Dec 23. Review. 2014.

Massberg S., Grahl L., von Bruehl M.L., Manukyan D., Pfeiler S., Goosmann C., Brinkmann V., Lorenz M., Bidzhekov K., Khandagale A.B., Konrad I., Kennerknecht E., Reges K., Holdenrieder S., Braun S., Reinhardt C., Spannagl M., Preissner K.T., Engelmann B. "Reciprocal coupling of coagulation and innate immunity via neutrophil serine proteases". *Nat Med.* 16(8):887-96. 2010.

Matsushima H., Shimohama S., Tanaka S., Tiniiguchi T., Hagiwara M., Hidaka H., Kimura J. "Platelets protein kinase CC levels in Alzheimer's disease". *Neurobiol. Aging*. 15: 671-674. 1994.

Matsushima H., Shimohama S., Fujimoto S., Takenawa T., Kimura J. "Reduction of platelet phospholipase C activity in patient with Alzheimer's disease". *Alzheimer's Dis*. *Assoc. Disord*. 9: 213-217. 1995.

Maxwell M.J., Westein E., Nesbitt W.S., Giuliano S., Dopheide S.M., Jackson S.P. "Identification of a 2-stage platelet aggregation process mediating shear-dependent thrombus formation". *Blood* .109: 566-576. 2007.

Menashi S., Davis C., Crawford N. "Calcium uptake associated with an intracellular membrane fraction prepared from human blood platelets by high-voltage, free-flow electrophoresis". *FEBS Lett.* 140(2): 298-302. 1982.

Mészáros Z., Borcsiczky D., Máté M., Tarcali J., Tekes K., Magyar K. "MAO inhibitory side effects of neuroleptics and platelet serotonin content in schizophrenic patients". *J Neural Transm Suppl*.52:79-85. 1998.

Metzler K.D., Fuchs T.A., Nauseef W.M., Reumaux D., Roesler J., Schulze I., Wahn V., Papayannopoulos V., Zychlinsky A. "Myeloperoxidase is required for neutrophil extracellular trap formation: implications for innate immunity". *Blood*. 117(3):953-9. 2011.

Mielke M.M., Rosenberg P.B., Tschanz J., Cook L., Corcoran C., Hayden K.M.,

Norton M., Rabins P.V., Green R.C., Welsh-Bohmer K.A., Breitner J.C., Munger R., Lyketsos C.G. "Vascular factors predict rate of progression in Alzheimer disease". Neurology. 69(19):1850-8. 2007.

Möller H. J., Graeber M. B. "The case described by Alois Alzheimer in 1911. Historical and conceptual perspectives based on the clinical record and neurohistological sections". *Eur Arch Psychiatry Clin Neurosci*. 248(3): 111-22. 1998.

Momi S., Falcinelli E., Giannini S., Ruggeri L., Cecchetti L., Corazzi T., Libert C., Gresele P. "Loss of matrix metalloproteinase 2 in platelets reduces arterial thrombosis in vivo". *J Exp Med.* 206(11):2365-79. 2009.

Momi S., Caracchini R., Falcinelli E., Evangelista S., Gresele P."Stimulation of platelet nitric oxide production by nebivolol prevents thrombosis". *Arterioscler Thromb Vasc Biol*. 2014 Apr;34(4):820-9

Müller U., Cristina N., Li Z.W., et al."Behavioral and anatomical deficits in mice homozygous for a modified beta-amyloid precursor protein gene". Cell.79(5):755-765. 1994.

Müller H.P., Kassubek J., Vernikouskaya I., Ludolph A.C., Stiller D., Rasche V. "Diffusion tensor magnetic resonance imaging of the brain in APP transgenic mice: a cohort study". *PLoS One*. 8(6):e67630. 2013.

Müller U.C., Deller T. "The Physiological Functions of the APP Gene Family". *Front Mol Neurosci*. 2017.

Multhaup G., Schlicksupp A., Hesse L., Beher D., Ruppert T., Masters C.L., Beyreuther K. "The amyloid precursor protein of Alzheimer's disease in the reduction of copper(II) to copper(I)". *Science*. 271(5254):1406-9. 1996.

Munter L.M., Voigt P., Harmeier A., Kaden D., Gottschalk K.E., Weise C., Pipkorn R., Schaefer M., Langosch D., Multhaup G. "GxxxG motifs within the amyloid precursor protein transmembrane sequence are critical for the etiology of Abeta42". *EMBO J*. 26(6):1702-12. 2007.

Mukaetova-Ladinska E.B., Abdell-All Z., Andrade J., da Silva J.A., Boksha I., Burbaeva G., Kalaria R.J., O'Brien J.T. "Platelet Tau Protein as a Potential Peripheral Biomarker in Alzheimer's disease: An Explorative Study". *Curr Alzheimer Res*. 2013.

Muresan Z., Muresan V. "c-Jun NH2-terminal kinase-interacting protein-3 facilitates phosphorylation and controls localization of amyloid-beta precursor protein". *J Neurosci*. 25(15):3741-51. 2005.

Nalivaeva N.N., Turner A.J. "The amyloid precursor protein: a biochemical enigma in brain development, function and disease". *FEBS Lett*. 587(13):2046-54. doi: 10.1016/j.febslet.2013.05.010. Epub 2013 May 16. Review. 2013.

Neeli I., Radic M. "Opposition between PKC isoforms regulates histone deimination and neutrophil extracellular chromatin release". *Front Immunol*. 4:38. 2013.

Nieswandt B., Brakebusch C., Bergmeier W., Schulte V., Bouvard D., Mokhtari-Nejad R., Lindhout T., Heemskerk J.W., Zirngibl H., Fässler R. "Glycoprotein VI but not alpha2beta1 integrin is essential for platelet interaction with collagen".EMBO J. 20(9):2120-30. 2001.

Ninomiya H., Roch J.M., Sundsmo M.P., Otero D.A., Saitoh T. "Amino acid sequence RERMS represents the active domain of amyloid beta/A4 protein precursor that promotes fibroblast growth". *J Cell Biol*. 121(4):879-86. 1993.

Nishimoto I., Okamoto T., Matsuura Y., Takahashi S., Okamoto T., Murayama Y., Ogata E. "Alzheimer amyloid protein precursor complexes with brain GTP-binding protein G(o)". *Nature*. 362(6415):75-9. 1993.

Nurden A.T., Caen J.P. "Specific roles for platelet surface glycoproteins in platelet function". *Nature*. 255(5511):720-2. 1975.

Offermanns S. "Activation of platelet function through G protein-coupled receptors". *Circ Res*.99:1293–1304. 2006.

Octave J.N., Pierrot N., Ferao Santos S., Nalivaeva N.N., Turner A.J. "From synaptic spines to nuclear signaling: nuclear and synaptic actions of the amyloid precursor protein". *J Neurochem*. 126(2):183-90. 2013.

Oddo S., Caccamo A., Kitazawa M., Tseng B.P., LaFerla F.M. "Amyloid deposition precedes tangle formation in a triple transgenic model of Alzheimer's disease*". Neurobiol Aging*. 24(8):1063-70. 2003.

Oddo S., Caccamo A., Shepherd J.D., Murphy M.P., Golde T.E., Kayed R., Metherate R., Mattson M.P., Akbari Y., LaFerla F.M. "Triple-transgenic model

of Alzheimer's disease with plaques and tangles: intracellular Abeta and synaptic dysfunction". *Neuron*. 39(3):409-21. 2003.

Palmert M.R., Podlisny M.B., Witker D.S., Oltersdorf T., Younkin L.H., Selkoe D.J., Younkin S.G. "The beta-amyloid protein precursor of Alzheimer disease has soluble derivatives found in human brain and cerebrospinal fluid". *Proc Natl Acad Sci U S A*.86(16):6338-42. 1989.

Pangalos M. N., Efthimiopoulos S., Shioi J., Robakis N. K. "The chondroitin sulfate attachment site of appican is formad by splicing out exon 15 of the amyloid precursor gene". *J Biol Chem*. 270: 10388-10391. 1995.

Papayannopoulos V., Metzler K.D., Hakkim A., Zychlinsky A. "Neutrophil elastase and myeloperoxidase regulate the formation of neutrophil extracellular traps". *J Cell Biol*. 191(3):677-91. 2010.

Passer B., Pellegrini L., Russo C., Siegel R.M., Lenardo M.J., Schettini G., Bachmann M., Tabaton M., D'Adamio L. "Generation of an apoptotic intracellular peptide by gamma-secretase cleavage of Alzheimer's amyloid beta protein precursor". *J Alzheimers Dis*. 2: 289–301. 2000.

Pereira L.F., Marco F.M., Boimorto R., Caturla A., Bustos A., De la Concha E.G., Subiza J.L. "Histones interact with anionic phospholipids with high avidity; its relevance for the binding of histone-antihistone immune complexes". *Clin Exp Immunol*. 97(2):175-80. 1994.

Pierrot N., Tyteca D., D'auria L., Dewachter I., Gailly P., Hendrickx A., Tasiaux B., Haylani L.E., Muls N., N'kuli F., Laquerrière A., Demoulin J.B., Campion D., Brion J.P., Courtoy P.J., Kienlen-Campard P., Octave J.N. "Amyloid precursor protein controls cholesterol turnover needed for neuronal activity". *EMBO Mol Med*. 5(4):608-25. 2013.

Prodan C.I., Ross E.D., Vincent A.S., Dale G.L. "Differences in coated-platelet production between frontotemporal dementia and Alzheimer disease". *Alzheimer Dis Assoc Disord*. 23:234–23. 2009.

Querfurth H. W., LaFerla F M. "Alzheimer's disease". *N. Engl J Med*. 362: 329-44. 2010.

Rau J.C., Beaulieu L.M., Huntington J.A., Church F.C. "Serpins in thrombosis, haemostasis and fibrinolysis". *J Thromb Haemost*. 5 Suppl 1:102-15. Review. 2007.

Reed G.L., Fitzgerald M.L., Polgar J. "Molecular mechanisms of platelet exocytosis: insights into the "secrete" life of thrombocytes". *Blood*. 96:3334–3342. 2000.

Reinhard C., Hébert S.S., De Strooper B. "The amyloid-beta precursor protein: integrating structure with biological function". *EMBO J*. 24(23):3996-4006. Review. 2005.

Rendu F. and Brohard-Bohn B. "Platelets in thrombotic and non-thrombotic disorders: pathophysiology, pharmacology and therapeutics". Edited in 2002 by P. Gresele

Rivera J., Lozano M.L., Navarro-Núñez L., Vicente V. "Platelet receptors and signaling in the dynamics of thrombus formation". *Haematologica*. 94(5):700-11. 2009.

Rossjohn J., Cappai R., Feil S.C., Henry A., McKinstry W.J., Galatis D., Hesse L., Multhaup G., Beyreuther K., Masters C.L., Parker M.W. "Crystal structure of the N-terminal, growth factor-like domain of Alzheimer amyloid precursor protein". *Nat Struct Biol*. 6(4):327-31. 1999.

Ruggeri Z.M. "Mechanisms initiating platelet thrombus formation".*Thromb Haemost*. 78(1):611-6. 1997.

Sato T., Tanimura Y., Hirotani N., Saido T.C., Morishima-Kawashima M., Ihara Y. "Blocking the cleavage at midportion between gamma- and epsilon-sites remarkably suppresses the generation of amyloid beta-protein". *FEBS Lett*. 579(13):2907-12. 2005.

Scheinfeld M.H., et al: "Amyloid beta protein precursor is phosphorylated by JNK-1 independent of, yet facilitated by, JNK-interacting protein (JIP)-1". *J Biol Chem*. 278(43):42058-63. 2003.

Scheuermann S., Hambsch B., Hesse L., Stumm J., Schmidt C., Beher D., Bayer T.A., Beyreuther K., Multhaup G. "Homodimerization of amyloid precursor protein and its implication in the amyloidogenic pathway of Alzheimer's disease". *J Biol Chem*. 276(36):33923-9. 2001.

Schmaier A.H., Dahl L.D., Rozemuller A.J.M., Roos R.A.C., Wagner S.L., Chung R., Van Nostrand W.E. "Protease nexin-2/amyloid ß-protein precursor: a tight binding inhibitor of coagulation factor IXa". *J. Clin. Invest*. 92 2540–2545. 1993.

Schulze H. and Shivdasani R.A. "Mechanisms of thrombopoiesis". *J Thromb Haemost*. 3(8):1717-24. 2005.

Selkoe D. J. "Alzheimer's disease: genes, proteins and therapy". *Physiol Rev*. 81: 741-766. 2001.

Selkoe D.J., Wolfe M.S. "Presenilin: running with scissors in the membrane". *Cell*. 131(2):215-21. Review. 2007.

Semeraro F., Ammollo C.T., Morrissey J.H., Dale G.L., Friese P., Esmon N.L., Esmon C.T. "Extracellular histones promote thrombin generation through platelet-dependent mechanisms: involvement of platelet TLR2 and TLR4". *Blood*. 118(7):1952-61. 2011.

Seubert P., Oltersdorf T., Lee M. G., Barbour R., Blomquist C., Davis D.L., Bryant K, Fritz L C, Galasko D, Thal L J, Lieberburg I, Schenk D.B. "Secretion of βamyloid precursor protein cleaved at the amino terminus of the β-amyloid peptide". *Nature*. 361:260-263. 1993.

Sevuh S., Jy W., Horstman L.L., et al. "Platelet activation in Alzheimer disease". *Arch. Neurol*. 55 (4): 530-536. 1998.

Shattil S.J. and Newman P.J. "Integrins: dynamic scaffolds for adhesion and signaling in platelets". *Blood*.104:1606–1615. 2004.

Shattil S.J., Kim C., Ginsberg M.H. "The final steps of integrin activation: the end game". *Nat Rev Mol Cell Biol*.11:288–300. 2010.

Shen M. Y., Hsiao G., Fong T. H., et al. "Amyloid beta peptide-activated signal pathways in human platelets". Eur. J. Pharmacol. 588 (2-3): 259-266. 2008.

Si-Tahar M., Pidard D., Balloy V., Moniatte M., Kieffer N., Van Dorsselaer A., Chignard M. "Human neutrophil elastase proteolytically activates the platelet integrin alphaIIbbeta3 through cleavage of the carboxyl terminus of the alphaIIb subunit heavy chain. Involvement in the potentiation of platelet aggregation". *J Biol Chem*. 272(17):11636-47. 1997.

Small D. H., Nurcombe V., Reed G., Clarris H., Moir R., Beyreuther K., et al. "A heparin-binding domain in the amyloid protein precursor of Alzheirmer's disease is involved in the regulation of neurite outgrowth".*J Neurosci*. 14: 2117-2127. 1994.

Smith R.P., Higuchi D.A., Broze Jr. G.J. "Platelet coagulation factor XIa-inhibitor, a form of Alzheimer amyloid precursor protein". *Science*. 248 1126–1128. 1990.

Soba P., Eggert S., Wagner K., Zentgraf H., Siehl K., Kreger S., Löwer A., Larger A., Merdes G., Paro R., Masters C. L., Müller U., Kins S., Beyreuther K. "Homo- and heterodimerization of APP family members promotes intracellular adhesion". *EMBO J*. 24: 3624-3634. 2005.

Sonkar V.K., Kulkarni P.P., Dash D. "Amyloid β peptide stimulates platelet activation through RhoA-dependent modulation of actomyosin organization".FASEB J.; 28(4):1819-29. 2014.

Stellos K., Panagiota V., Kögel A., Leyhe T., Gawaz M., Laske C. "Predictive value of platelet activation for the rate of cognitive decline in Alzheimer's disease patients". *J Cereb Blood Flow Metab*. 30(11):1817-20. 2010.

Steppich B.A., Seitz I., Busch G., Stein A., Ott I. "Modulation of tissue factor and tissue factor pathway inhibitor-1 by neutrophil proteases". *Thromb Haemost*. 100(6):1068-75. 2008.

Stover et al., "Early detection of cognitive deficits in the 3xTg-AD mouse model of Alzheimer's disease". Behav Brain Res. 289:29-38. 2015.

Struhl G. and Adachi A. "Requirements for presenilin-dependent cleavage of notch and other transmembrane proteins*". Mol Cell*. 6: 625–636. 2000.

Sullam P.M., Hyun W.C., Szöllösi J., Dong Jf., Foss W.M., López J.A. "Physical proximity and functional interplay of the glycoprotein Ib-IX-V complex and the Fc receptor FcgammaRIIA on the platelet plasma membrane".*J Biol Chem.* 273(9):5331-6. 1998.

Tangelder G.J., Slaaf D.W., Arts T., Reneman R.S. "Wall shear rate in arterioles in vivo: least estimates from platelet velocity profiles". *Am J Physiol*. 254(6 Pt 2):H1059-64. 1988.

Tanzi R.E., McClatchey A.I., Lamperti E.D., Villa-Komaroff L., Gusella J.F., Neve RL.

"Protease inhibitor domain encoded by an amyloid protein precursor mRNA associated with Alzheimer's disease".*Nature*. 331(6156):528-30. 1988.

Tanzi R.E., Bertram L. "Twenty years of the Alzheimer's disease amyloid hypothesis: A genetic perspective". *Cell*. 120: 545–555. 2005.

Thal D.R., Griffin W S., de Vos R.A, Ghebremedhin E. "Cerebral amyloid angiopathy and its relationship to Alzheimer's disease". *Acta Neuropathol*.; 60: 1707-1712. 2008.

Thinakaran G., Koo E.H. "Amyloid precursor protein trafficking, processing, and function".
J Biol Chem. 283(44):29615-9. Epub 2008 Jul 23. Review. 2008.

Torti M., Bertoni A., Canobbio I., Sinigaglia F., Lapetina E.G., Balduini C. "Rap1B and Rap2B translocation to the cytoskeleton by von Willebrand factor involves Fc gamma II receptor-mediated protein tyrosine phosphorylation". *J Biol Chem*. 274: 13690-97. 1999.

Tremoli E., Camera M., Toschi V., Colli S. "Tissue factor in atherosclerosis". *Atherosclerosis*. 144(2):273-83. Review. 1999.

Triplett DA. "Coagulation and bleeding disorders: review and update". *Clin Chem*. 46(8 Pt 2):1260-9. Review. 2000.

Turner A.J., Belyaev N.D., Nalivaeva N.N. "Mediator: the missing link in amyloid precursor protein nuclear signalling". *EMBO Rep*. 12(3):180-1. 2011.

Van Nostrand W.E., Wagner S.L., Suzuki M., Choi B.H., Farrow J.S., Geddes J.W., Cotman C.W., Cunningham D.D. "Protease nexin-II, a potent anti-chymotrypsin, shows identity to amyloid ß-protein precursor". *Nature*. 341 546–549. 1989.

Van Nostrand W.E., Wagner S.L., Farrow J.S., Cunningham D.D. "Immunopurification and protease inhibitory properties of protease nexin-2/amyloid ß-protein precursor". *J. Biol. Chem*. 265 9591–9594. 1990.

Van Nostrand W.E., Farrow J.S., Wagner S.L., Bhasin R., Goldgaber D., Cotman C.W., Cunningham D.D"The predominant form of the amyloid beta-protein precursor in human brain is protease nexin 2". *Proc Natl Acad Sci U S A*. 88(22):10302-6. 1991.

Van Nostrand W.E., Melchor J.P., Keane D.M., Saporito-Irwin S.M., Romanov G., Davis J., Xu F. "Localization of a fibrillar amyloid ß- protein binding domain on its precursor". *J. Biol. Chem*. 277 - 36392–36398. 2002.

Varga-Szabo D, Pleines I, Nieswandt B. "Cell adhesion mechanisms in platelets".*Arterioscler Thromb Vasc Biol*. 28(3): 403-12. 2008.

Vassar R., Bennett B.D., Babu-Khan S., Kahn S., Mendiaz E.A., Denis P., Teplow D.B., Ross S., Amarante P., Loeloff R., Luo Y., Fisher S., Fuller J., Edenson S., Lile J., Jarosinski M.A., Biere A.L., Curran E., Burgess T., Louis J.C., Collins F., Treanor J., Rogers G., Citron M. "Beta-secretase cleavage of Alzheimer's amyloid precursor protein by the transmembrane aspartic protease BACE". *Science*. 286(5440):735-41. 1999.

Vassar R., Citron M. "Abeta-generating enzymes: recent advances in beta- and gamma-secretase research". *Neuron*. 27(3):419-22. Review. 2000.

Veitinger M., Varga B., Guterres S.B., Zellner M. "Platelets, a reliable source for peripheral Alzheimer's disease biomarkers?" *Acta Neuropathol Commun*. J. 2:65. Review. 2014.

von Brühl M.L., Stark K., Steinhart A., Chandraratne S., Konrad I., Lorenz M., Khandoga A., Tirniceriu A., Coletti R., Köllnberger M., Byrne R.A., Laitinen I., Walch A., Brill A., Pfeiler S., Manukyan D., Braun S., Lange P., Riegger J., Ware J., Eckart A., Haidari S., Rudelius M., Schulz C., Echtler K., Brinkmann V., Schwaiger M., Preissner K.T., Wagner D.D., Mackman N., Engelmann B., Massberg S. "Monocytes, neutrophils, and platelets cooperate to initiate and propagate venous thrombosis in mice in vivo". *J Exp Med*. 209(4):819-35. 2012.

von Rotz R.C., Kohli B.M., Bosset J., Meier M., Suzuki T., Nitsch R.M., Konietzko U. "The APP intracellular domain forms nuclear multiprotein complexes and regulates the transcription of its own precursor". *J Cell Sci*. 117: 4435–4448. 2004.

Xu F., Davis J., Miao J., Previti M.L., Romanov G., Ziegler K., Van Nostrand W.E. "Protease nexin-2/amyloid beta-protein precursor limits cerebral thrombosis. *Proc Natl Acad Sci U S A*. 102(50):18135-40. 2005.

Xu F., Previti M.L., Van Nostrand W.E. "Increased severity of hemorrhage in transgenic mice expressing cerebral protease nexin-2/amyloid beta-protein precursor". *Stroke*. 38(9): 2598-601. 2007.

Xu F., Previti M.L., Nieman M.T., Davis J., Schmaier A.H., Van Nostrand W.E. "AbetaPP/APLP2 family of Kunitz serine proteinase inhibitors regulate cerebral thrombosis". *J Neurosci*. 29(17):5666-70. 2009.

Xu F., Davis J., Hoos M., Van Nostrand W.E. "Mutation of the Kunitz-type proteinase inhibitor domain in the amyloid β-protein precursor abolishes its anti-thrombotic properties in vivo". *Thromb Res*. 155:58-64. 2017.

Walsh D.M., Fadeeva J.V., LaVoie M.J., Paliga K., Eggert S., Kimberly W.T., Wasco W., Selkoe D.J. "Gamma-secretase cleavage and binding to FE65 regulate the nuclear translocation of the intracellular C-terminal domain (ICD) of the APP family of proteins". *Biochemistry*. 42: 6664–6673. 2003.

Wang Y., Li M., Stadler S., Correll S., Li P., Wang D., Hayama R., Leonelli L., Han H., Grigoryev S.A., Allis C.D., Coonrod S.A. "Histone hypercitrullination mediates chromatin decondensation and neutrophil extracellular trap formation". *J Cell Biol*. 184(2):205-13. doi: 10.1083/jcb.200806072. 2009.

Wang H., Bang K.W., Blanchette V.S. et al. "Phosphatidylserine exposure, microparticle formation and mitochondrial depolarization in Glanzmann throbasthenia platelets". *Thromb Haemost.* 111:1184-6. 2014.

Wang H., Reiser G. "Thrombin signaling in the brain: the role of protease-activated receptors". *Biol Chem*. 384(2):193-202. Review. 2003.

Wang Y., Ha Y. "The X-ray structure of an antiparallel dimer of the human amyloid precursor protein E2 domain". M*ol Cell*. 15(3):343-53. 2004.

Wasco W., Bupp K., Magendantz M., Gusella J.F., Tanzi R.E., Solomon F. "Identification of a mouse brain cDNA that encodes a protein related to the Alzheimer disease-associated amyloid beta protein precursor". *Proc Natl Acad Sci U S A*. 89(22):10758-62. 1992.

Wasco W., Brook J.D., Tanzi R.E. "The amyloid precursor-like protein (APLP) gene maps to the long arm of human chromosome 19". *Genomics*. 15(1):237-9. 1993.

Wasco W., Pettingell W.P., Jondro P.D., Schmidt S.D., Gurubhagavatula S., Rodes L., DiBlasi T, Romano D.M., Guenette S.Y., Kovacs D.M., et al. "Familial Alzheimer's chromosome 14 mutations". *Nat Med*. 1(9):848. 1995.

Watson K., Gooderham N.J., Davies D.S., Edwards R.J. "Nucleosomes bind to cell surface proteoglycans". *J Biol Chem*. 274(31):21707-13. 1999.

Watson S.P., Gibbins J. "Collagen receptor signalling in platelets: extending the role of the ITAM". *Immunol Today*. 19:260–264. 1998.

Watson S.P., Auger J.M., McCarty O.J., Pearce A.C. "GPVI and integrin alphaIIb beta3 signaling in platelets". *J Thromb Haemost*.3:1752–1762. 2005.

White J.G. "Shape change*". Thromb Diath Haemorrh*.60: 159–71. 1974.

Willoughby S., Holmes A., Loscalzo J. "Platelets and cardiovascular disease". *Eur J Cardiovasc Nurs*. 1(4): 273-88. 2002.

Wolozin B., Maheshwari S., Jones C., Dukoff R., Wallace W., Racchi M., Nagula S., Shulman N.R., Sunderland T., Bush A. "Beta-amyloid augments platelet aggregation: reduced activity of familial angiopathy-associated mutants". *Mol Psychiatry*. 3(6):500-7. 1998.

Wu Y., Suzuki-Inoue K., Satoh K., Asazuma N., Yatomi Y., Berndt M.C., Ozaki Y. "Role of Fc receptor gamma-chain in platelet glycoprotein Ib-mediated signaling". *Blood*. 97:3836-45. 2001.

Yamazaki T., Koo E.H., Selkoe D.J. "Cell surface amyloid beta-protein precursor colocalizes with beta 1 integrins at substrate contact sites in neural cells". *J Neurosci*. 17(3):1004-10. 1997.

Yin H., Liu J., Li Z., Berndt M.C., Lowell C.A., Du X. "Src family tyrosine kinase Lyn mediates VWF/GPIb-IX-induced platelet activation via the cGMP signaling pathway". *Blood*.112:1139–1146. 2008.

Yoshikai S., Sasaki H., Doh-ura K., Furuya H., Sakaki Y. "Genomic organization of the human amyloid beta-protein precursor gene". *Gene*. 87(2):257-63. 1990.

Young-Pearse T.L., Chen A.C., Chang R., Marquez C., Selkoe D.J. "Secreted APP regulates the function of full-length APP in neurite outgrowth through interaction with integrin beta1". *Neural Dev*. 3:15. 2008.

Zhang W., Huang W., Jing F. "Contribution of blood platelets to vascular pathology in Alzheimer's disease". *J. of Blood Med*.4: 141-147. 2013.

Zheng H., Jiang M., Trumbauer M.E., Sirinathsinghji D.J., Hopkins R., Smith D.W., Heavens R.P., Dawson G.R., Boyce S., Conner M.W., Stevens K.A., Slunt H.H., Sisoda S.S., Chen H.Y., Van der Ploeg L.H. "beta-Amyloid precursor protein-deficient mice show reactive gliosis and decreased locomotor activity". *Cell*. 81(4):525-31. 1995.

Zheng H., Koo E.H. "Biology and pathophysiology of the amyloid precursor protein". *Mol Neurodegener*. 6(1):27. 2011.